AD-A164 523 STUDY OF OFF-AXIS RADIATION EXPOSURE FROM RELATIVISTIC 1/2
ELECTRONS TRAVERSING THROUGH MATTER(U) NAVAL
POSTGRADUATE SCHOOL MONTEREY CA R D FITZPATRICK DEC 85
UNCLASSIFIED F/G 20/8 NL

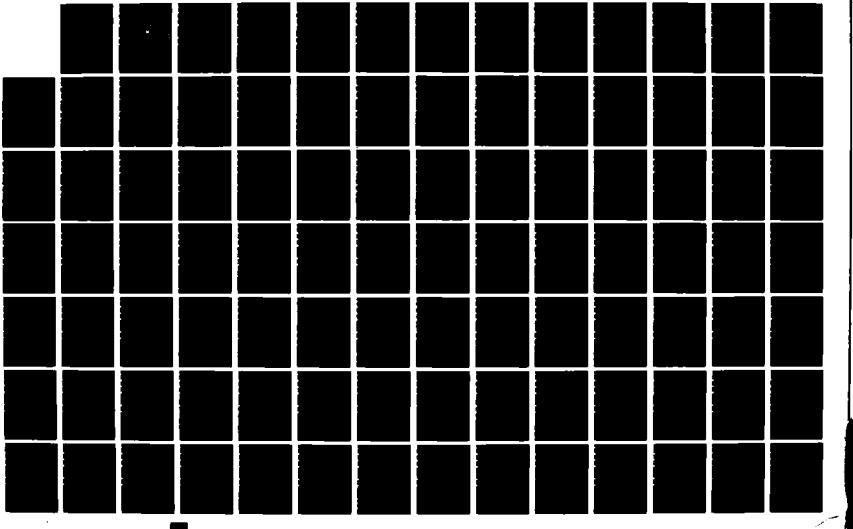

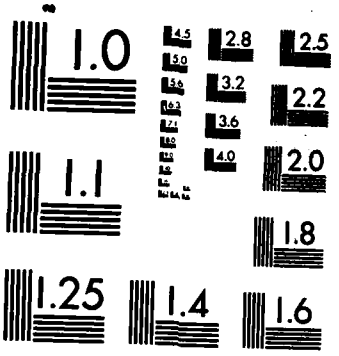

(2)

AD-A164 523

NAVAL POSTGRADUATE SCHOOL
Monterey, California

THESIS

STUDY OF OFF-AXIS RADIATION EXPOSURE FROM RELATIVISTIC ELECTRONS TRAVERSING THROUGH MATTER

by

Richard D. Fitzpatrick

December 1985

Thesis Advisor: X.K. Maruyama

Approved for public release: distribution is unlimited.

UNCLASSIFIED

SECURITY CLASSIFICATION OF THIS PAGE

AD-A164523

REPORT DOCUMENTATION PAGE

1a. REPORT SECURITY CLASSIFICATION	1b. RESTRICTIVE MARKINGS
2a. SECURITY CLASSIFICATION AUTHORITY	3. DISTRIBUTION/AVAILABILITY OF REPORT Approved for public release; distribution is unlimited.
2b. DECLASSIFICATION/DOWNGRADING SCHEDULE	
4. PERFORMING ORGANIZATION REPORT NUMBER(S)	5. MONITORING ORGANIZATION REPORT NUMBER(S)
6a. NAME OF PERFORMING ORGANIZATION: Naval Postgraduate School 6b. OFFICE SYMBOL (If applicable): Code 61	7a. NAME OF MONITORING ORGANIZATION: Naval Postgraduate School
6c. ADDRESS (City, State, and ZIP Code): Monterey, California 93943-5100	7b. ADDRESS (City, State, and ZIP Code): Monterey, California 93943-5100
8a. NAME OF FUNDING/SPONSORING ORGANIZATION 8b. OFFICE SYMBOL (If applicable)	9. PROCUREMENT INSTRUMENT IDENTIFICATION NUMBER
8c. ADDRESS (City, State, and ZIP Code)	10. SOURCE OF FUNDING NUMBERS PROGRAM ELEMENT NO. / PROJECT NO. / TASK NO. / WORK UNIT ACCESSION NO

11. TITLE (Include Security Classification)
STUDY OF OFF-AXIS RADIATION EXPOSURE FROM RELATIVISTIC ELECTRONS TRAVERSING THROUGH MATTER

12. PERSONAL AUTHOR(S)
Fitzpatrick, Richard D.

13a. TYPE OF REPORT	13b. TIME COVERED	14. DATE OF REPORT (Year, Month, Day)	15. PAGE COUNT
Master's Thesis	FROM _____ TO _____	1985, December	144

16. SUPPLEMENTARY NOTATION

17. COSATI CODES			18. SUBJECT TERMS (Continue on reverse if necessary and identify by block number)
FIELD	GROUP	SUB-GROUP	Off-Axis Radiation; Dosimetry; CYLTRAN

19. ABSTRACT (Continue on reverse if necessary and identify by block number)

Results are presented from the study of the off-axis radiation field caused by a relativistic, mono-directional electron beam passing through water. Using the Naval Postgraduate School 100 MeV linear accelerator, off-axis radiation dose was measured with calcium fluoride thermo-luminescent dosimeters placed at various path lengths out to two radiation lengths. The off-axis dose was calculated using the electron transport code CYLTRAN of the integrated TIGER series of coupled electron/photon Monte Carlo transport codes.Calculations were performed at Los Alamos National Laboratory. Comparison with the results is made and CYLTRAN is found to be in agreement with experimentally measured values. The extension of results from one medium(water) to another (air) appears to be valid.

20. DISTRIBUTION/AVAILABILITY OF ABSTRACT	21. ABSTRACT SECURITY CLASSIFICATION
☒ UNCLASSIFIED/UNLIMITED ☐ SAME AS RPT. ☐ DTIC USERS	Unclassified
22a. NAME OF RESPONSIBLE INDIVIDUAL: Prof. Fred R. Buskirk	22b. TELEPHONE (Include Area Code): (408) 646-2765 / 22c. OFFICE SYMBOL: Code 61Bs

DD FORM 1473, 84 MAR — 83 APR edition may be used until exhausted. All other editions are obsolete.

SECURITY CLASSIFICATION OF THIS PAGE

Approved for public release; distribution is unlimited.

Study of Off-Axis Radiation Exposure From Relativistic Electrons Traversing Through Matter

by

Richard Douglas Fitzpatrick
Lieutenant, United States Navy
B.S., United States Naval Academy, 1979

Submitted in partial fulfillment of the
requirements for the degree of

MASTER OF SCIENCE IN PHYSICS

from the

NAVAL POSTGRADUATE SCHOOL
December 1985

Author: Richard D. Fitzpatrick
Richard Douglas Fitzpatrick

Approved by: Xavier K. Maruyama (B, F B)
X.K. Maruyama, Thesis Advisor

Fred R Buskirk
F.R. Buskirk, Second Reader

G E Schacher
Gordon E. Schacher, Chairman, Department of Physics

John Dyer
John N. Dyer, Dean of Science and Engineering

ABSTRACT

Results are presented from the study of the off- axis radiation field caused by a relativistic, mono-directional electron beam passing through water. Using the Naval Postgraduate School 100 MeV linear accelerator, off-axis radiation dose was measured with calcium fluoride thermo-luminescent dosimeters placed at various path lengths out to two radiation lengths. The off-axis dose was calculated using the electron transport code CYLTRAN of the integrated TIGER series of coupled electron/photon Monte Carlo transport codes. Calculations were performed at Los Alamos National Laboratory. Comparison with the results is made and CYLTRAN is found to be in agreement with experimentally measured values. The extension of experimental results in one medium (water) to another (air) appears to be valid.

TABLE OF CONTENTS

ACKNOWLEDGMENT

Special thanks are due to Dr. Joseph Mack of Los Alamos National Laboratory and Ms. Louise Miles of the Naval Surface Weapons Center who both contibuted significant time and expertise towards this project. Also deserving recognition is Mr. Don Snyder of the Naval Postgraduate School Accelerator Laboratory whose involvement with the students proved invaluable.

I. INTRODUCTION

Recent development of new high energy, high current accelerators has renewed interest in the ability to accurately predict radiation exposure in the vicinity of a monodirectional electron beam. In addition to personnel safety requirements, the areas of vulnerability and lethality as they apply to charged particle beams are becoming increasingly important. The majority of the literature on radiation dosimetry applies to low or moderate energy sources. The experimental verification of the calculations as they apply to high energy electron beams has been sparse and comparison of several computational methods has been inconclusive.

Recent experiments at the Naval Postgraduate School by P.F. Cromar attempted to address some of these questions by studying the off-axis radiation field in liquid nitrogen as a function of radiation length [Ref. 1: p.4]. Focused electrons of 100 MeV incident energy were delivered to insulated containers filled with liquid nitrogen. The measured dose was compared to calculations using the electron transport code CYLTRAN . Cromar's results compared favorably (within a factor of 2) with the results predicted by the calculations. However, where comparisons could be made, Cromar's results appeared to differ from an earlier calculation by R.A. Lindgren using the code ETRAN-16,which referred to 50 Mev electrons in air [Ref. 1: p.39] . It is the objective of this thesis to address, through a series of experiments, several questions concerning the validity of calculations and

experimental methods as they apply to high energy electron beams. Passive dosimetry will be used to determine:

1) Can the computer computations accurately predict the experimental results?

2) Can the results in one medium be used to predict the response in a second medium?

3) Is there an energy dependence to the response?

4) If the responses are different, what is the significance as it applies to the energy spectrum?

II. BACKGROUND

A. INTERACTION OF RADIATION WITH MATTER

When a primary electron passes through an absorber it will only have a well-defined range for energies of less than a few MeV. At these low energies, energy loss is by ionization and excitation of the atomic electrons in the atoms of the absorber[Ref.2: p.508]. The energy loss of electrons due to ionization is given by [Ref.3: p.38]:

$$-\left(\frac{dE}{dx}\right)_{ion} = \frac{4\pi e^4 n}{mc^2}\left[\log\frac{2mc^2}{I} - \frac{3}{2}\log(1-\beta^2)^{1/2} - \frac{1}{2}\log\delta + \frac{1}{16}\right]$$

where e = charge on the electron (cgs)

n = electron density

m = mass of electron

c = speed of light

I = ionization potential

β = ratio of electron velocity to c

As the electron energy increases, radiative energy loss becomes more important than ionization. This energy loss is given by [Ref. 3: p.68]:

$$-\left(\frac{dE}{dx}\right)_{Rad} = \frac{4Z^2 n}{137} r_0 h\nu_{max} \log\frac{183}{Z^{1/3}}$$

where r_0 = classical radius of the electron

h = Planck's constant

Z = atomic number

υ = frequency of the highest energy photon produced

The energy loss by radiation, called bremsstrahlung, is proportional to Z^2 of the material and increases linearly with the electrons energy, whereas losses due to ionization and excitation are only proportional to Z. Thus the radiation loss predominates at the higher energies. The approximate ratio of the two losses is [Ref.3: p.64]

$$\frac{\left(\frac{dE}{dx}\right)_{Rad}}{\left(\frac{dE}{dx}\right)_{ion}} = \frac{EZ}{1600\,mc^2} = \frac{EZ}{800}$$

There is a critical energy, E_c, for which the two energy losses are equal:

$$E_c\ (MeV) = \frac{800}{Z}$$

If, in a given material, the incident energy is much larger than the critical energy, then radiation loss predominates over ionization loss and can be considered to be the only significant loss mechanism [Ref.3: p.72].

When electrons of high initial energy pass through matter, they lose their energy mainly by emitting bremsstrahlung photons. These high-energy photons, or gamma rays, in turn lose their energy mainly by the electron pair-production process. By a series of similar interactions and a succession of these simple elementary processes, a multiplication process comes about. An avalanche of electrons and photons develops and is referred to as cascade shower or electron-photon cascade.[Ref.4: p.91][Ref.5: p.221]

The energy of the primary electron is divided among the cascade particles, their sum equaling the primary energy except for the amount lost due to ionization. A rapid multiplication of shower particles results with the number of particles growing exponetially as long as their energies exceed the critical energy, E_c. As the number of particles reaches a maximum value *and the energy per particle is smaller*, the ionization losses become more important than the bremsstrahlung losses. Multiplication of shower particles ceases and as energy is spent in ionization and excitation processes the number of particles decreases. [Ref.4:pp.92-93]

The maximum number of shower particles amounts to :

$$N_{max} = \frac{E_0}{E_c}$$

This maximum is observed at an absorber depth of:

$$t_{max} = \frac{\ln(E_o/E_c)}{\ln 2}$$

with t_{max} being measured in radiation lengths.[Ref.4: p.93]

Photon production by bremsstrahlung and their angular distribution is largely a statistical process. The spectrum of energies produced by an electron beam will be broad and the percentage of energy transferred to any given photon following an interaction will follow a probability distribution function determined by the energy of the incident electron and the atomic number of the material. The result is that many secondary electrons which are emitted cause further ionization and excitation, and may penetrate far beyond the range of the primary electrons [Ref.2: p.509]. The precise mathematical development of showers is complicated and can contain large fluctuations from the average behavior. In practice, it becomes necessary to use Monte Carlo techniques to calculate the shower induced dose.

The difficulty in separating the effects of the primary and secondary electrons makes range an inappropriate measure of electron absorption above a few MeV energy [Ref.2: p.509.]. The concept of radiation length, X_0, is useful in the interpretation of this energy-loss phenomena and is defined by Fenyves and Haiman [Ref.4: p.25] as:

$$\frac{1}{X_0} = 4\alpha\frac{N}{A}Z(Z+1)r_0^2\left[\ln(183\,Z^{-1/3})\right]\left[1+0.12\left(\frac{Z}{82}\right)^2\right]^{-1}$$

Radiation length can be visualized as the distance in which the electron energy is reduced to 1/e of its initial value and is independent of electron

energy. In practice it is more convenient to express the quantity in units of gm/cm^2 (Table 1) in which the calculated values form a smooth curve as a function of Z. [Ref.2: pp.510-512]

TABLE 1

VALUES OF RADIATION LENGTH FOR VARIOUS SUBSTANCES

Substance	Z	A	Radiation lengths (gm/cm2)	(cm)	Critical energy (Mev)
Carbon	6	12	44.6	30.0	102
Nitrogen	7	14	39.4		88.7
Air	7.37	14.78	37.7	31.0×10^3	84.2
Water	7.23	14.3	37.1	37.1	83.8
Oxygen	8	16	35.3		77.7

III. ISSUES

Previous experiments dealing with the experimental verification of calculations as they apply to high energy particle beams raised several issues. Direct comparisons between experiments and calcualtions have been difficult due to differing experimental geometries, varying incident energies, and multiple computational computer codes. This experiment will address some of these issues.

A. EXPERIMENTAL GEOMETRY

The recent experiments by P.F. Cromar [Ref. 1] were conducted in an insulated container filled with liquid nitrogen. The use of liquid nitrogen as the test medium precluded the immersion of the dosimeters in the environmental matrix. The dosimeters were placed in air on the exterior of a one inch thick hard foam container. Ideally, direct comparison with calculation should be done with the dosimeters placed inside the test medium so that the side and back scatter contributions are the same for experiment and calculations.

Separate tanks were required for measurements at different distances from the beam entrance. As a result, several independent runs were necessary to compile the data at all distances. If the dosimeters could be placed directly in the test medium all measurements could be done

simultaneously to minimize experimental beam condition variability. For this experiment, thermoluminescent dosimeters were sealed in plastic and placed directly in water.

B. ENERGY DEPENDENCE

The experiment by Cromar was conducted at a single energy of 100 MeV. This is roughly the critical energy of liquid nitrogen where there is equal contribution from bremsstrauhlung and ionization to the energy loss mechanism. The contributions to energy deposition are different from that for energy loss. It is possible that the continuous slowing down approximation in the computational code may not be adequate at all energies.

Experiments were conducted at 100 MeV and 20 MeV. The experimental results from the 20 MeV run were not returned for inclusion is this paper, but results of other published results at varying energies are discussed.

C. COMPUTATION

It is not clear from the published data and the calculations of Cromar that all versions of the electron transport codes produce the same computational results. The apparent disagreement between ETRAN-16 and CYLTRAN needs to be investigated. In translating the calculated dose in liquid nitrogen to that which might be observed in air, a single geometrical extrapolation was used. This may not be adequate as multiple scattering angles and radiation lengths in the beam axis and the perpendicular direction interplay.

In this experiment, the results of the two-dimensional CYLTRAN code for the energy deposition in water have been converted to a one-dimensional geometry and compared with the published results for ETRAN. In addition, CYLTRAN results for water and liquid nitrogen are scaled and compared to the CYLTRAN predictions for air.

D. DOSIMETRY

CaF_2 dosimeters have a non-linear response as a function of photon energy below 200 keV as shown in Figure 3.1.

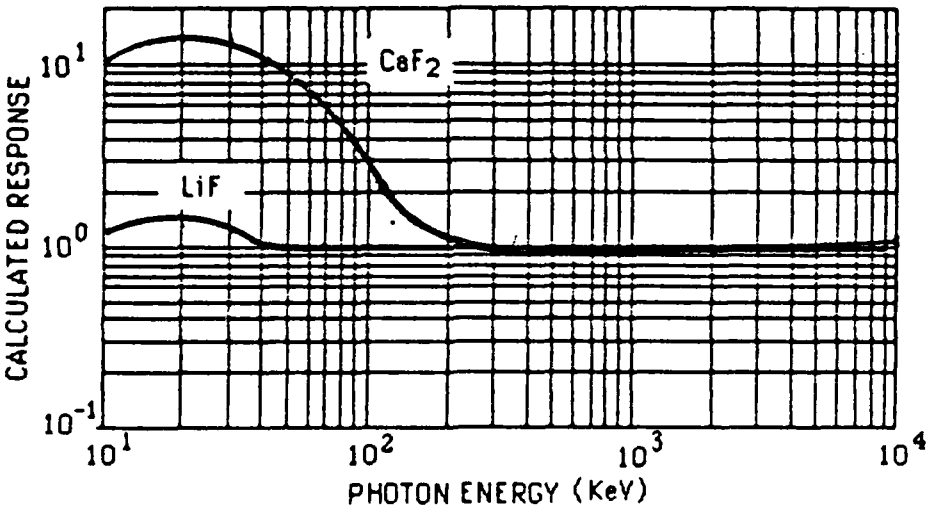

Figure 3.1 Calculated Response of CaF_2 and LiF

Should the radiation field in the vicinity of the electron beam result in a large fraction of the deposited energy being due to lower energy photons, then the dose measured could be in serious error. The dosimeters have been

calibrated with respect to a ^{60}Co source. The spectrum due to a line electron source is not identical to that from ^{60}Co.

Dosimeters of CaF_2 and LiF were placed in symmetrical positons for a direct comparison of the measured dose. This portion of the experiment remains incomplete as the results for the LiF dosimeters were not returned due to a faulty set of calibration curves at the reading facility.

IV. CALCULATIONS

A. DESCRIPTION

The calculations of electron/photon showers were performed using the computer program CYLTRAN of the Integrated TIGER Series of Transport Codes[Ref. 6]. The purpose of the calculation was to determine the off-axis dose resulting from discharging a monodirectional beam of electrons into several different media.

The cylindrical geometry of the computer code CYLTRAN is well suited for the desired output. A 0.8 cm diameter electron beam of 20,000 particles was incident normal to targets of water, air, and liquid nitrogen. Each target, as indicated in Figure 4.1, was divided into zones with energy deposition being recorded at distances that corresponded to 0.0, 0.25, 0.50, 1.0, 1.5, and 2.0 radiation lengths in each medium. At each distance, ten concentric sub-zones, Figure 4.2, were created to measure the off-axis energy deposition. Zone thickness was kept thin to provide semi-discrete data points at specific distances of penetration into the medium. However, sufficient thickness was necessary to allow for the finite track segments used in the computer calculations and to provide for statistical validity of the results.

The output of the code included the target material, zone or sub-zone location and mass, energy deposited by primary and knock-on electrons, energy deposited by photons, and the total energy deposited within each

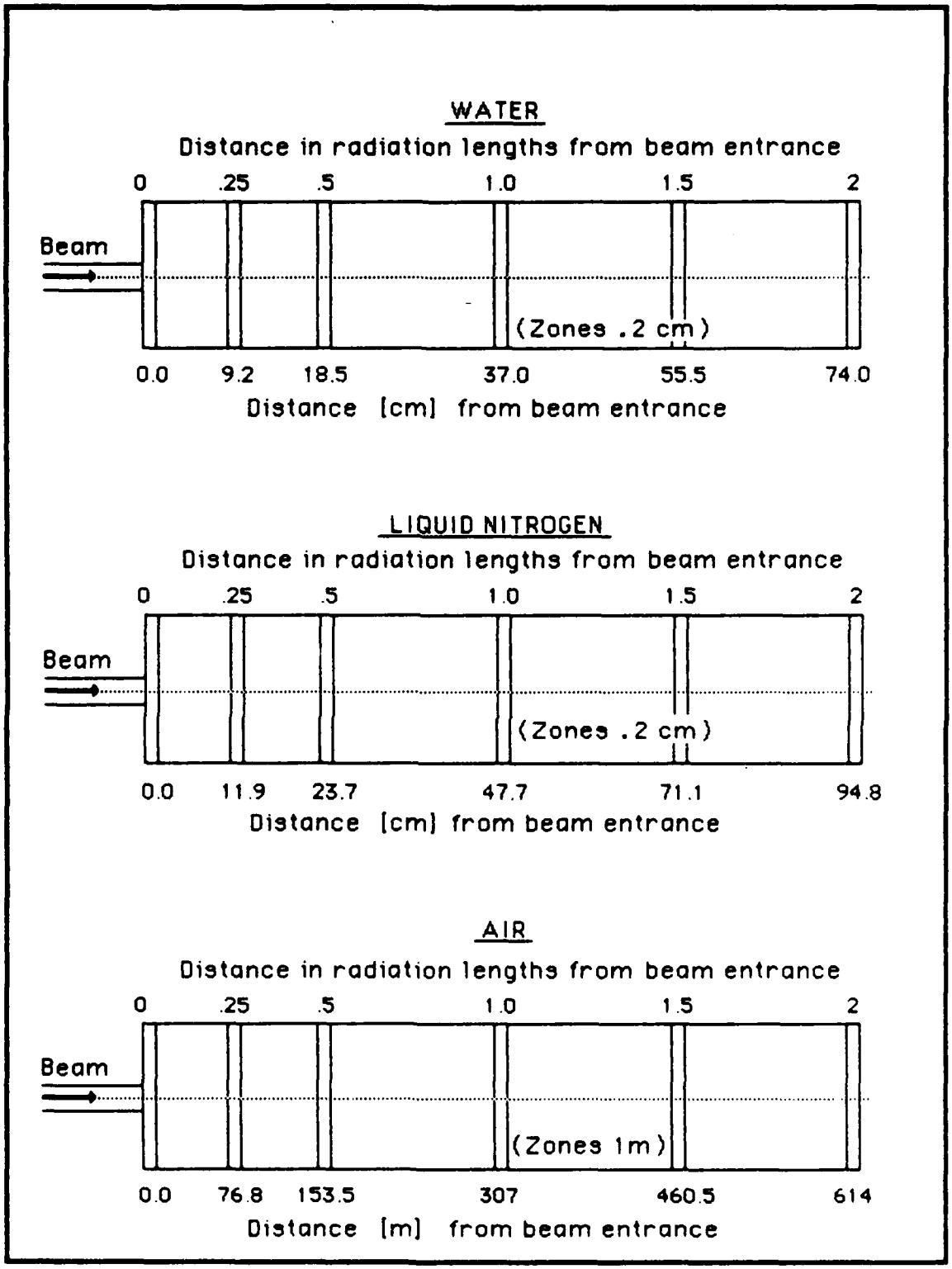

Figure 4.1 CYLTRAN Geometry

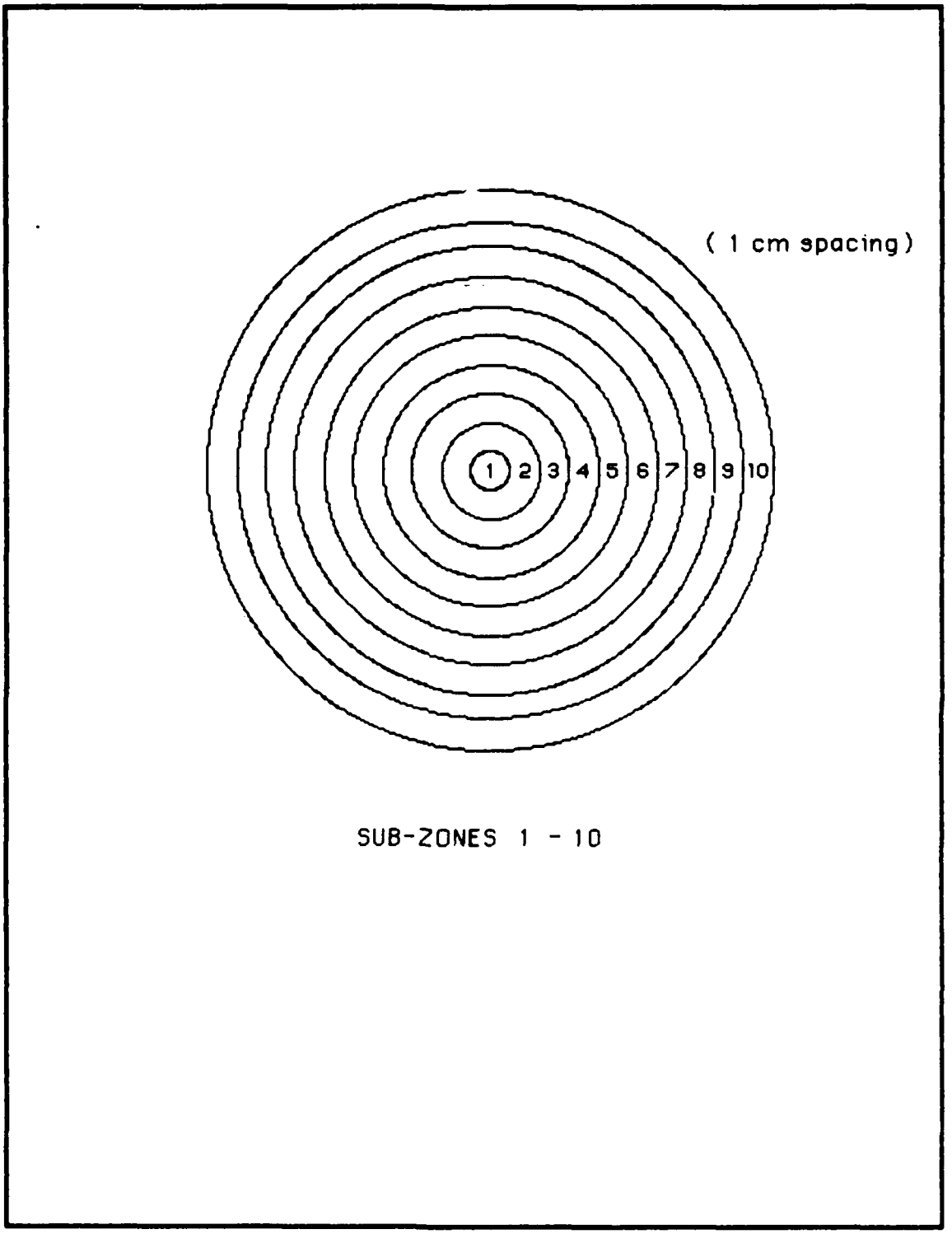

Figure 4.2 CYLTRAN Sub-Zones for Water

sub-zone. The simulation was run in ten batches of 2000 particles each with statistical values being computed after each batch. Each value of energy deposition is followed by a two digit number that represents the one-sigma uncertainty that results from the Monte-Carlo routine, with low numbers indicating narrow bounds of uncertainty.

At distances well within the targets the statistical uncertainties grew due to the fewer number of particles with sufficient energy to penetrate to these zones. Decreasing the statistical uncertainties can be accomplished by increasing the number of incident particles, however the relationship between numbers of particles and uncertainties is not linear. Each simulation run of 20,000 particles used about twenty minutes of Cental Processor Unit time on the Cray computers at Los Alamos. Increasing the number of particles to 45,000 would have reduced the uncertainty by only about ten percent but would have increased the CPU time by a factor of two.

Since the primary purpose of the computer simulations was to provide immediate comparisons with the experimental results, no attempt was made to fully optimize the numerical calculations. When reasonable, all default values within the codes were used. This led to track segments that were larger than ideal at the higher energies near the entrance, while the track segments were too small for the less energetic particles well within the target. It is believed that for the comparisons desired, the integration of the large number of incident particles is adequate to provide meaningful results inspite of the less than optimum analysis.

Appendix A contains a description of CYLTRAN and sample input data streams for the generation of the cross-sections (Table A1) and the execution of the program (Table A2). The CYLTRAN output of the energy deposition normalized to one incident particle for 100 MeV electrons in water, air, liquid nitrogen, and 20 MeV electrons in water is contained in Tables A3-A25.

B. RESULTS

The total energy deposited in each sub-zone was converted to Rads/Coulomb for comparison with the experimental results. The normalized dose due to 100 MeV electrons for each sub-zone in water is contained in Table B1 of Appendix B. The resultant graphs of the off-axis dose for each penetration depth are given in Figures B1 through B7. Appendix's C, D, and E contain similar results for the 100 MeV electrons in air and liquid nitrogen, and the 20 MeV electrons in water.

The curves drawn on the graphs are not intended to necessarily be the mathematically best fit approximation for the data although in most cases the difference is minimal. Instead, the curves were generated using the exponential and polynomial equations of Appendix F, in order to construct the three dimensional half-axis surface plots of Figures 4.3 through 4.6 and the contour, or isodose, curves of Figures 4.7 through 4.10. The vertical error bars result from the indicated one-sigma errors generated by CYLTRAN. The plots have been smoothed only in the off-axis direction.

Smoothing parallel to the beam axis would have involved a good deal of numerical experimentation and iteration and would not have added any meaingful interpretation to the results. In spite of the modest smoothing, the relatively small number of data points resulted in the rough surface plots of Figures 4.7 through 4.10 and it is felt that no additional smoothing could be justified based on these few points.

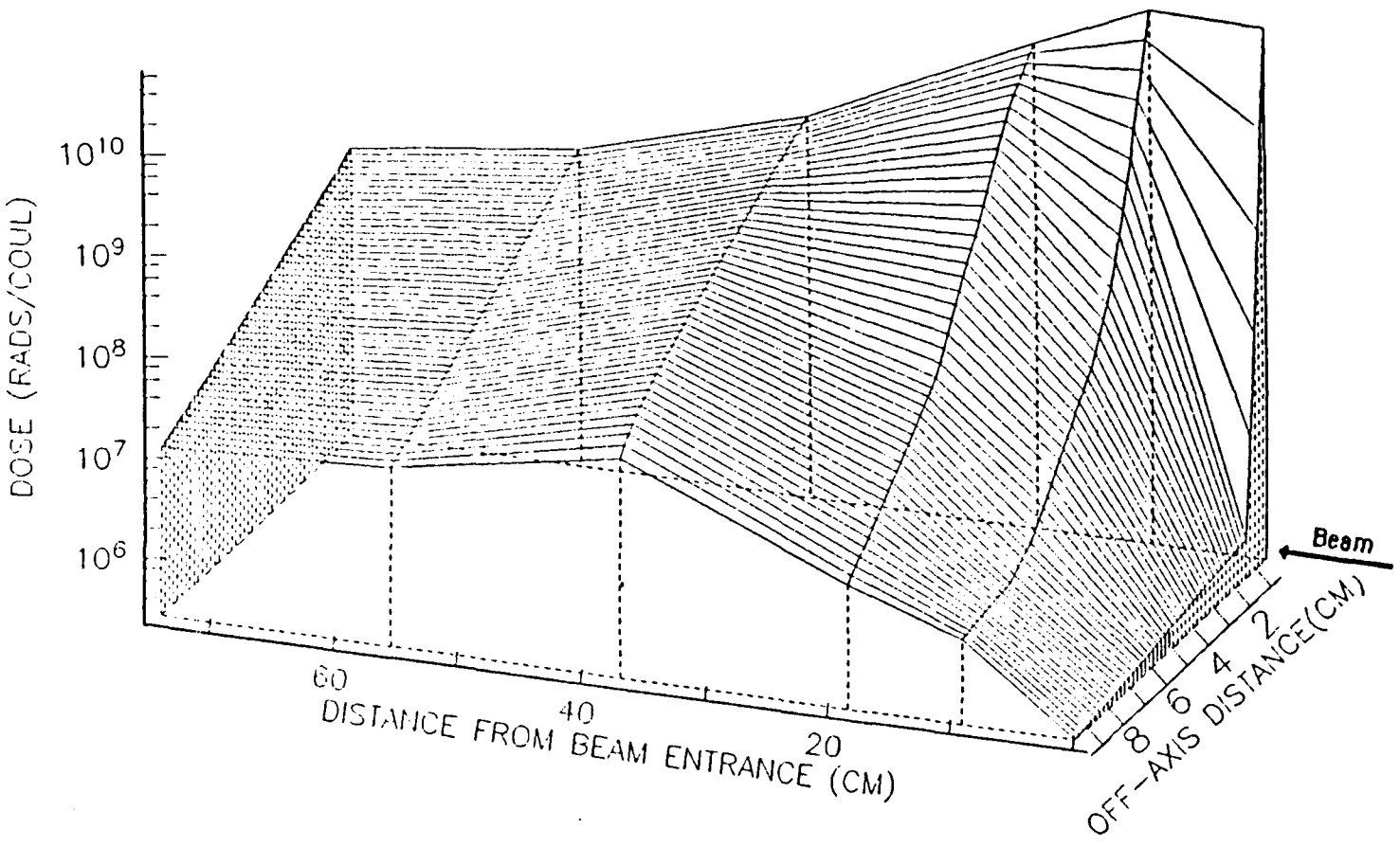

Figure 4.3 : Surface Plot of Dose Due to 100 MeV Electrons in Water

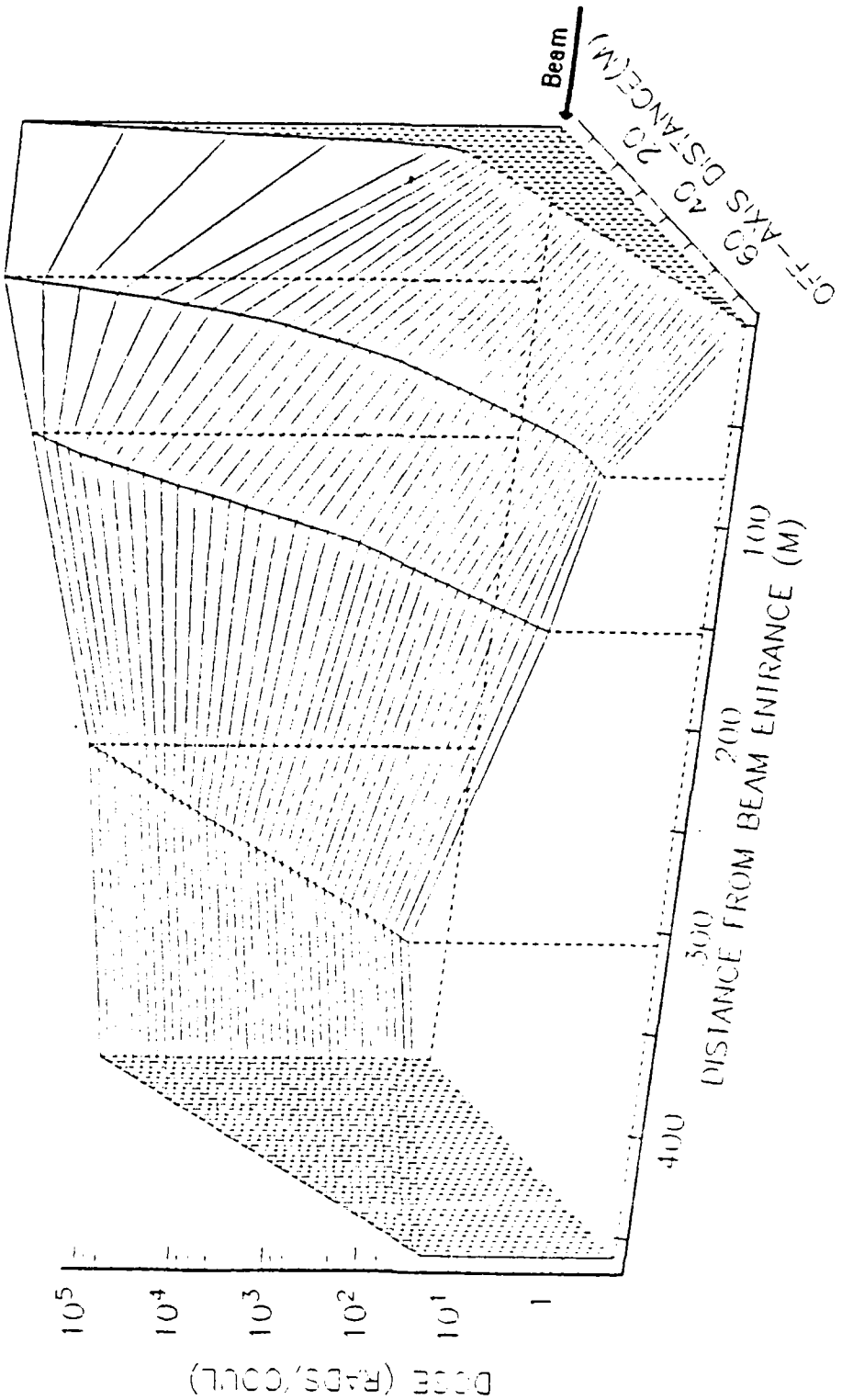

Figure 4.4 : Surface Plot of Dose Due to 100 MeV Electrons in Air

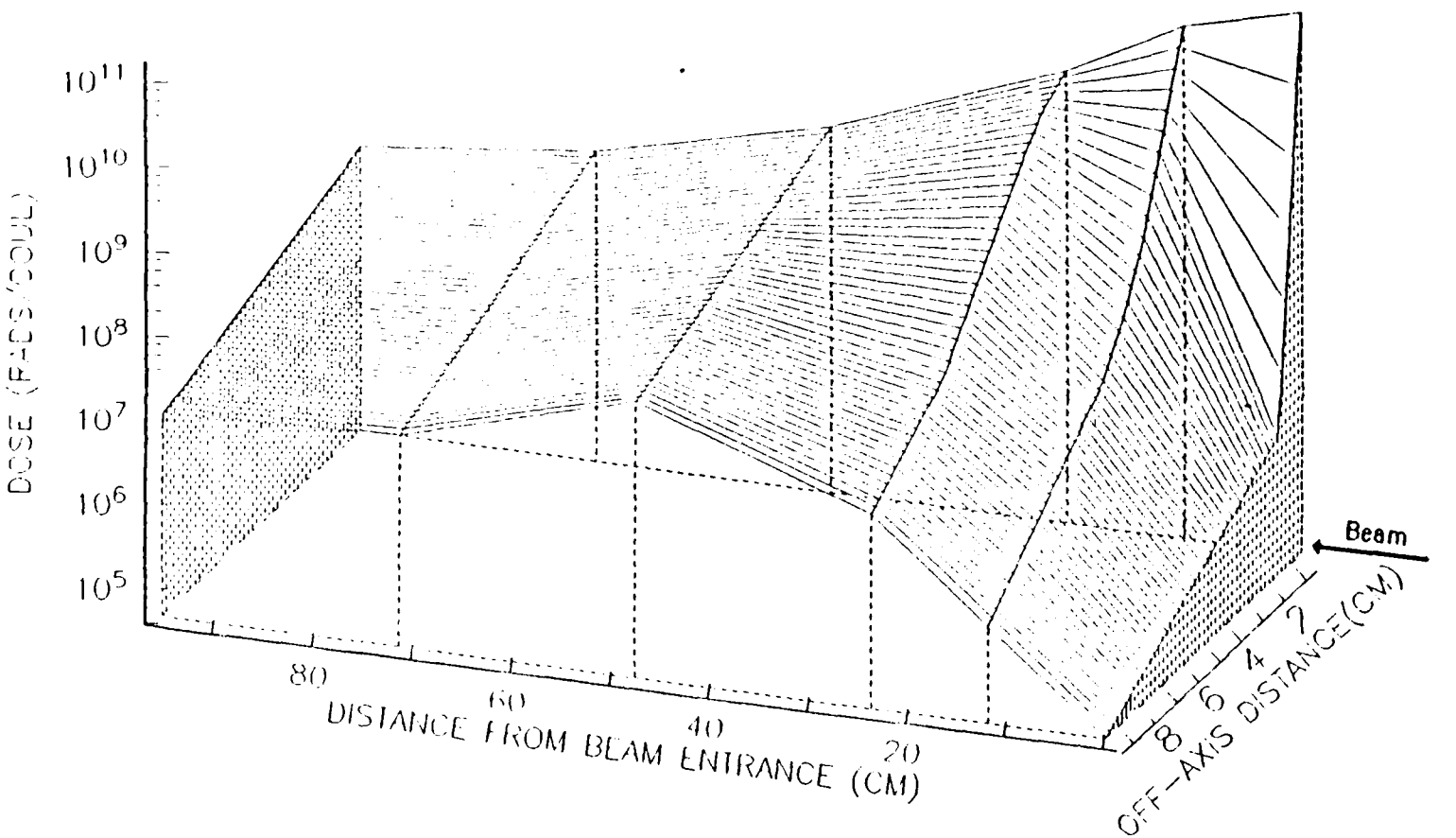

Figure 4.5 : Surface Plot of Dose Due to 100 MeV Electrons in LN_2

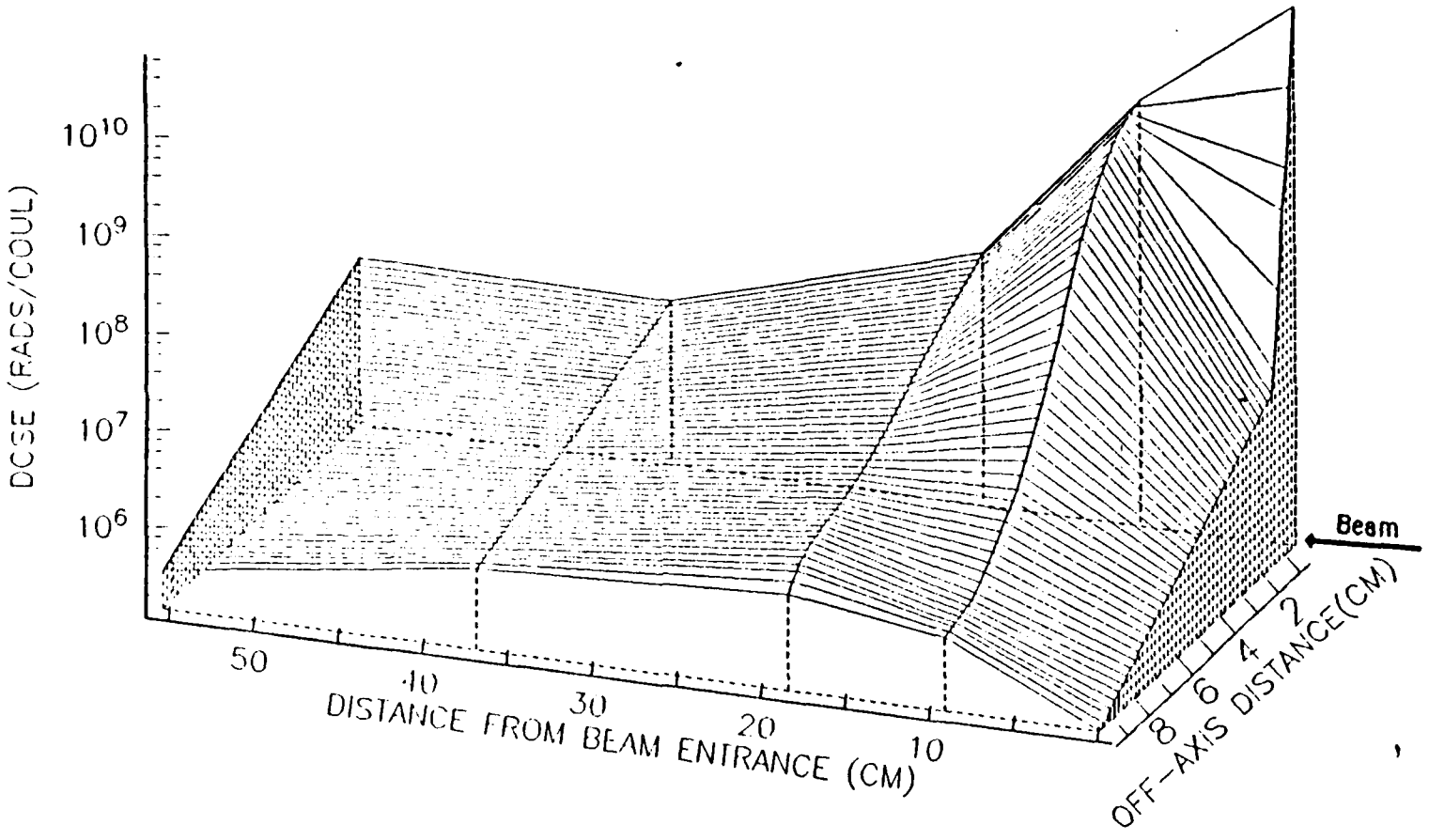

Figure 4.6 : Surface Plot of Dose Due to 20 MeV Electrons in Water

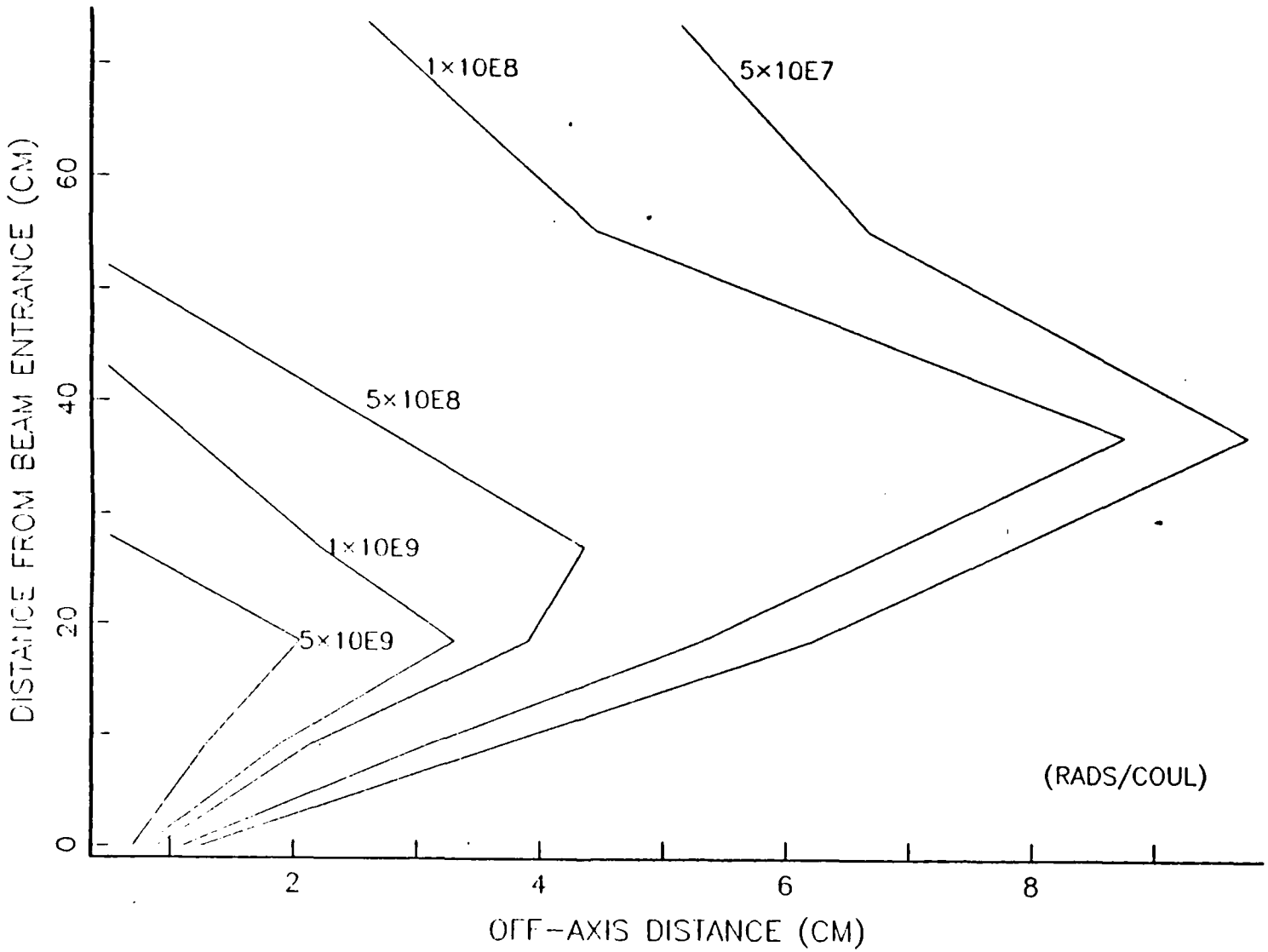

Figure 4.7 : Contour Plot of Dose Due to 100 MeV Electrons in Water

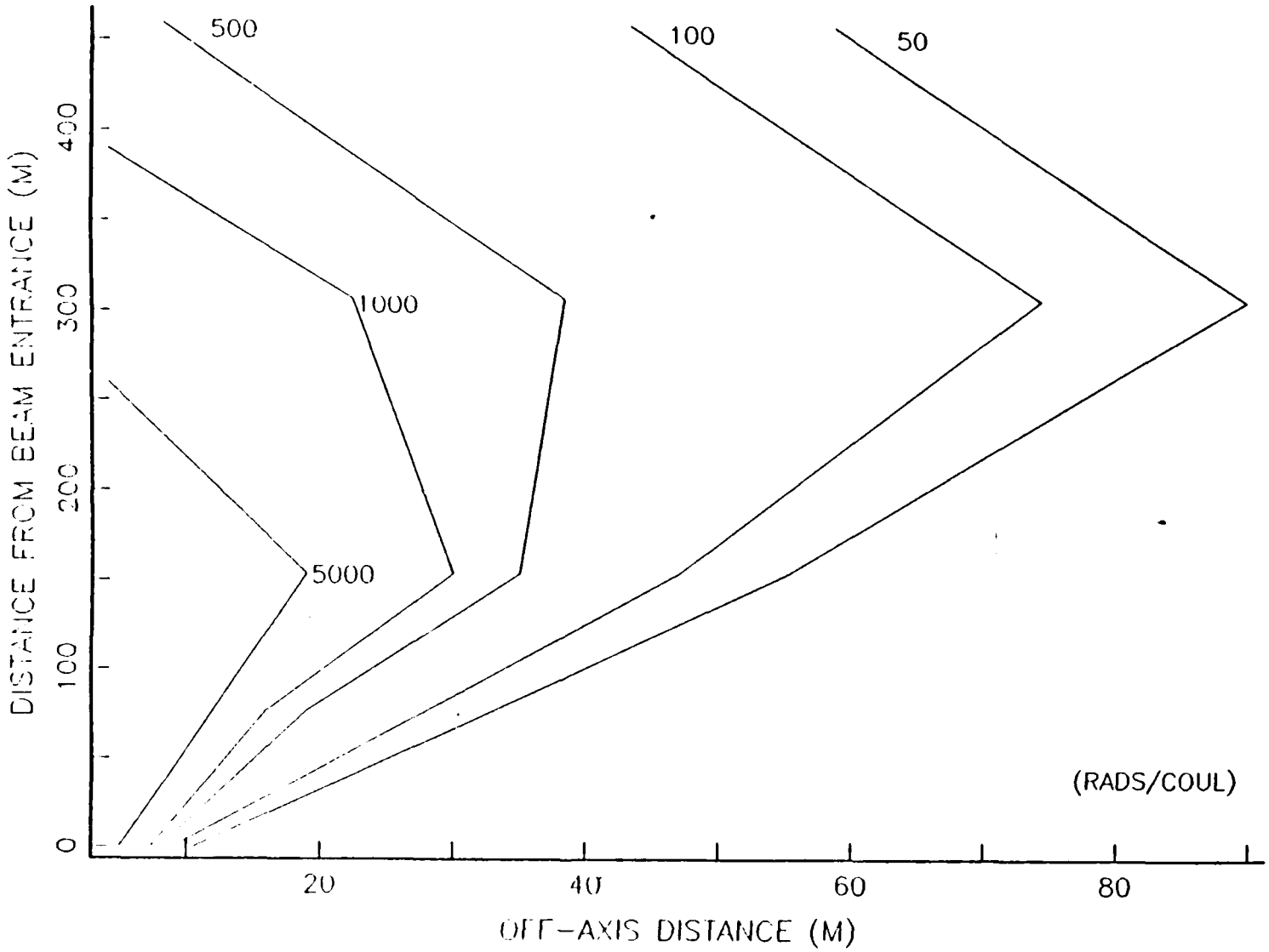

Figure 4.8 : Contour Plot of Dose Due to 100 MeV Electrons in Air

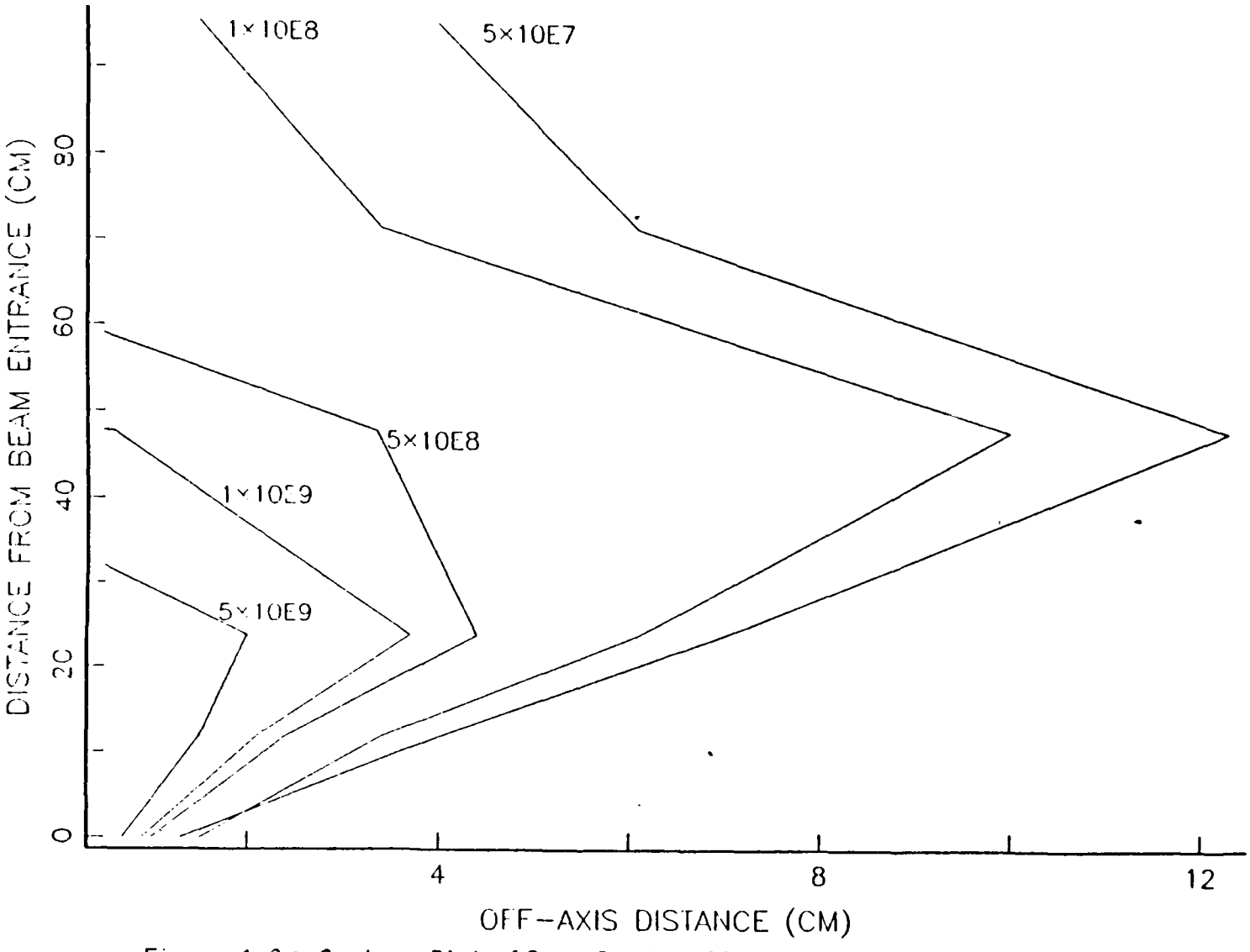

Figure 4.9 : Contour Plot of Dose Due to 100 MeV Electrons in LN_2

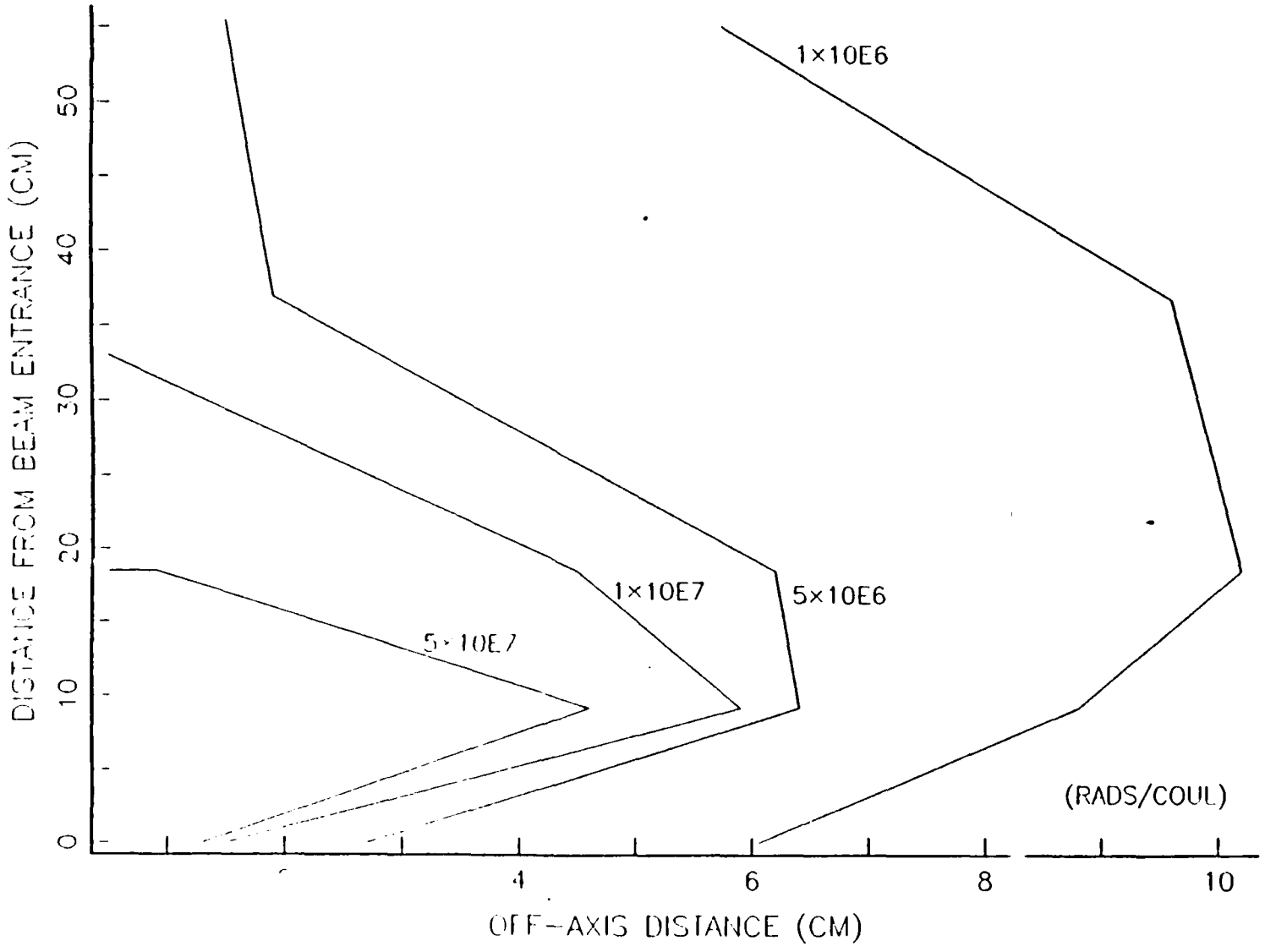

Figure 4.10 : Contour Plot of Dose Due to 20 MeV Electrons in Water

V. EXPERIMENTS

A. DISCUSSION

All experimental measurements were conducted at the Naval Postgraduate School Accelerator Lab using the 100 MeV linear electron accelerator. A rectangular container (100 x 46 x 38 cm^3) of 4 mm polyethylene plastic was used to contain the experimental matrix. This allowed for a usable test area of 10 cm on either side of the central axis with a minimum of 9 cm of water beyond this to provide a uniform scattering medium without side effects. The length of the tank allowed measurements out to two radiation lengths in water.

Calcium fluoride thermoluminescent dosimeters (TLDs) were provided by Naval Surface Weapons Center. The TLDs were wrapped in a single layer of 1 mil aluminum and were enclosed in a thin plastic film to prevent moisture from contaminating the crystals. The TLDs were mounted to soft wood stretchers at intervals indicated in Figure 5.1 and Figure 5.2. Wood contains hydrogen and carbon and is similar to water in atomic properties. Pairs of TLDs (one CaF2 and one LiF) were mounted in symmetric positions. The TLDs were generally located at one centimeter spacing, but alternating between sides of the central axis, i.e. 1,3,5 cm right and 2,4,6 cm left . This served to reduce interference between adjacent dosimeters and was intended to provide a means of interpreting the results in case of a slightly off-axis beam or drifting of the stretcher from centerline. TLD positions were known

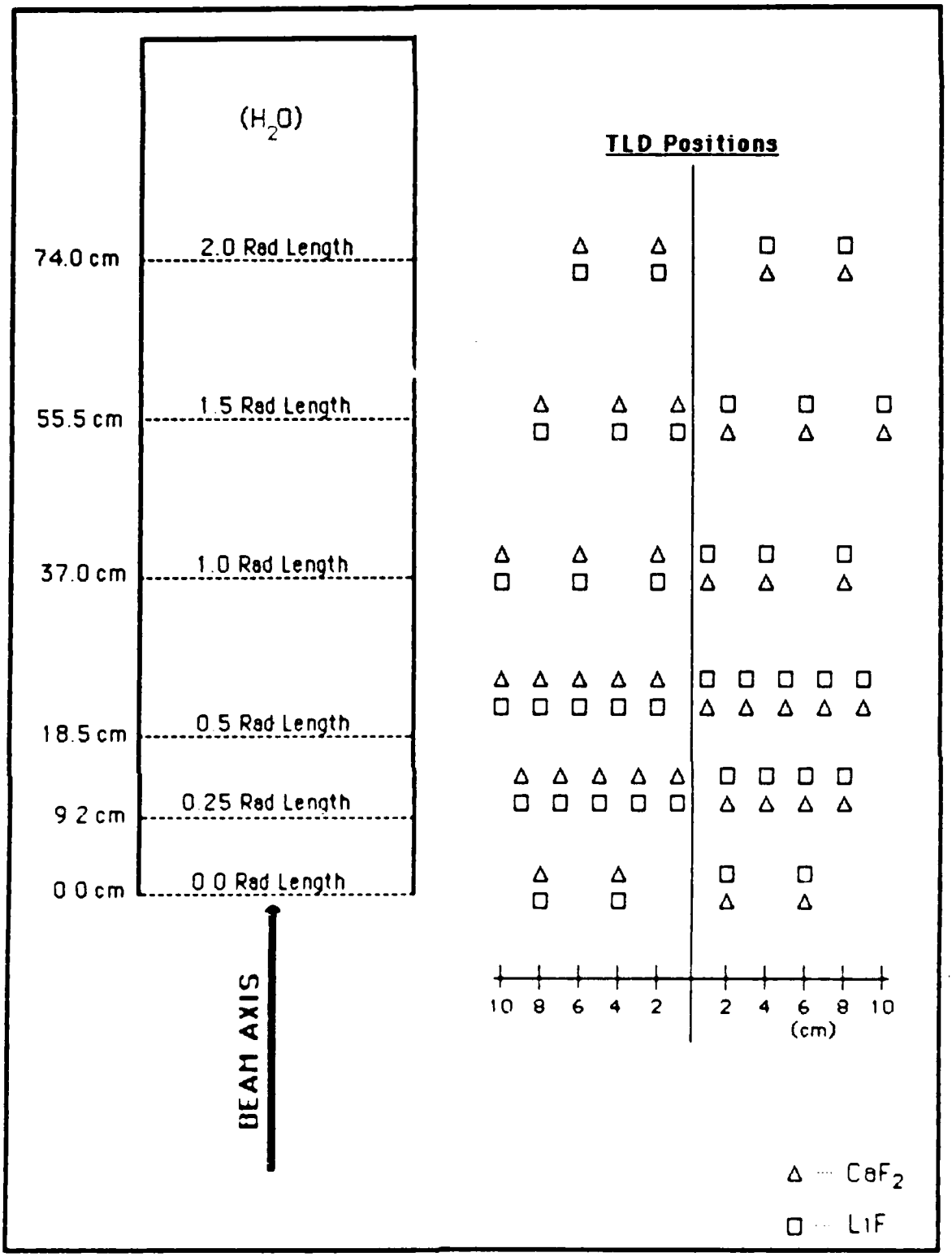

Figure 5.1 TLD Positioning Within Test Tank for 100 Mev Run

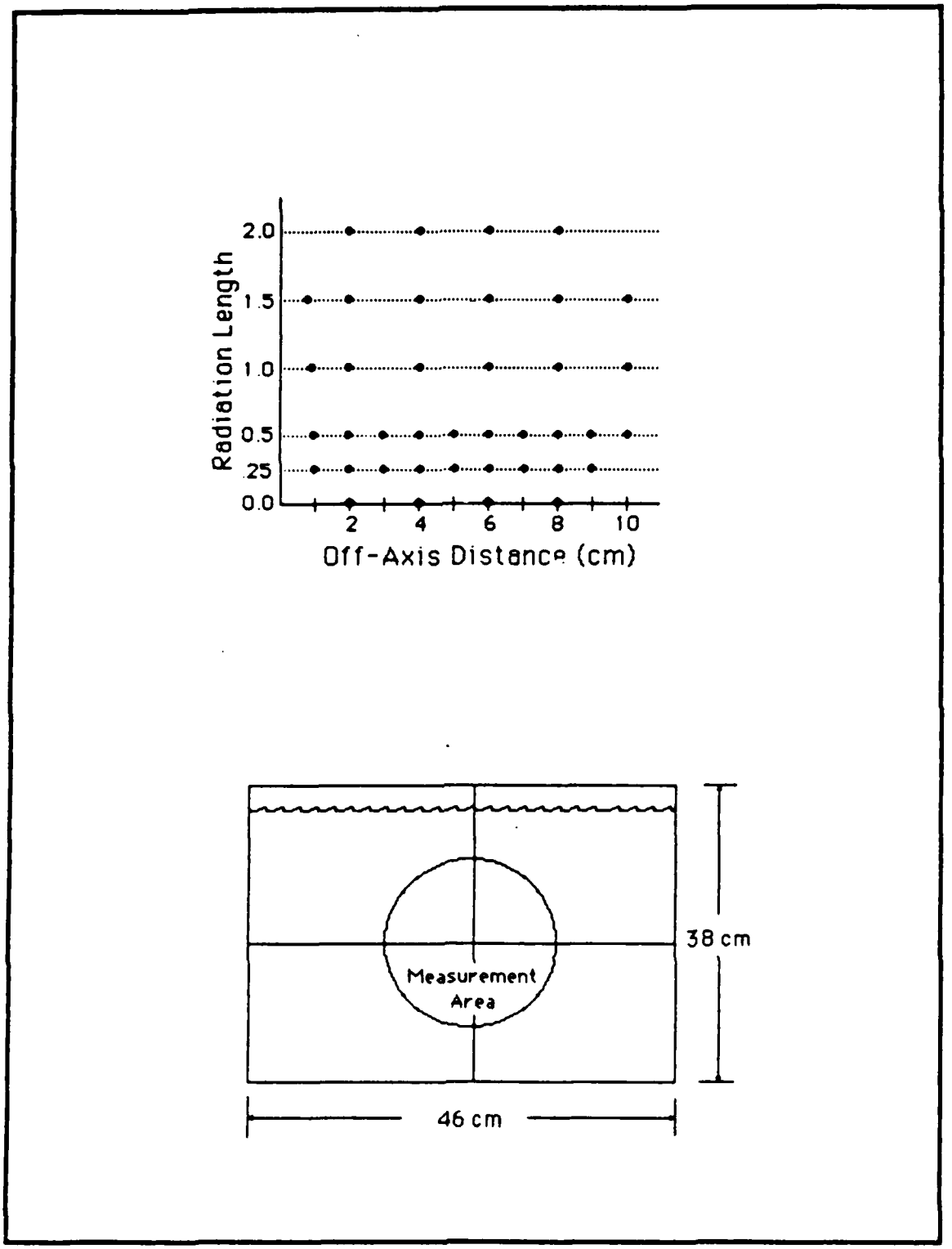

Figure 5.2 Test Tank Dimensions and TLD Positioning

to within 0.5 cm on the stretcher while the stretcher position was known to within one centimeter.

Pulsed beams of 100 MeV and 20 MeV electrons were normally incident on the target at a repetition rate of 60 Hz. The beam passed through a vacuum test chamber which was sealed with a five mil aluminum window and then through 25 cm of air prior to entering the test tank.

The total charge delivered was monitored by a Secondary Emission Monitor (SEM). A vibrating reed electrometer coupled with a one micro-farad capacitor was used to determine the charge delivered to the SEM. With an SEM efficiency of .028, the total charge delivered to the matrix could be determined. Due to uncertainties in this efficiency factor, it is estimated the total charge delivered can only be determined to within five percent. Electron energy was controlled by the use of a magnetic deflection system and is considered to be sufficiently stable that any fluctuations would not be noticable within the limits of this experiment.

Phosphor screens were placed at both ends of the tank on the central axis to align the beam. The TLDs were removed and the beam was passed through the empty tank. By remotely observing the phosphor screens, an attempt was made to make the beam as parallel as possible while within the tank. The beam diameter entering the tank averaged 0.5 cm as indicated by the phosphor screens, while beam divergence caused the exiting diameter to approach 2.0 cm.

Once alignment and focussing were completed the phosphor screens were removed, TLDs installed, and the tank filled with water. To prevent saturation of the TLDs close to the beam axis and yet still provide a meaningful dose on the distant TLDs, three irradiation segments were conducted for each run. Based on estimated dose calculations, selected TLDs were removed after each segment to prevent overexposure. Normalization of the data to Rads per Coulomb delivered will account for the different exposure times.

B. RESULTS

The TLDs were mailed to the Naval Surface Weapons Center, White Oak, Maryland for reading. The results of the TLD readings were reported in Rads and using the recorded charge delivered to each TLD, the readings were normalized to Rads per Coulomb. For the 100 MeV experiment a faulty set of calibration curves prevented proper reading of the LiF dosimeters and these results were not returned.

The normalized dose from the CaF_2 dosimeters is contained in Table G1 of Appendix G. Figures 5.3 through 5.8 are plots of the normalized off-axis dose at each length within the water. The vertical error bars are drawn based on a ten percent error in the normalized dose . The horizontal error bars are the result of the uncertainty in the TLD position on the stretcher (±0.5 cm), the strecher location with respect to the central axis of the test tank(± 1.0 cm), and the skewness of the beam with respect the center line of

the tank (±2.0 degrees). The curves drawn on the figures are the semi-smoothed results from the CYLTRAN calculations and are included for comparison.

The objective of the experiment was to provide quick but meaningful results for comparison with the calculations. As a result, the experimental apparatus was kept simple and straight forward. As a consequence, the cumulative errors at the extreme distances result in horizontal error bars that encompass a large portion of the horizontal axis. However, by placing sequential TLDs on alternate sides of the central axis, some simple yet justified and reasonable corrections can be applied to the data in order to present the true picture.

Figure 5.3 shows how the true off-axis position of the TLDs varies with the degree of skewness in the beam. Since alternate alternate TLDs were placed on alternate sides of the matrix x-axis, this skewness results in a displacement of the true off-axis distance measured from the centerline of the beam.

Table G2 of Appendix G contains a set of corrected positions for the TLDs based on varying degrees of skewness for the beam. A misalignment of only two degrees from parallel results in an error of the off-axis position of 2.58 cm at the furthest distance for which data was recorded. Figures 5.9 through 5.12 present the results if a uniform correction of 1.7 degrees is applied to all the data points. At the inner distances the uncertainty in the position of the stretcher is greater than the correction of the beam skewness

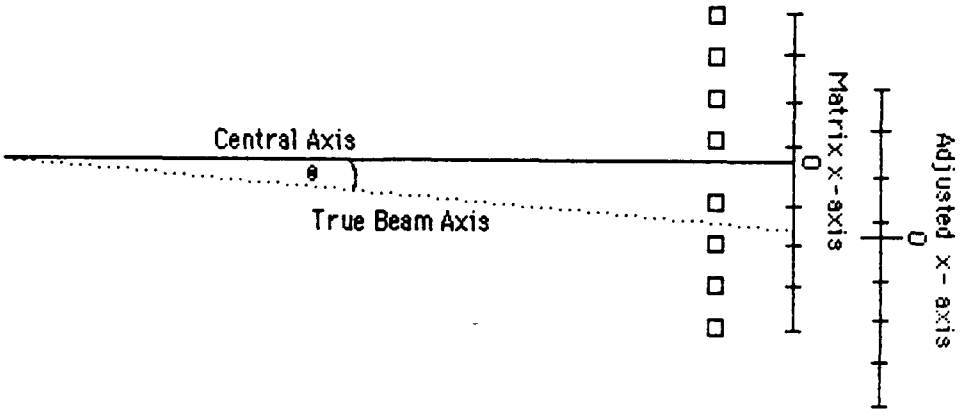

Figure 5.3: Effect of Beam Skewness on Off-axis Zero Point

and the effect of applying the skew correction is not as visable. In all cases, the data generally alternates between high and low points of the calculated curves, in relation to being on the right side or the left side of the central axis.

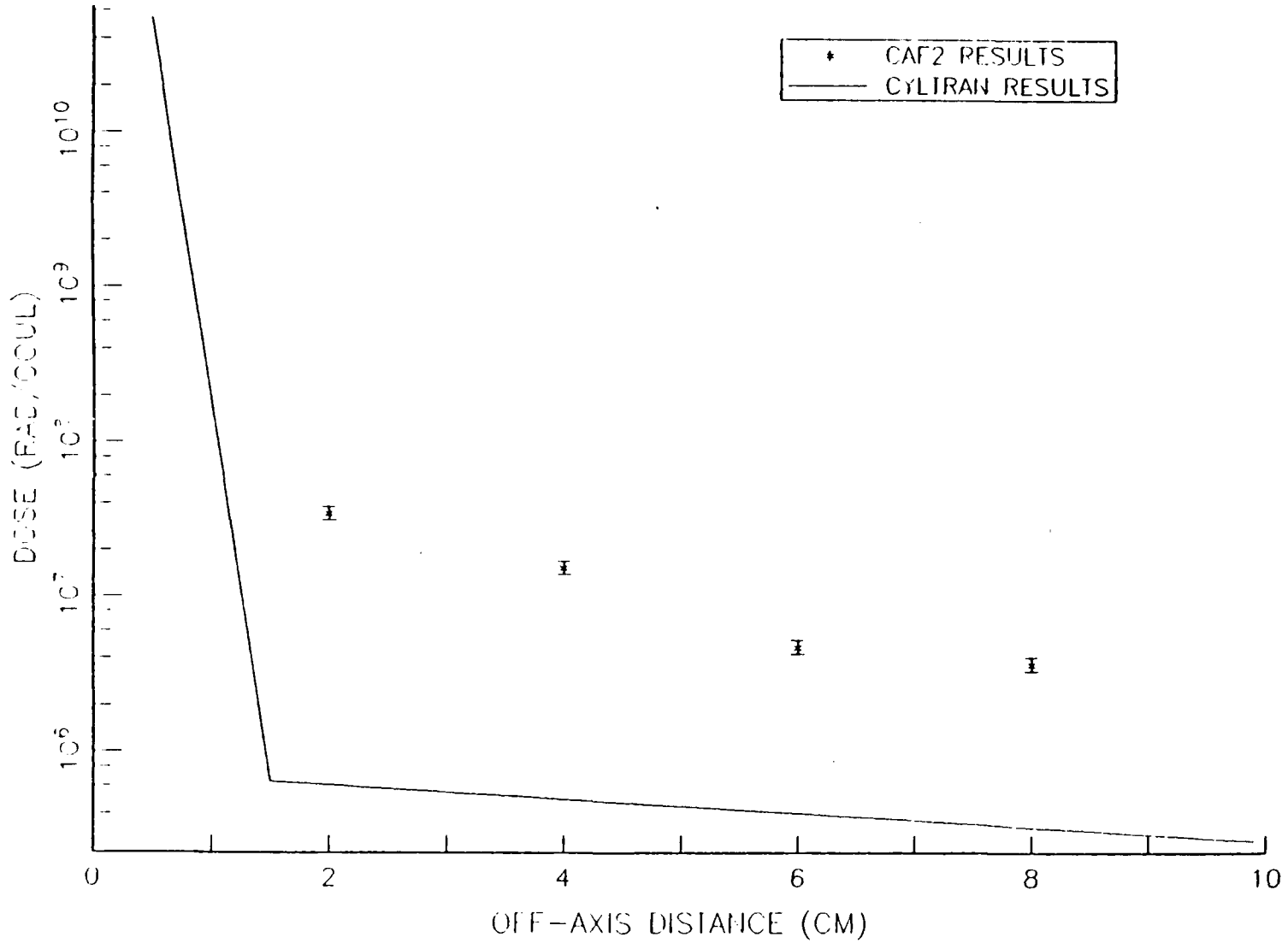

Figure 5.3: Experimental Results of 100 MeV Electrons in Water-0.0 cm

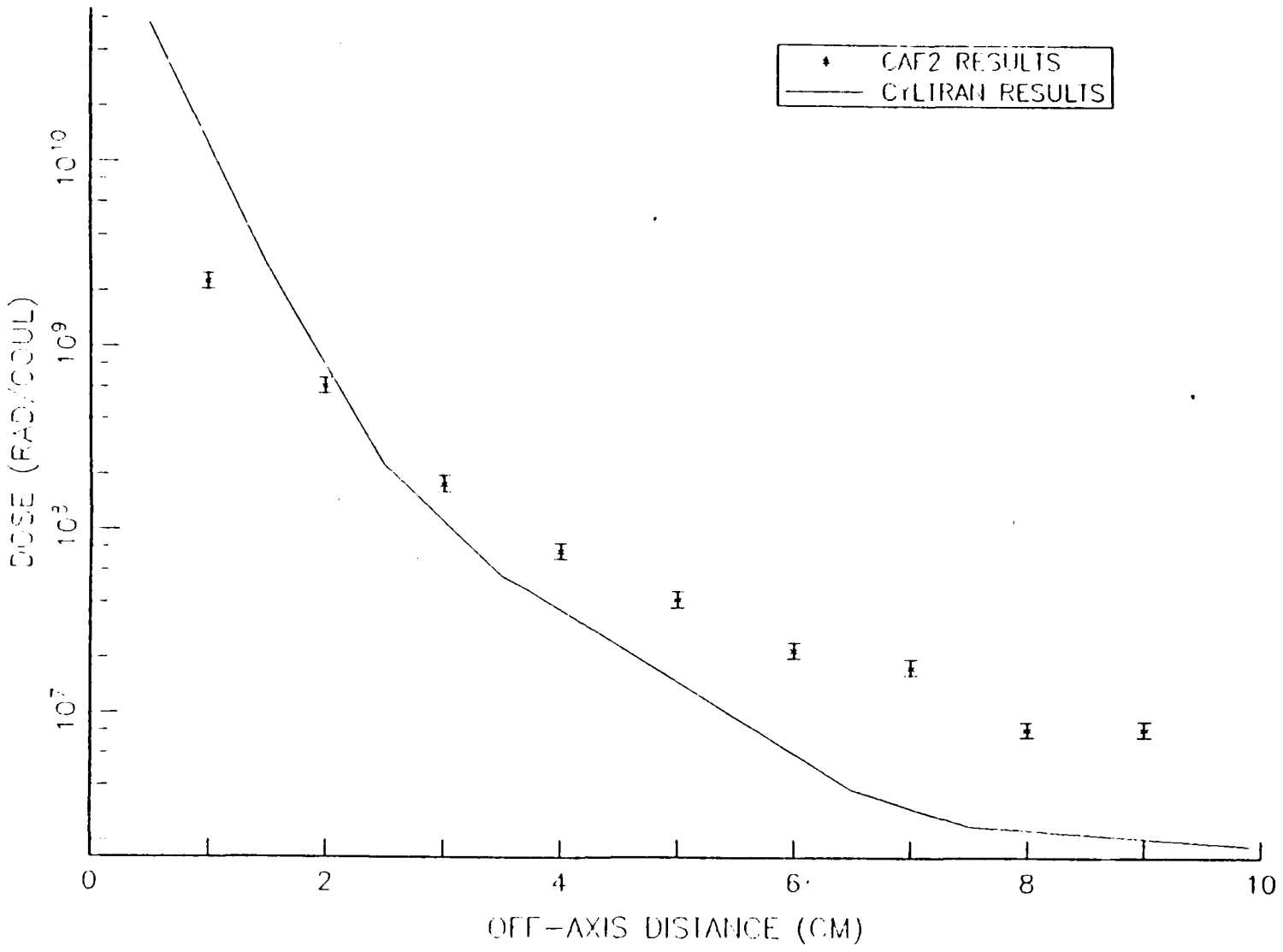

Figure 5.4 : Experimental Results of 100 MeV Electrons in Water-9.2 cm

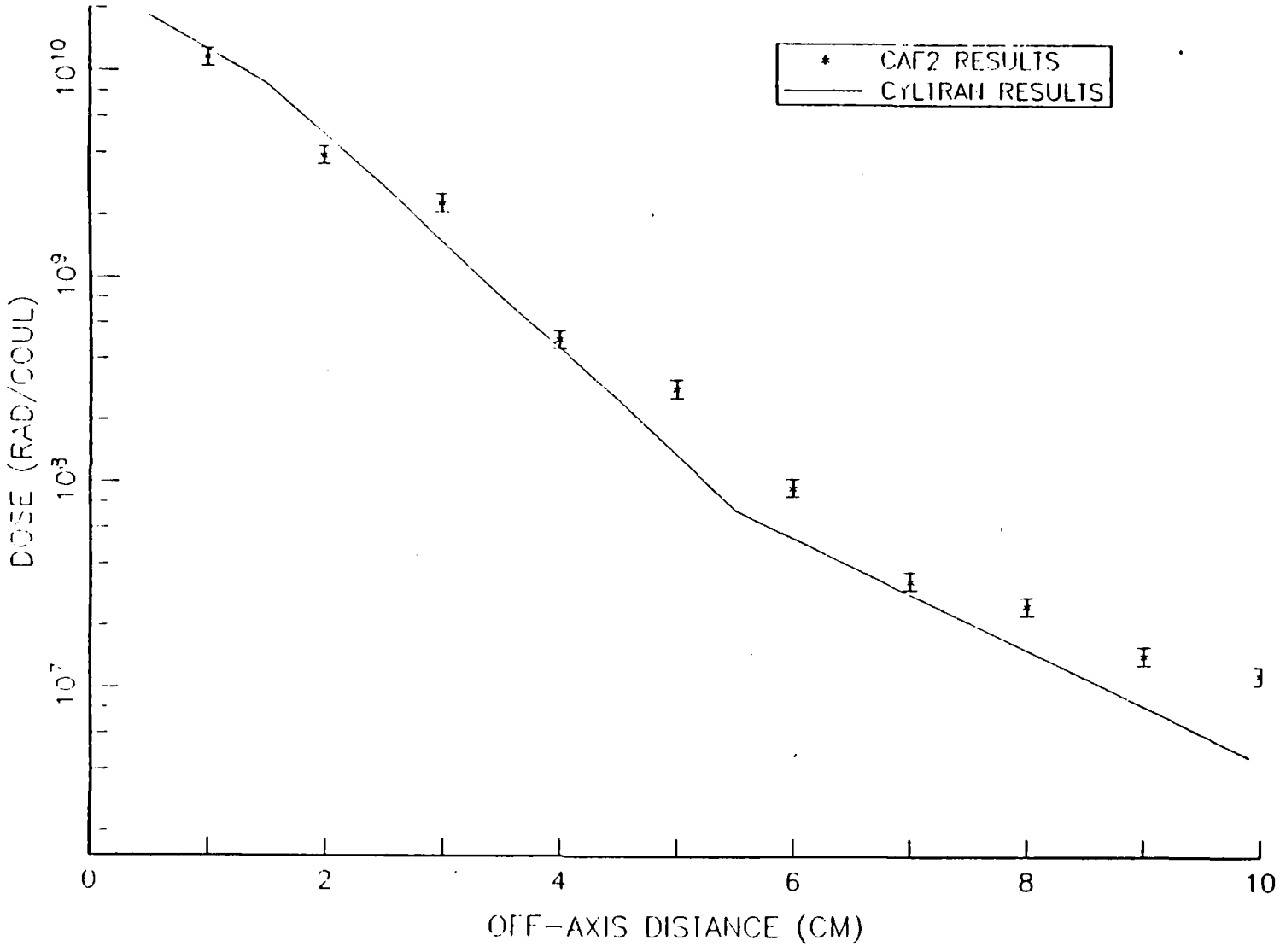

Figure 5.5 : Experimental Results of 100 MeV Electrons in Water-18.5 cm

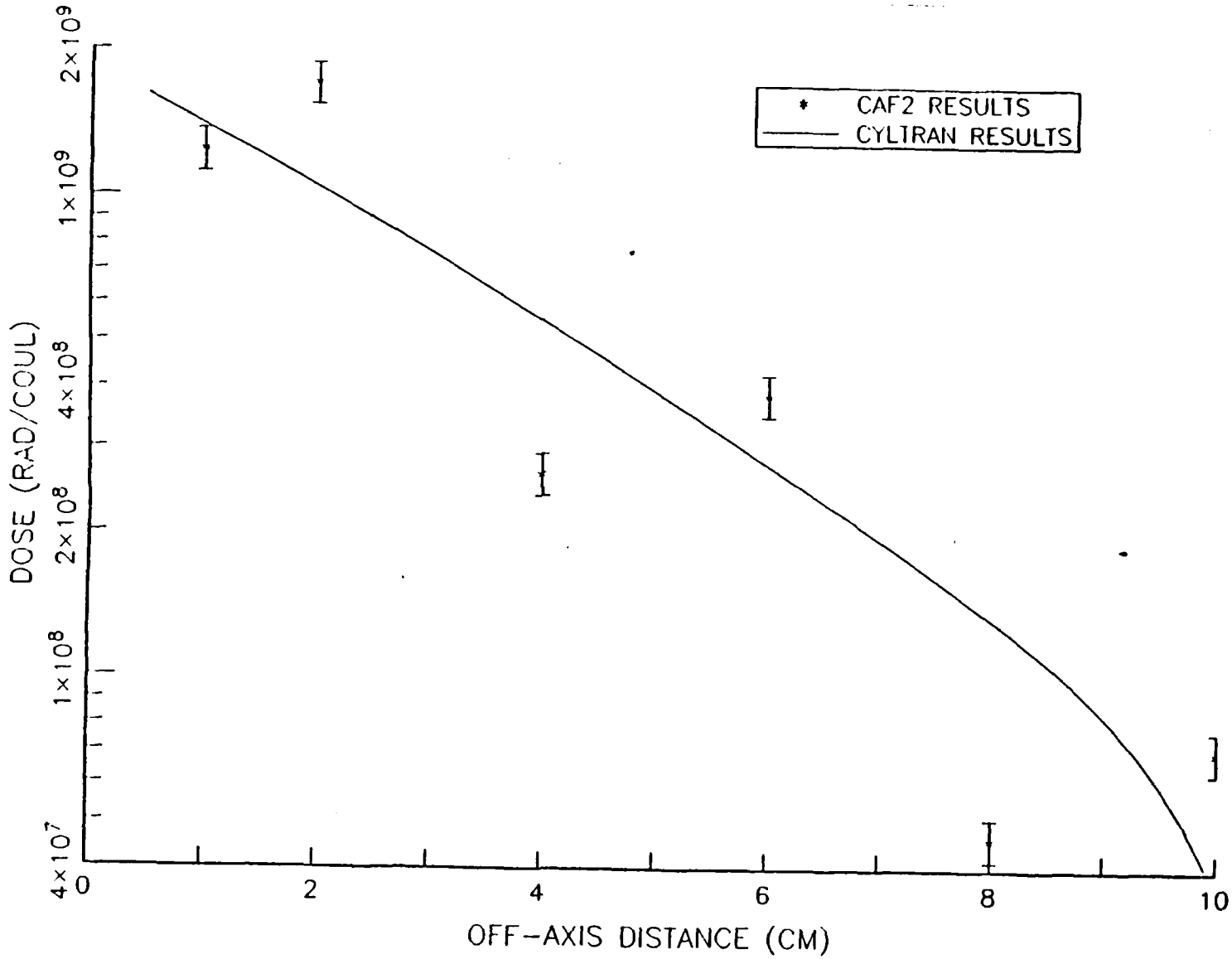

Figure 5.6 : Experimental Results of 100 MeV Electrons in Water-37.0 cm

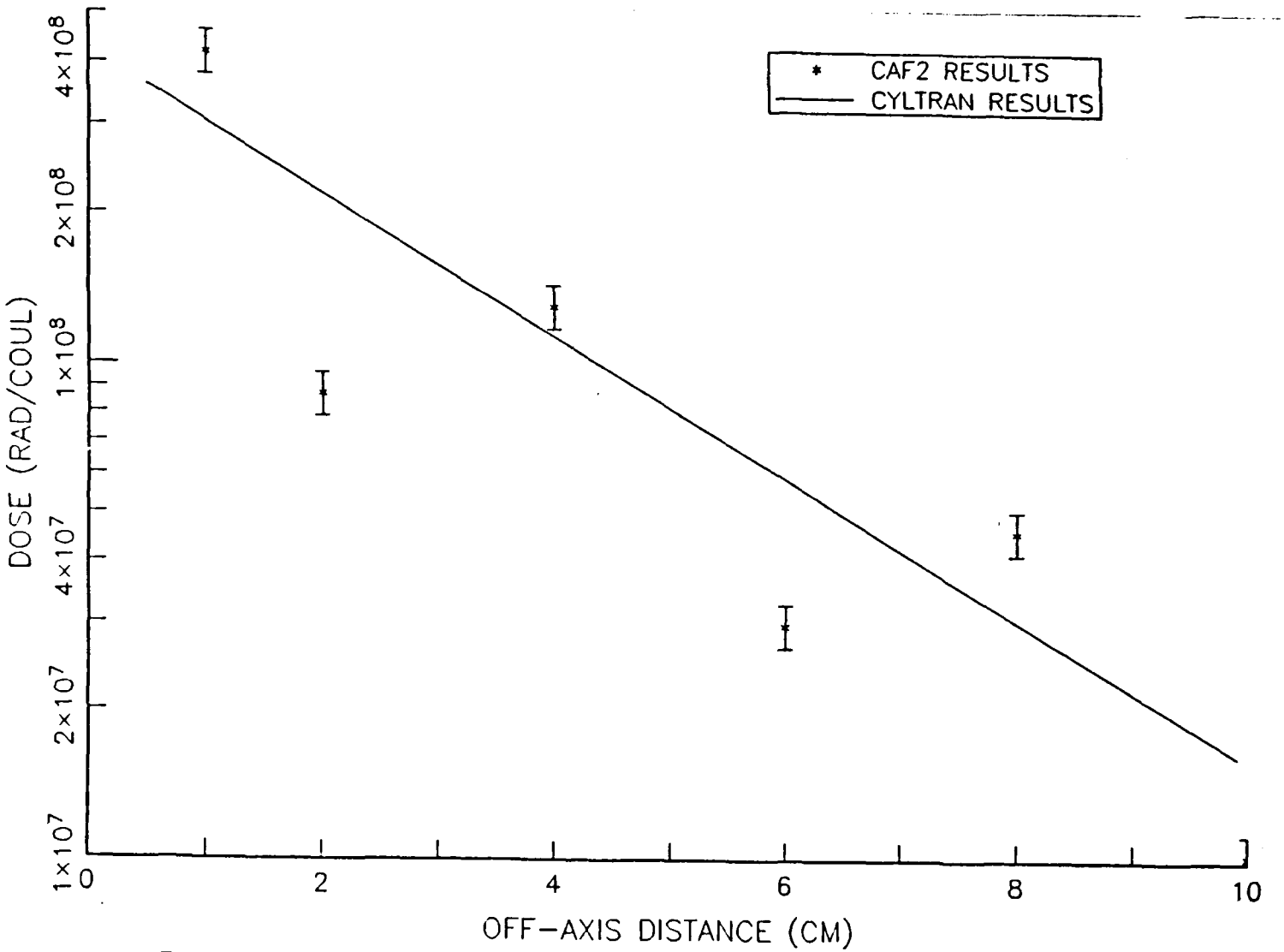

Figure 5.7 : Experimental Results of 100 MeV Electrons in Water-55.5 cm

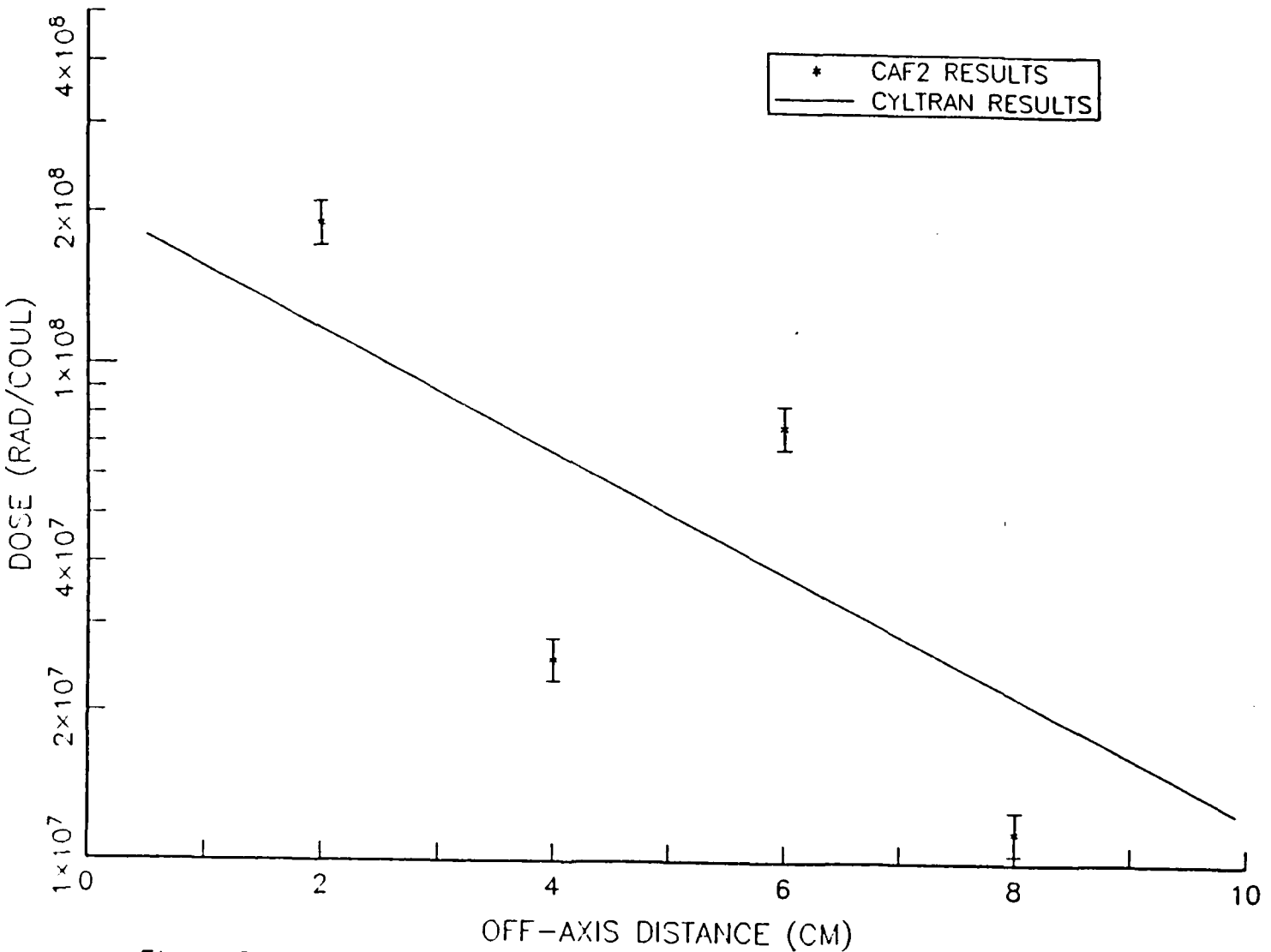

Figure 5.8 : Experimental Results of 100 MeV Electrons in Water-74.0 cm

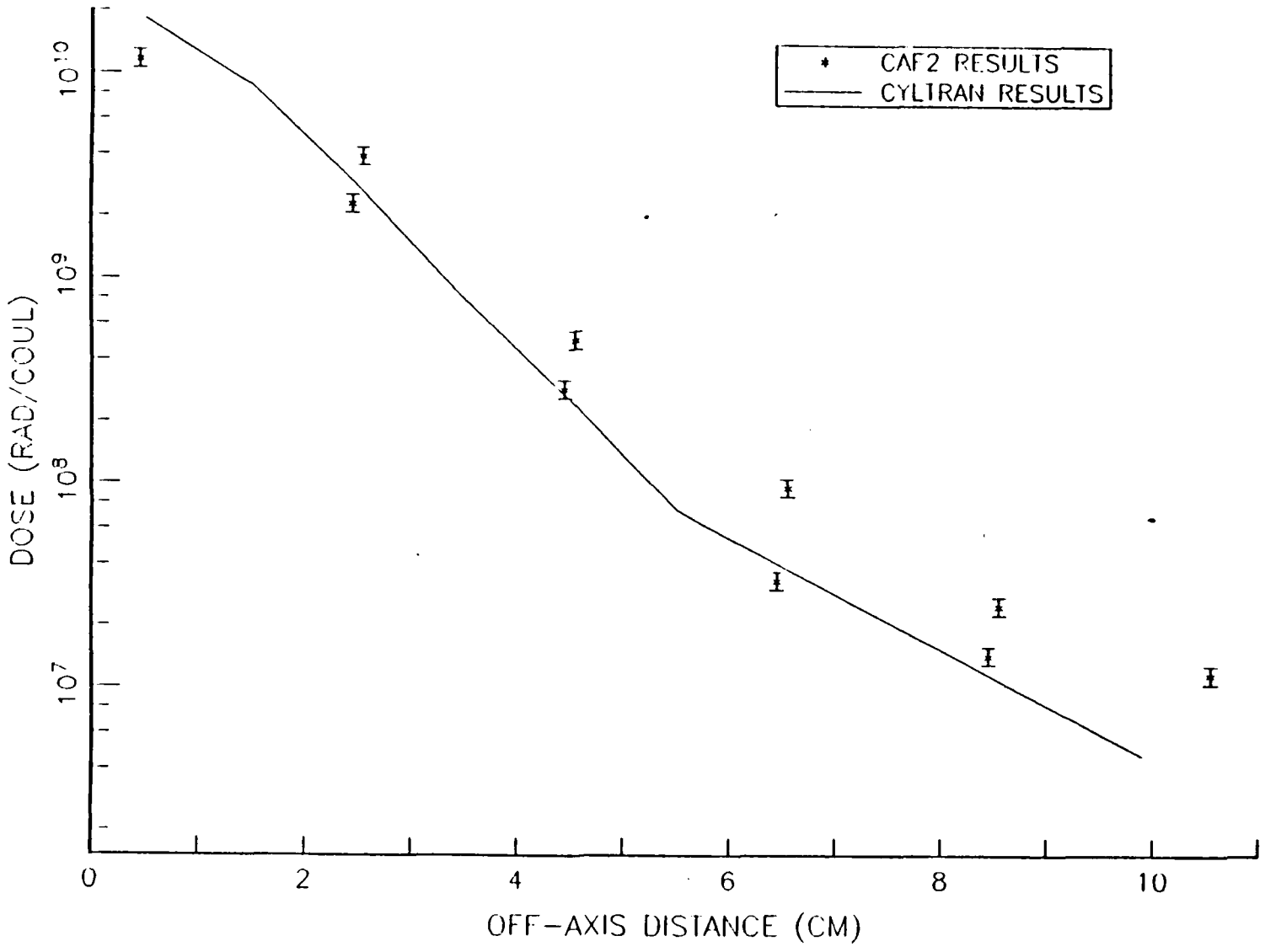

Figure 5.9: Experimental Results of 100 MeV Electrons in Water-18.5 cm (1.7°)

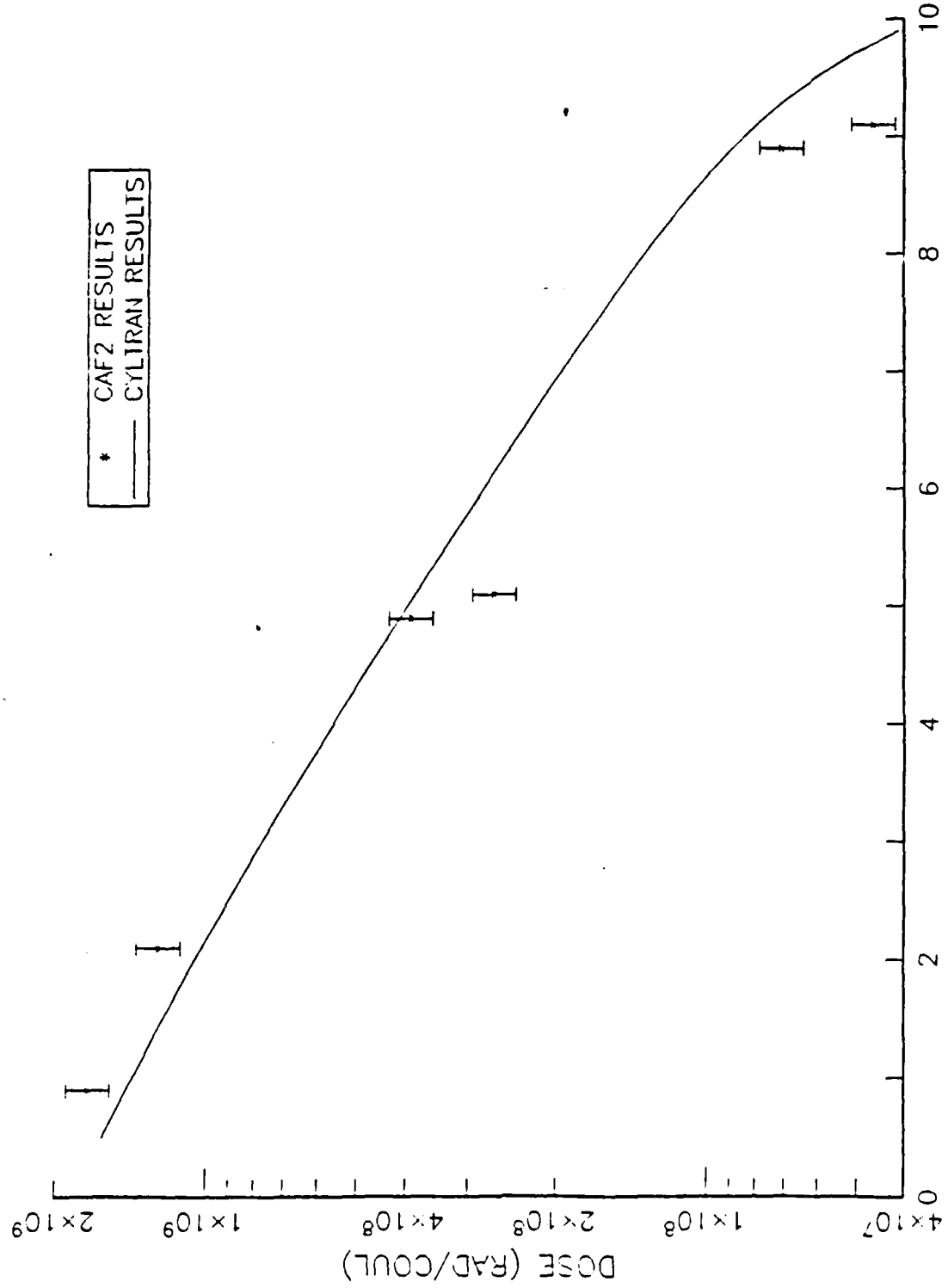

Figure 5.10 : Experimental Results of 100 MeV Electrons in Water-37.0 cm (1.7°)

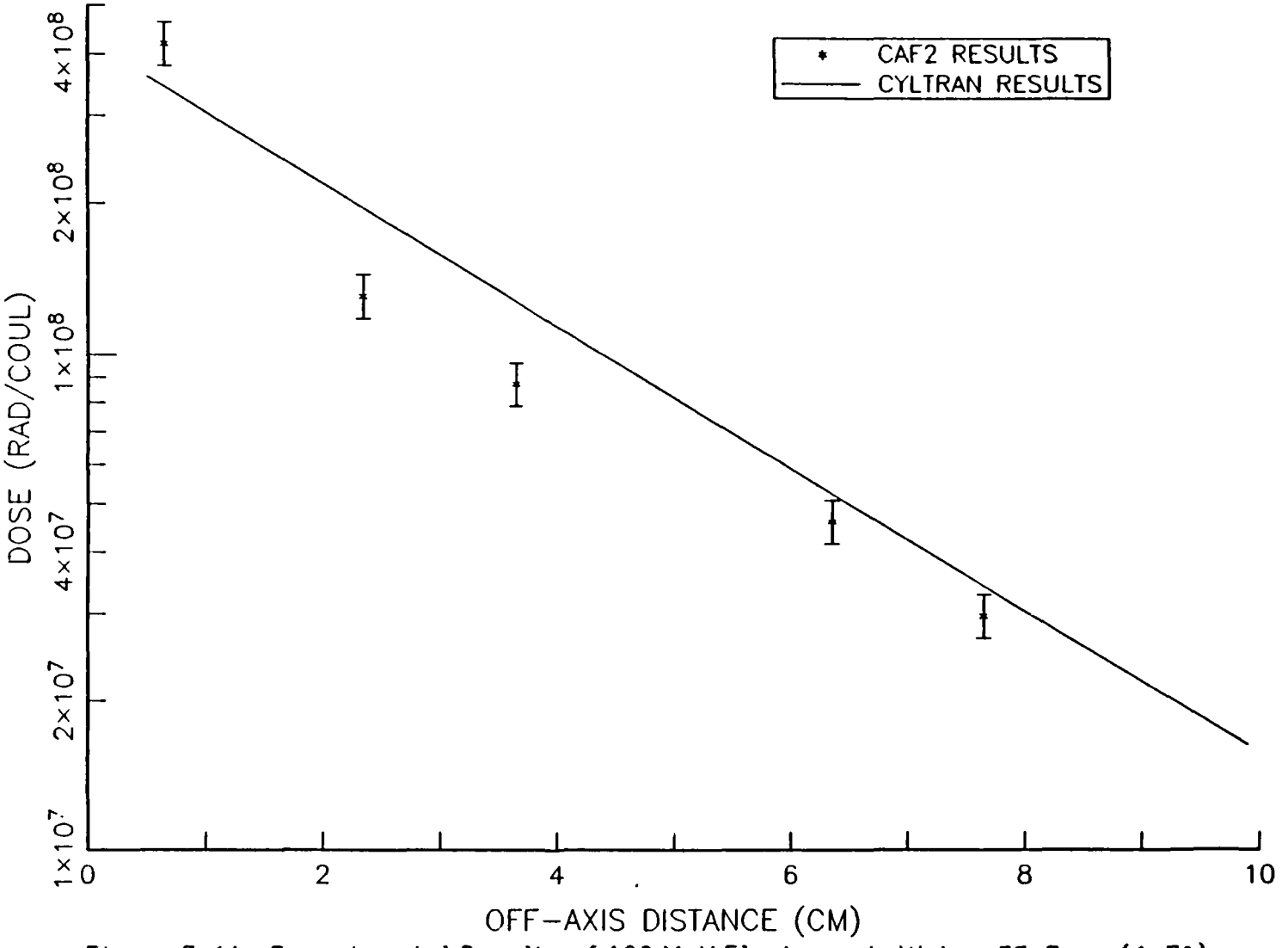

Figure 5.11 : Experimental Results of 100 MeV Electrons in Water-55.5 cm (1.7°)

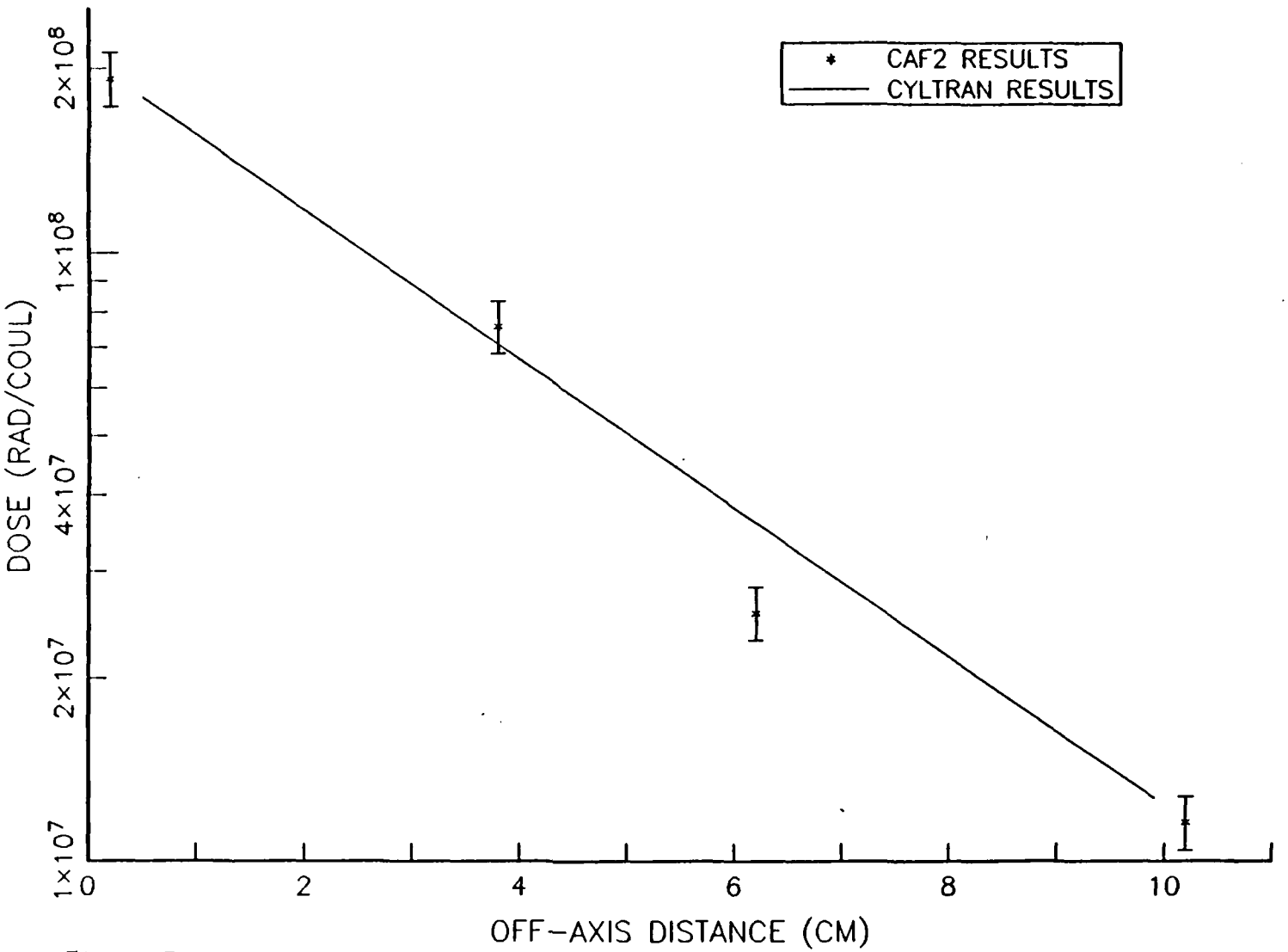

Figure 5.12 : Experimental Results of 100 MeV Electrons in Water-74.0 cm (1.7°)

VI. CONCLUSIONS

A. COMPARISON OF COMPUTER CALCULATIONS AND EXPERIMENTAL RESULTS

Within the limits of this experiment, there is good agreement between the measured and calculated normalized dose due to 100 MeV electrons in water. The experimental results at 0.0 cm and 9.2 cm were significantly higher than predicted. The TLDs at 0.0 cm were intended to measure the dose as a result of backscattering. However, the entrance to the test tank was not shielded and it is probable that these front TLDs were measuring a significant amount of radiation scattered from the aluminum window covering the exit of the vacuum chamber.

The results could be greatly improved with a few simple modifications to the TLD matrix. Alternating consecutive TLDs from one side of the central axis to the other showed that the beam was not directly on that axis. To adjust for this discrepancy it was necessary to try several iterative corrections of beam angle to bring the data back in line. If two TLDs had been placed at symmetrical positions on either side of the central axis, the two readings could be compared , providing a means of calibrating the off-axis positions of the TLDs with respect to the true beam position. In addition, use of a rigid frame to support the TLDs instead of the floating strechers that were used, would allow for much more accurate positioning of the entire array.

B. EXTENSIONS OF THE PREDICTIONS FROM ONE MEDIUM TO ANOTHER

The results were recorded at distances which correspond to fractions of the radiation length in the given medium. To extend the results from one medium to another, it is necessary to account for the change in size and mass of the detector as the radiation length varies [Ref. 1: p.34]. If a detector subtends the same solid angle and is located at an equivalent distance when measured in radiation lengths, the same energy should be deposited in the detector.

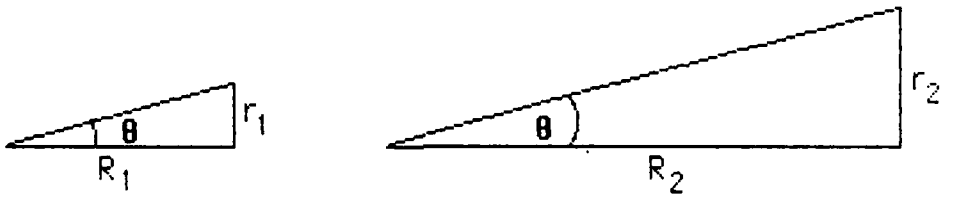

$$r_1 = R_1 \tan\theta \qquad r_2 = R_2 \tan\theta$$

$$\text{Area} = \pi r_1^2 = \pi (R_1 \tan\theta)^2 \qquad \text{Area} = \pi r_2^2 = \pi (R_2 \tan\theta)^2$$

$$\text{Ratio of Areas} = \frac{r_1}{r_2} \quad \frac{\pi (R_1 \tan\theta)^2}{\pi (R_2 \tan\theta)^2} = \left(\frac{R_1}{R_2}\right)^2$$

Figure 6.1 Ratio of the areas of two detectors

As shown if Figure 6.1, the new detector has an area and hence, a mass, that is larger by a factor of the square of the ratios of the distance to the detector. Since dose is related to the mass of the detector,

$$1 \text{ Rad} = 100 \text{ ergs / gm}$$

the dose at the new detector will be decreased by the same ratio. Water has

a radiation length of 37.0 cm and air has a radiation length of 307 meters, so for this experiment the ratio is:

$$\left(\frac{R_1}{R_2}\right)^2 = \left(\frac{.37}{307}\right)^2 = 1.45 \times 10^{-6}$$

Table 6.1 contains values of the dose in air predicted from the dose in water compared to the dose in air predicted by CYLTRAN. At the near distances, the results vary by about thirty percent, but this is largely due to the high one-sigma errors of the data at these distances. At one radiation length and above, the statistical errors in the initial data are much smaller and the resulting scaled dose is within ten percent of the dose in air predicted by CYLTRAN. Figure 6.2 through 6.6 present curves of the dose in water scaled to air, the dose in liquid nitrogen scaled to air, and the dose in air as predicted by CYLTRAN.

The critical energy for water, air, and liquid nitrogen are contained in Table 1. Since the experiment and the calculations were conducted at 100 MeV, close to the critical energies of the three media, the concept of radiation length is somewhat nebulous. Water with solid angle effects can be scaled to air with consistent results because they have similar Z. It is unlikely the results in water would scale to lead, for instance. At lower energies, a better length parameter is the range in gm/cm^2. Figure 6.7 and Figure 6.8 contain the off-axis dose in water. Figure 6.9 and Figure 6.10 contain the results in liquid nitrogen.

C. COMPARISONS WITH OTHER PAPERS

In his CYLTRAN predictions for liquid nitrogen, Cromar included a 0.2 cm layer of silicon in the geometry for the energy deposition [REF.1]. This special geometry required individual CYLTRAN runs for each distinct length used in the experiment, requiring a great deal of redundant calculations by the computer. To avoid this, the calulations in this paper were all done in a single run for each different medium. The energy deposition was recorded in sub-zones of the medium instead of silicon. To ensure the validity of this approach, the off-axis dose in liquid nitrogen predicted by this method is compared to the experimental results reported by Cromar. Figures 6.11 through 6.13 contain the two sets of data and in general show good agreement between the predicted and observed results.

Cromar's results were also compared to those reported by R.A Lindgren [Ref.7] which looked at the energy depositon in air due to 50 MeV electrons using the computer code ETRAN. The differences between the normalized doses were significant but several different assumptions were made in the two studies and the difference in the incident energy makes a direct comparison difficult.

An additional study of electron transport at energies up to 1000 MeV has been reported by S.M. Seltzer and M.J. Berger [Ref.8]. In their study, the computer code ETRAN was used. Since the TIGER series of codes all draw from the same source for the Monte-Carlo calculations the results shoud be the same as those presented in this paper generated from the CYLTRAN code.

Figure 6.14 shows the CYLTRAN data plotted with the ETRAN data at incident energies of 60 MeV and 125 MeV. The ETRAN curves were derived from replicate data of Ref. 8 and plotted at the midpoints of the histogram bins. ETRAN is a one-dimensional code and for comparison it was necessary to sum the ten radial sub-zones used by CYLTRAN to obtain a single value of energy deposition at a given penetration depth. The CYLTRAN zones were only 0.2 g/cm^2 in thickness so an additional factor of five was included to normalize the results to a unit depth. Figure 6.14 shows that once the geometries are equalized, there is no significant differences between the two computer codes.

D. ENERGY DEPENDENCE OF THE RESPONSE

An additional experimental run was conducted at 20 MeV incident energy however the results were not returned for inclusion in this paper. For future work, it is recommended that the Naval Postgrtaduate School purchase or obtain the use of its own TLD reader and a supply of reusable TLDs. This experiment alone used 80 TLDs at each energy. This was was considered the minimum necessary to obtain quick, but meaningful results. For a detailed study, the number of TLDs could easily run into the hundreds. Having to depend on a third party to process this number of TLDs is time consuming and imposses a huge burden of the processing facility. It would greatly facilitate the studies if the TLDs could be processed at the test facility.

E. SUMMARY

The results presented indicate that the CYLTRAN computer computations do accurately predict the experimental results. There does not appear to be any discreapncy between the one-dimensional computer code ETRAN and the two-dimensional computer code CYLTRAN. For materials of similar Z, the extension of experimental results in one medium to another appears to be valid.

TABLE 6.1

PREDICTIONS FOR AIR BASED ON RADS/COULOMB IN WATER

Factor=(30700/37)^2

Rad/Lth	Air (Pred) Rads/Coulomb	One-Sigma Error	Air (Cyltran) Rads/Coulomb	One-Sigma Error	Ratio
0.00	7.9245E+04	2	9.2801E+04	3	1.17
	8.1257E-01	56	3.1579E+00	91	3.89
	7.5299E-01	46	3.0577E-01	42	0.41
	4.6982E-01	48	2.2514E+00	62	4.79
	9.9008E-01	30	1.0680E+00	42	1.08
	8.3157E-01	28	3.1993E-01	34	0.38
	1.2156E+00	27	3.8732E-01	43	0.32
	5.5566E-01	20	4.8336E-01	36	0.87
	4.0331E-01	24	2.4460E-01	47	0.61
	2.1545E-01	27	1.8029E-01	51	0.84
0.25	8.2900E+04	3	9.5737E+04	3	1.15
	4.0395E+03	3	3.1162E+03	6	0.77
	3.2665E+02	7	3.0579E+02	9	0.94
	8.0173E+01	13	8.9421E+01	18	1.12
	3.8481E+01	16	3.2072E+01	28	0.83
	1.2797E+01	25	4.1353E+00	99	0.32
	5.5583E+00	26	8.7315E+00	40	1.57
	3.4629E+00	27	4.5326E+00	40	1.31
	3.1313E+00	27	3.2345E+00	55	1.03
	2.8272E+00	52	3.2645E+00	61	1.15

TABLE 6.1 (cont'd)

0.50	2.6881E+04	3	2.9248E+04	3	1.09
	1.2841E+04	2	1.3804E+04	2	1.07
	4.1262E+03	3	4.2394E+03	4	1.03
	1.1693E+03	5	1.1804E+03	6	1.01
	3.7070E+02	4	3.4757E+02	7	0.94
	1.0736E+02	13	1.1207E+02	17	1.04
	5.5645E+01	8	5.5706E+01	11	1.00
	3.2064E+01	11	3.5135E+01	15	1.10
	9.5732E+00	28	1.2687E+01	17	1.33
	8.5832E+00	15	8.8687E+00	29	1.03
1.00	2.3485E+03	6	2.2181E+03	7	0.94
	1.7406E+03	6	1.6862E+03	6	0.97
	1.3403E+03	3	1.1146E+03	6	0.83
	9.5150E+02	3	7.4772E+02	5	0.79
	6.8564E+02	4	5.8765E+02	6	0.86
	4.8474E+02	7	3.5625E+02	4	0.73
	3.4158E+02	2	2.4641E+02	9	0.72
	2.2934E+02	7	1.7884E+02	5	0.78
	1.5626E+02	3	1.1710E+02	8	0.75
	8.9038E+01	12	8.3028E+01	10	0.93
1.50	5.3640E+02	10	5.5813E+02	16	1.04
	3.7059E+02	7	4.4524E+02	5	1.20
	3.0896E+02	8	3.0862E+02	5	1.00
	1.7579E+02	12	1.8005E+02	7	1.02
	1.1369E+02	10	1.2701E+02	14	1.12
	1.0442E+02	7	7.9514E+01	10	0.76
	7.0638E+01	13	6.0580E+01	9	0.86
	5.6338E+01	12	4.2238E+01	15	0.75
	4.2163E+01	12	3.0173E+01	8	0.72
	2.4319E+01	13	2.5074E+01	18	1.03

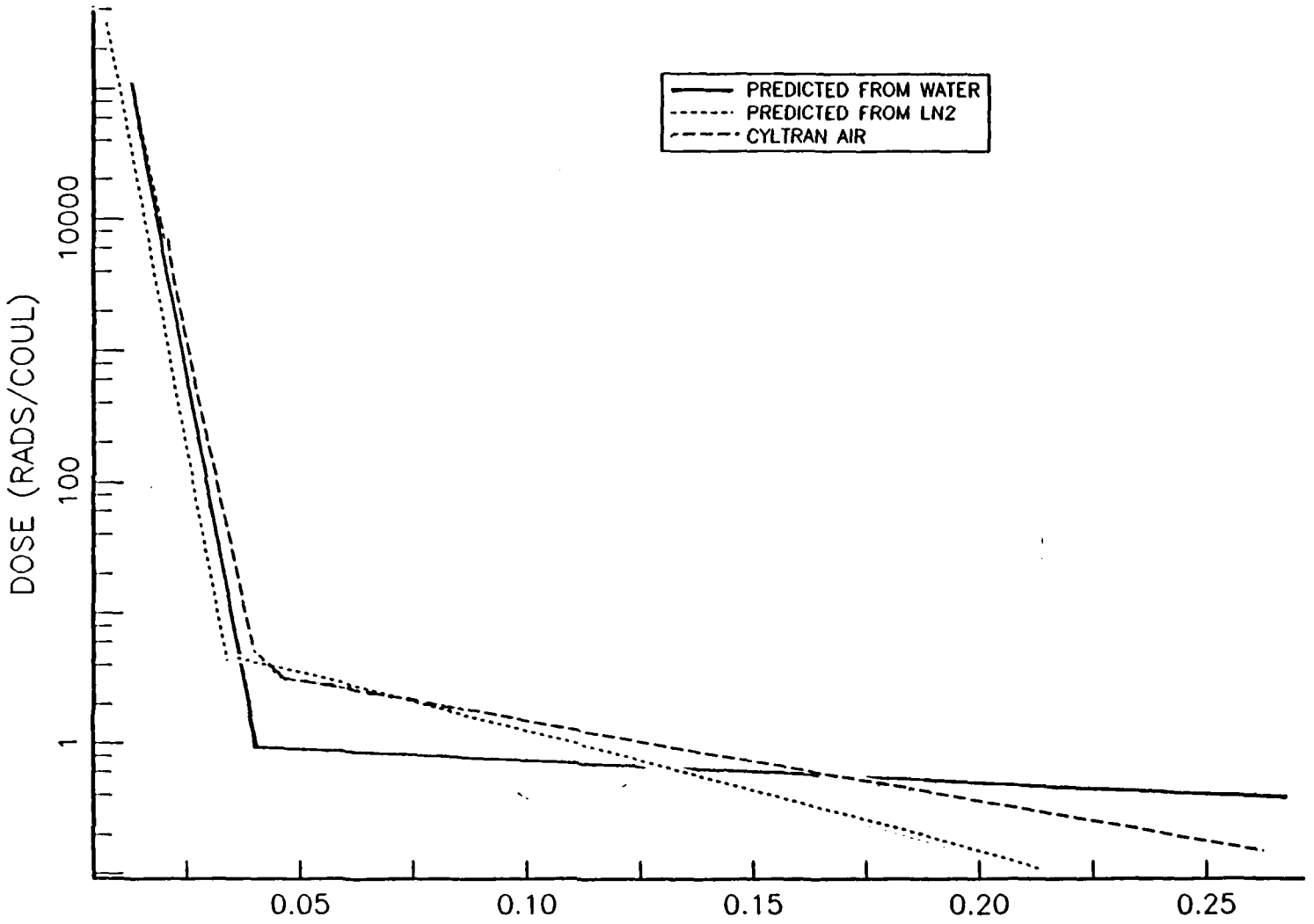

Figure 6.2 : Predicted Dose in Air (0.0 m)

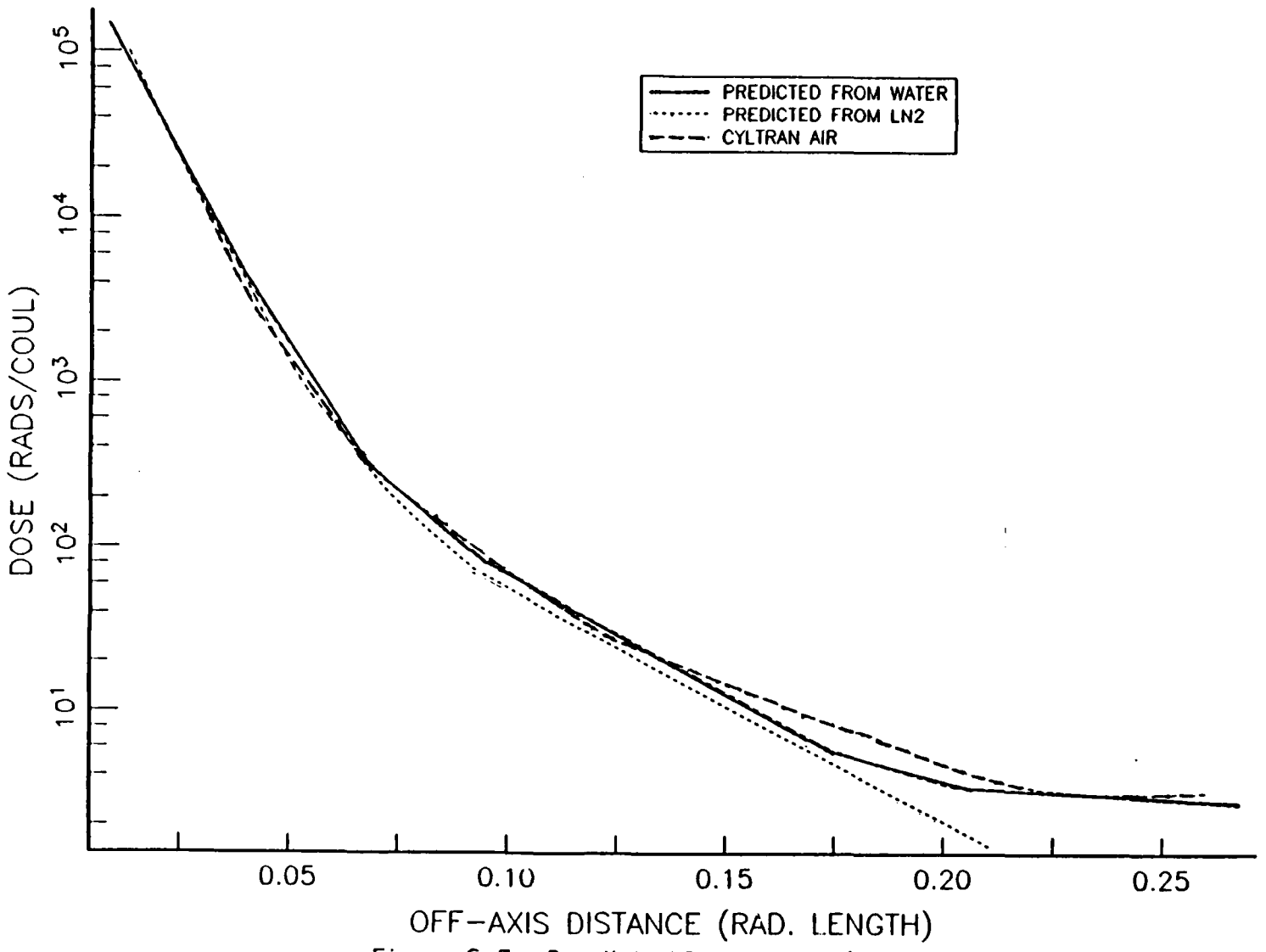

Figure 6.3 : Predicted Dose in Air (76.8 m)

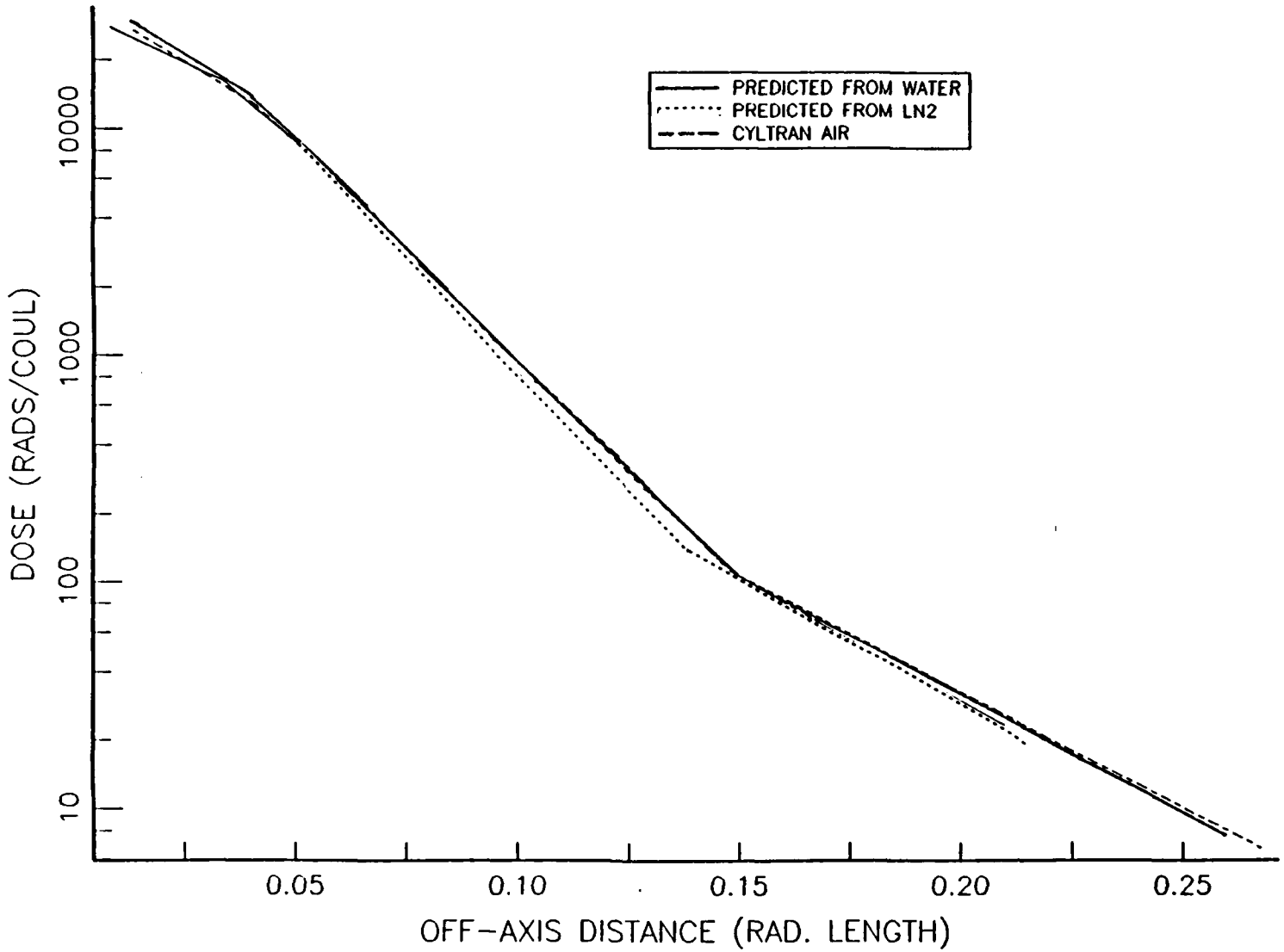

Figure 6.4 : Predicted Dose in Air (153.5 m)

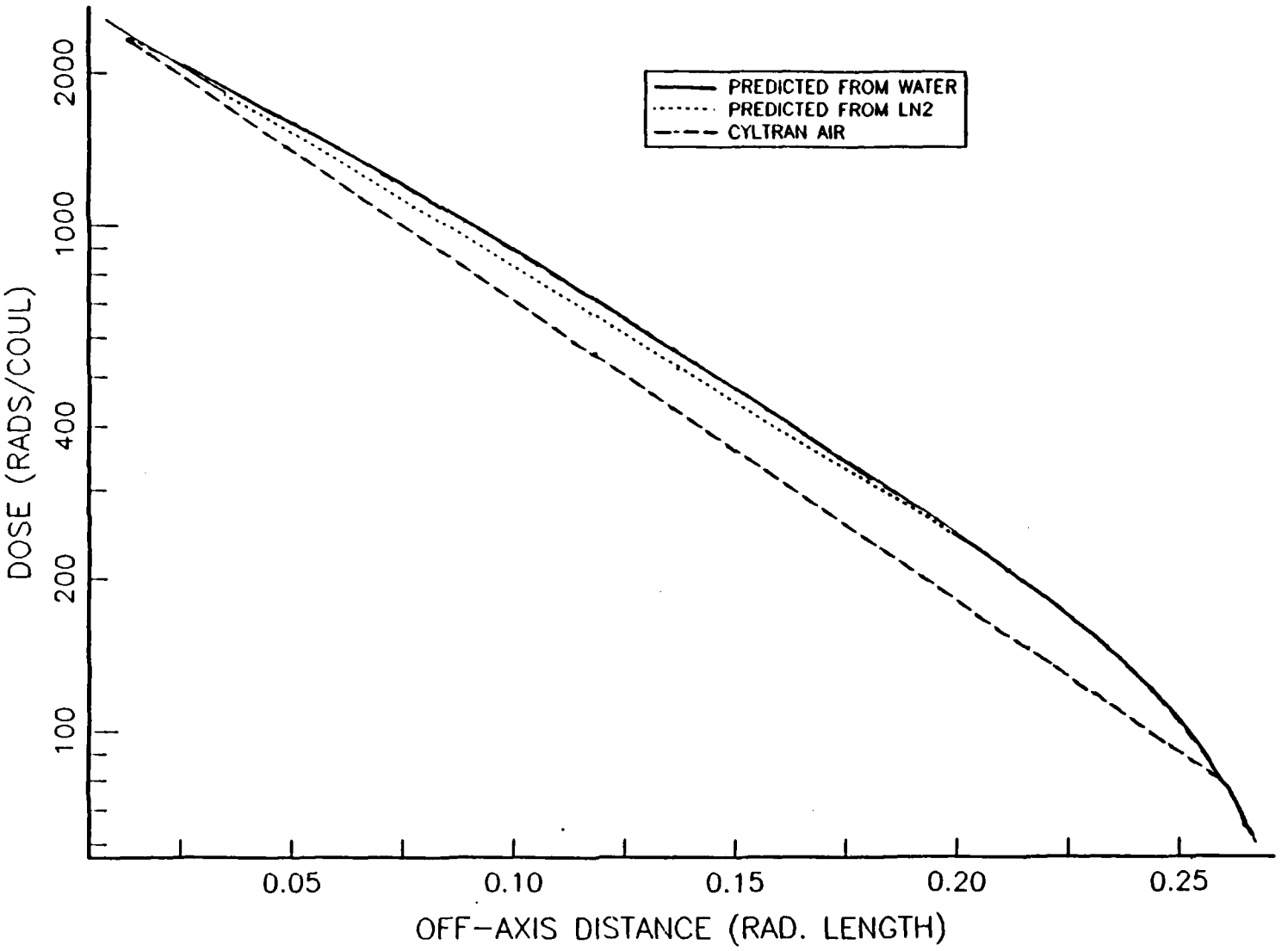

Figure 6.5 : Predicted Dose in Air (307.0 m)

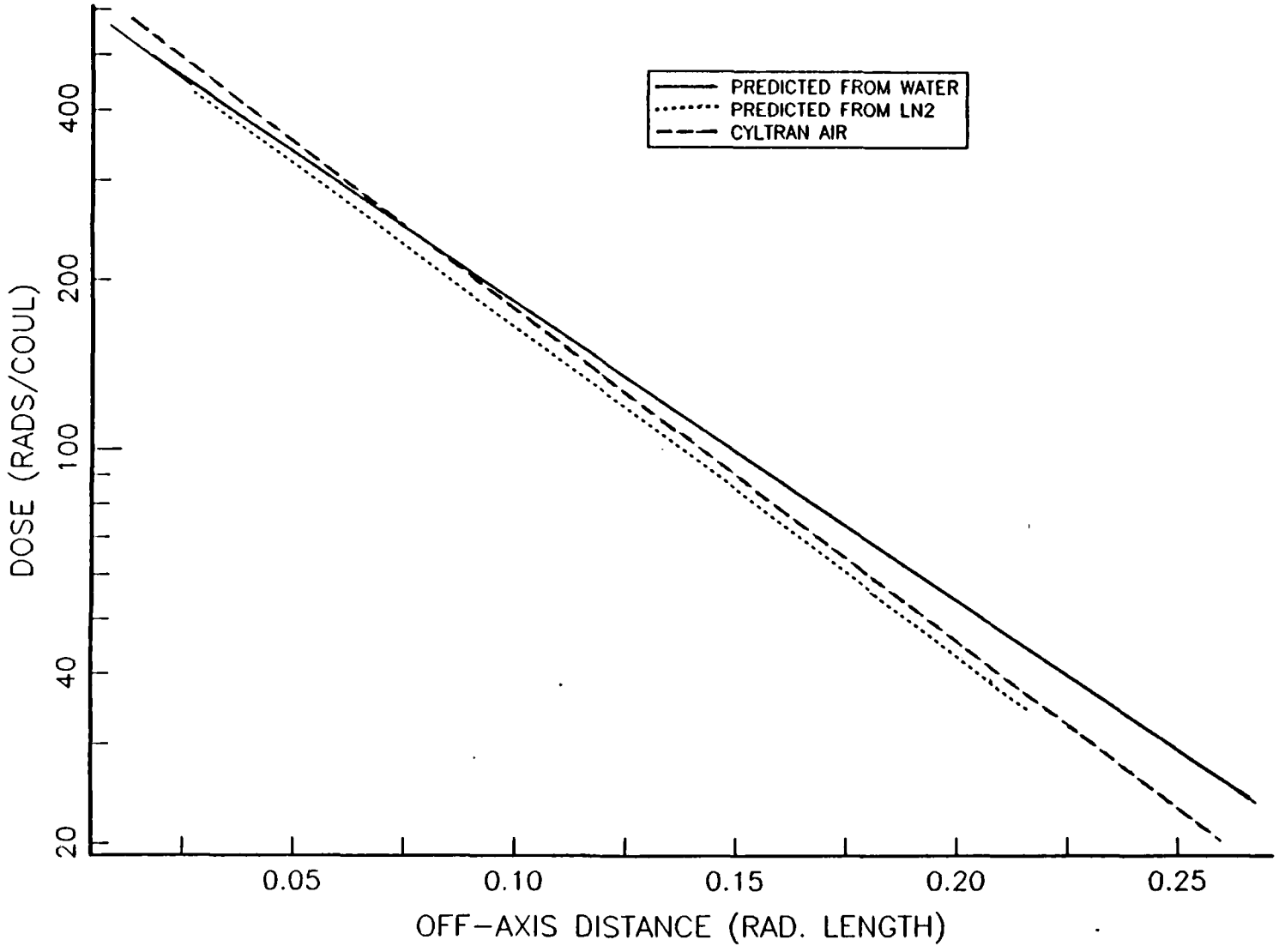

Figure 6.6 : Predicted Dose in Air (460.5 m)

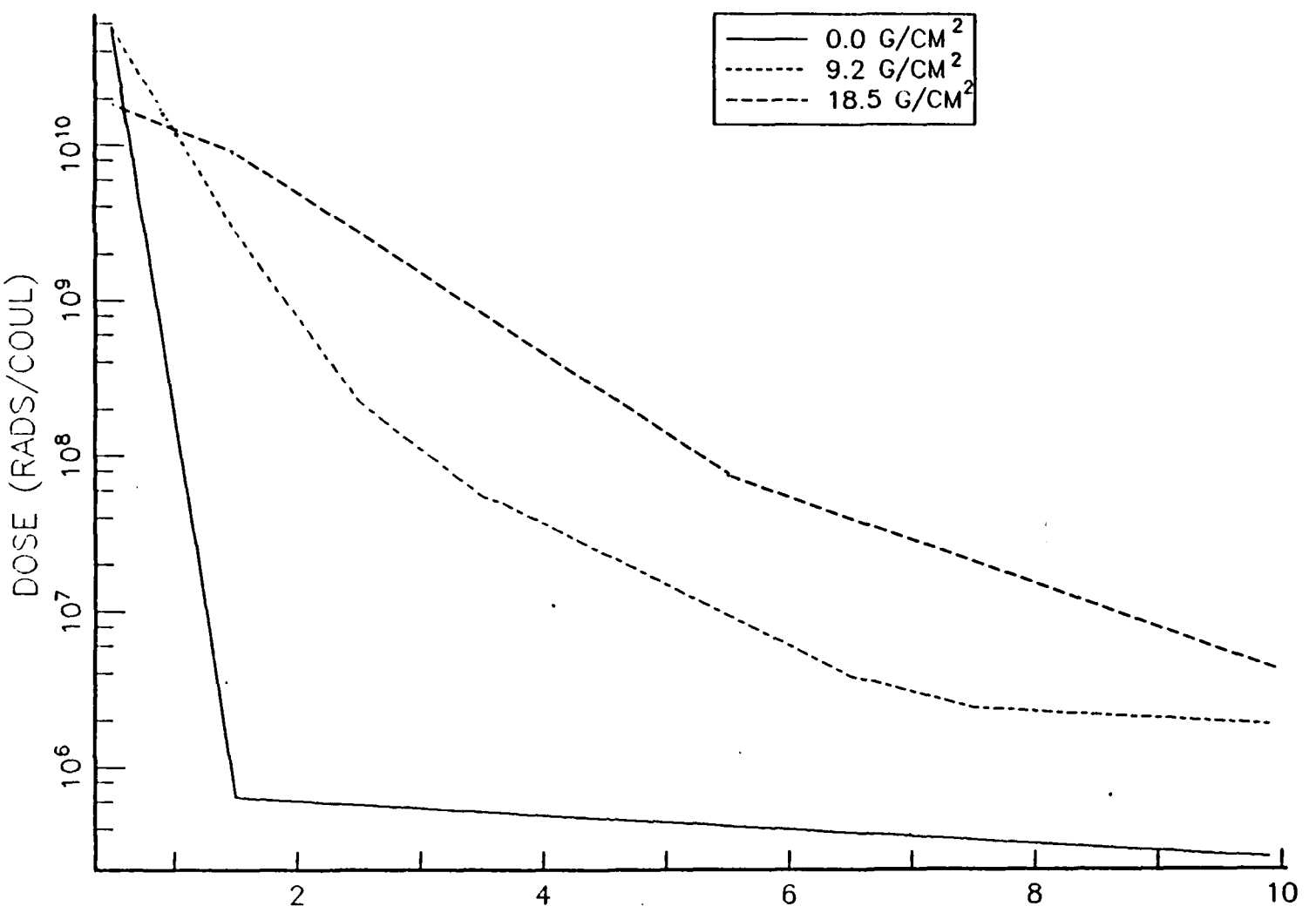

Figure 6.7 : CYLTRAN Dose in Water Due to 100 MeV Electrons

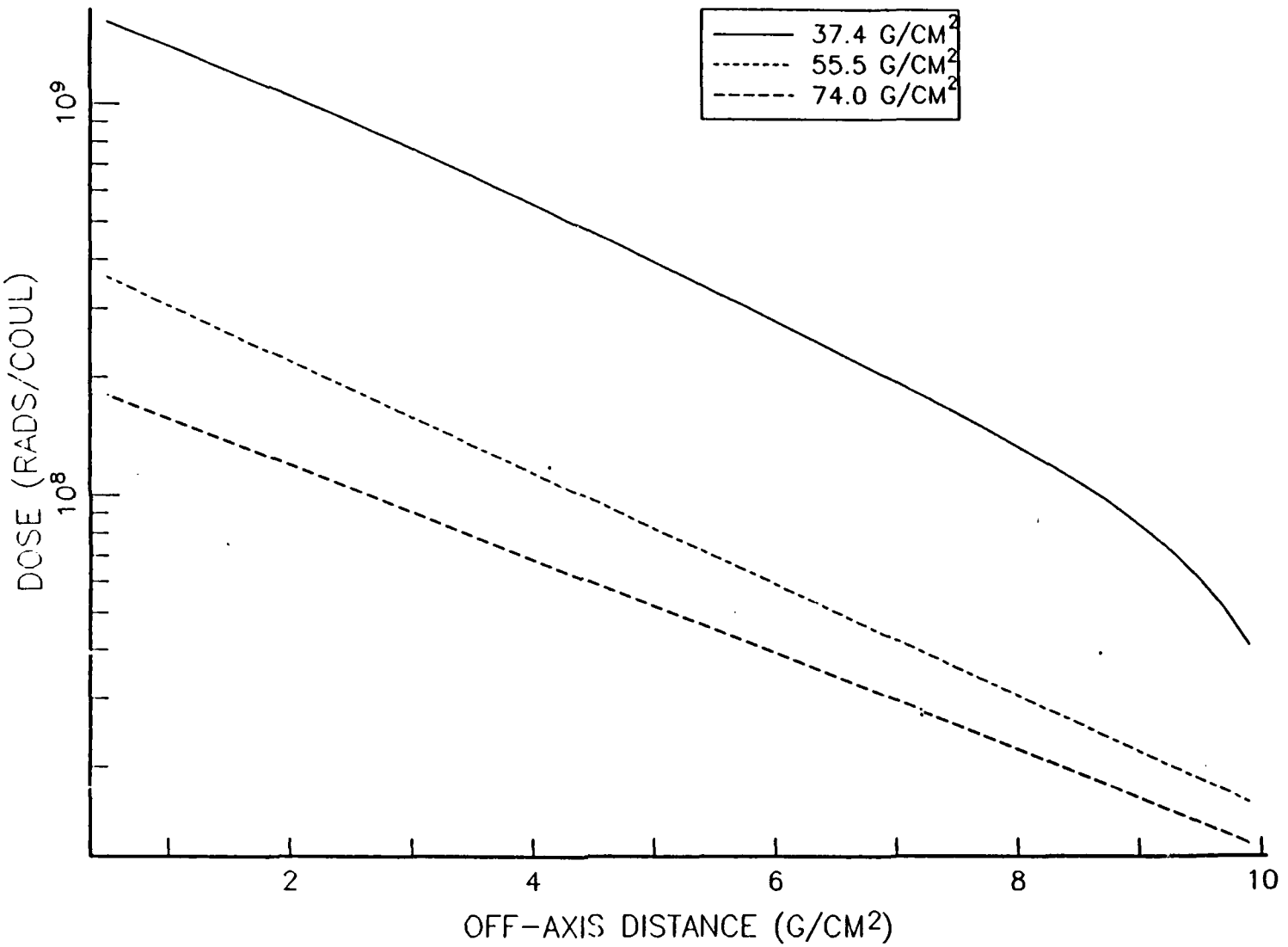

Figure 6.8 : CYLTRAN Dose in Water Due to 100 MeV Electrons

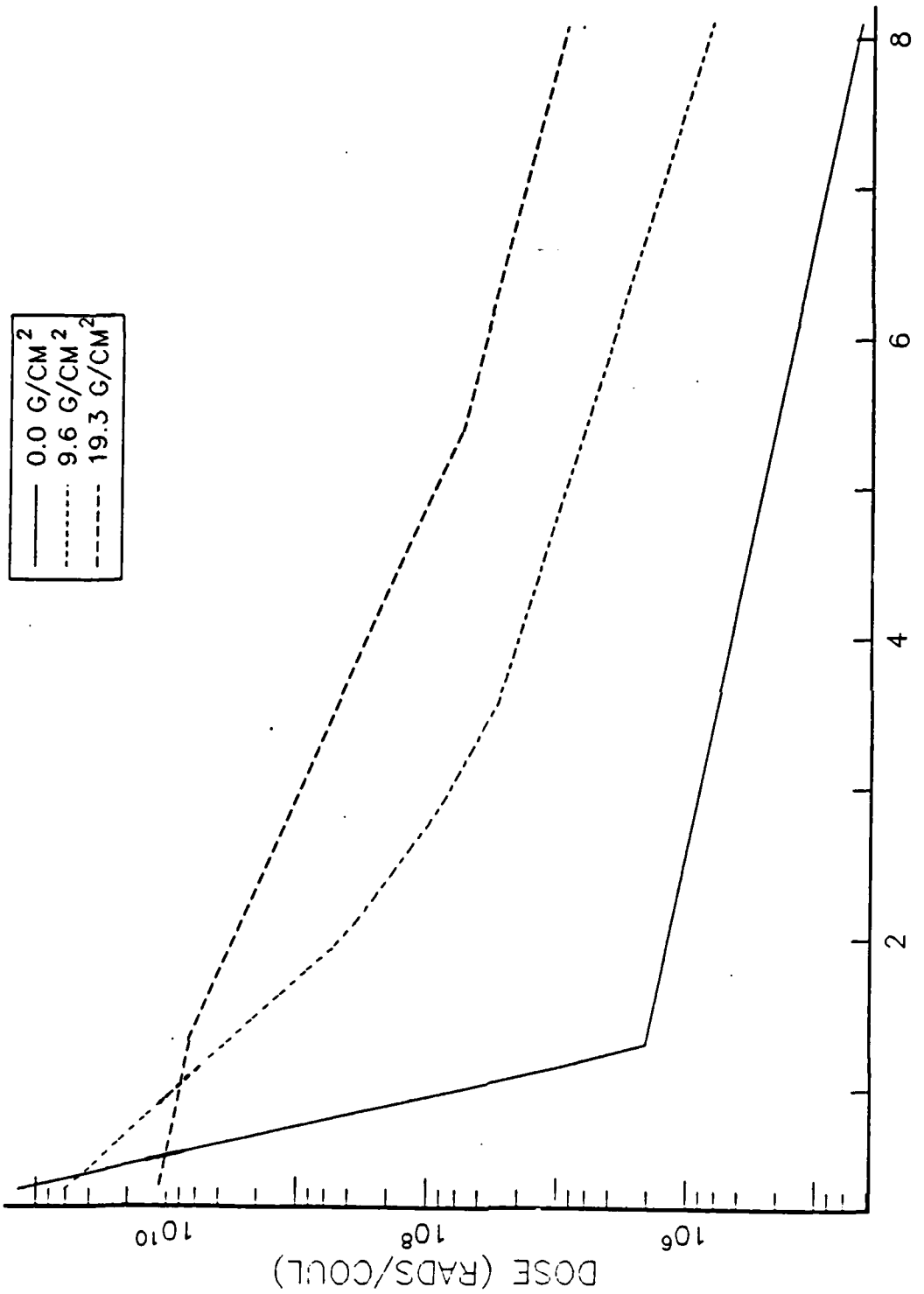

Figure 6.9 : CYLTRAN Dose In Liquid Nitrogen Due to 100 MeV Electrons

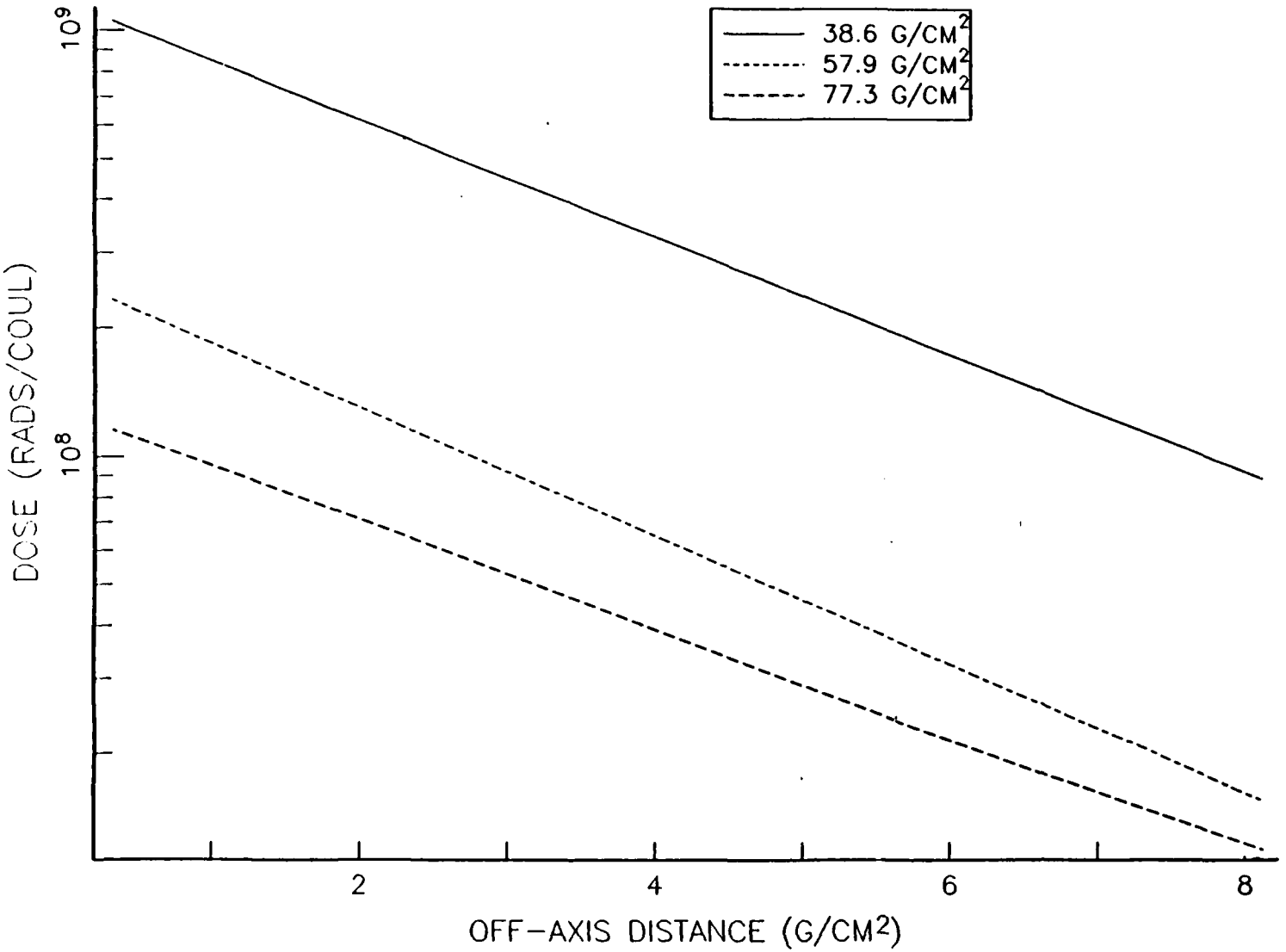

Figure 6.10 : CYLTRAN Dose in Liquid Nitrogen Due to 100 MeV Electrons

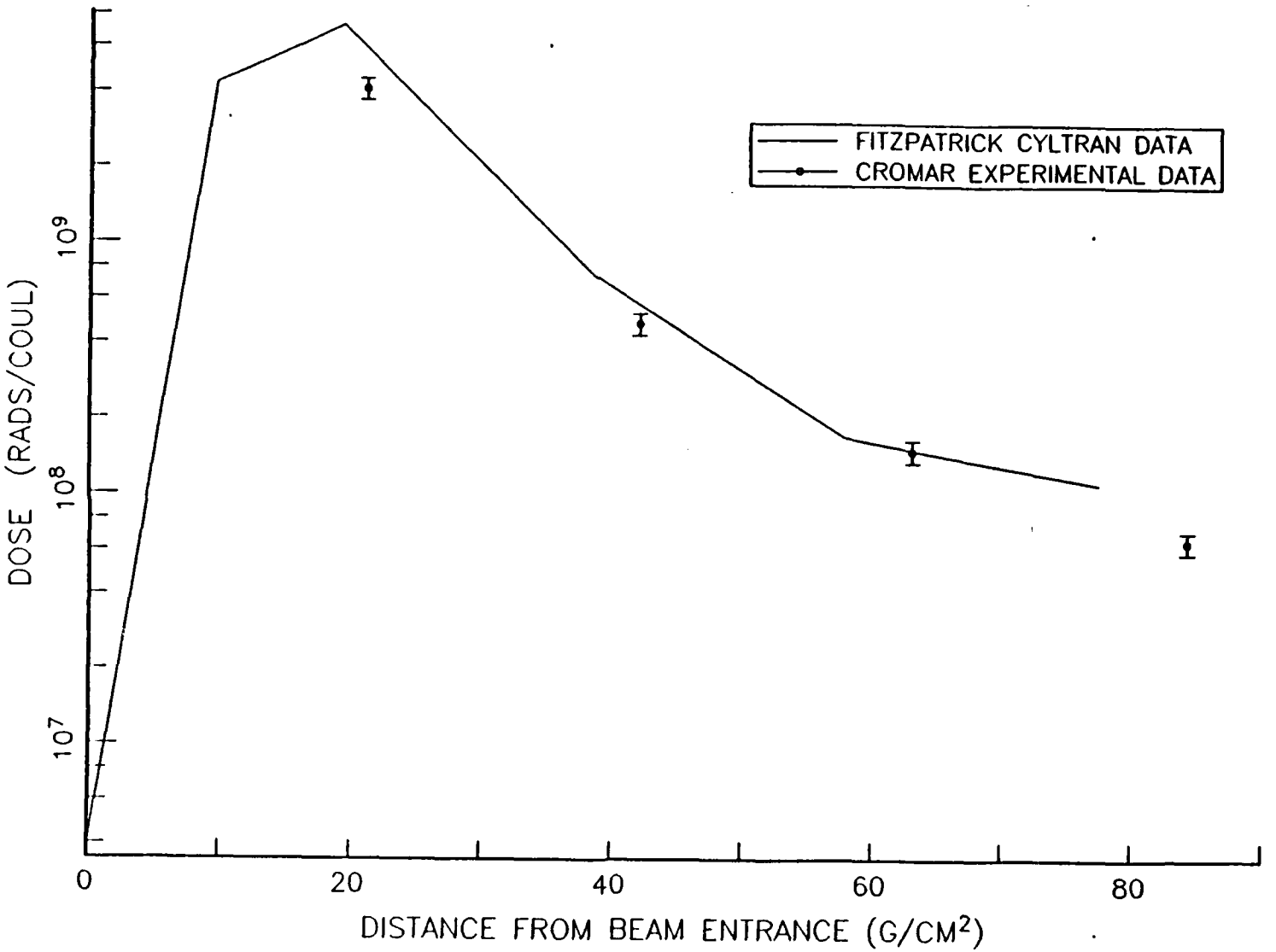

Figure 6.11 : Predicted and Experimental Dose In LN_2 ($z=1.2$ g/cm^2)

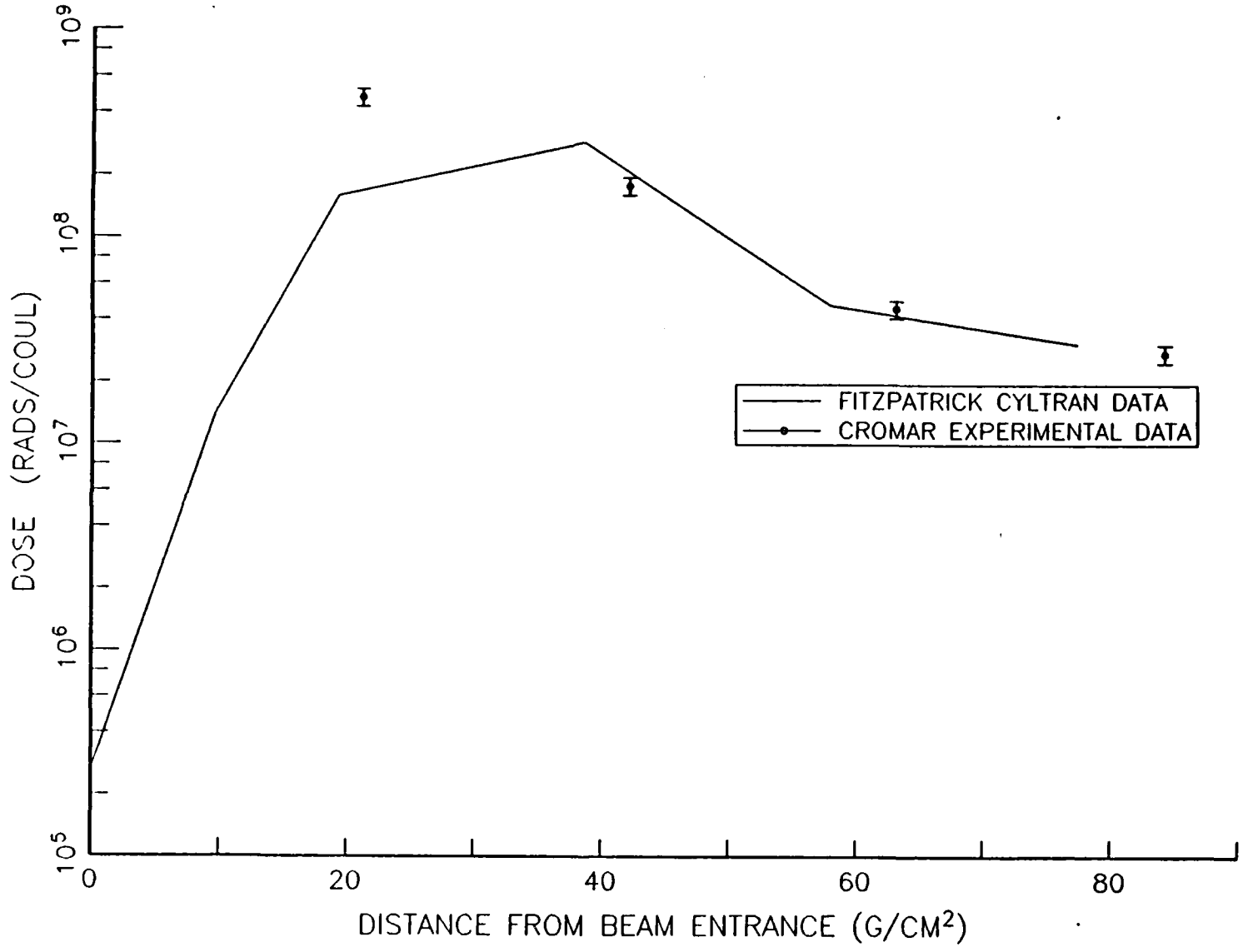

Figure 6.12 : Predicted and Experimental Dose In LN_2 ($z=4.5$ g/cm^2)

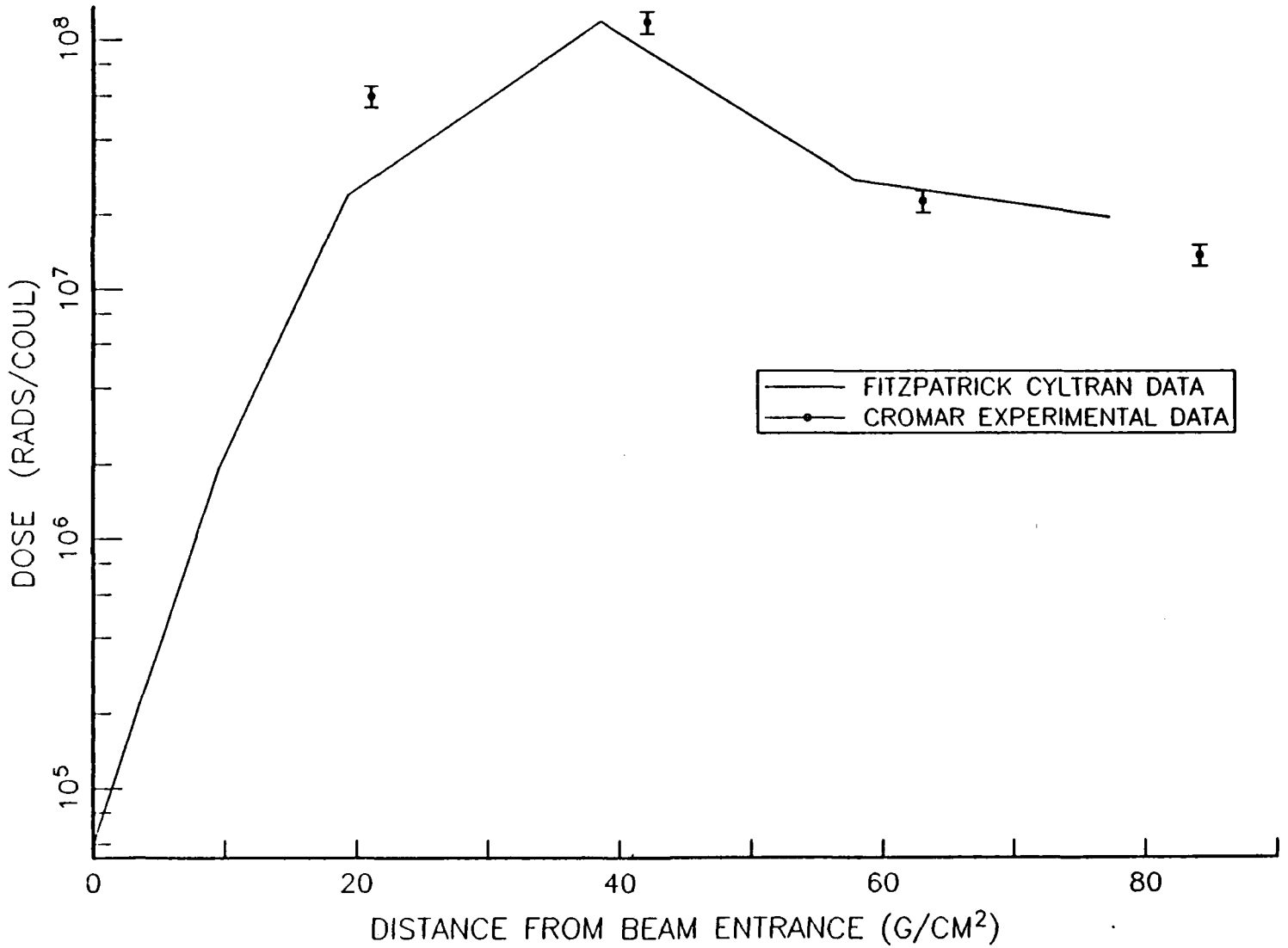

Figure 6.13 : Predicted and Experimental Dose In LN_2 (z=6.9 g/cm^2)

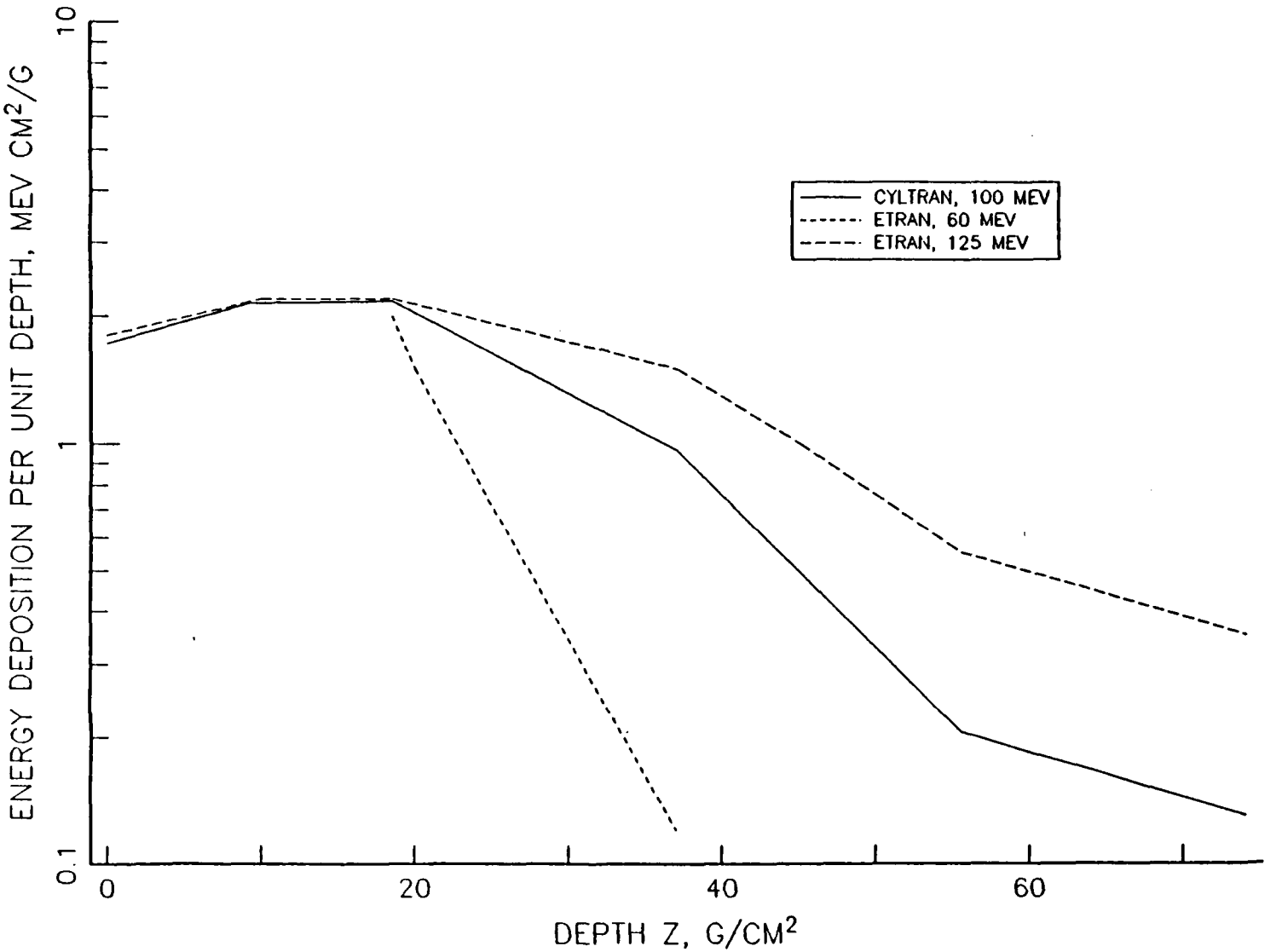

Figure 6.14 : Comparison of ETRAN and CYLTRAN Predictions

LIST OF REFERENCES

1. Cromar, P.F., Comparison of Calculations and Measurements of the Off-Axis Radiation Dose (Si) in Liquid Nitrogen as a Function of Radiation Length, M.S. Thesis, Naval Postgraduate School, Monterey, California, 1984.

2. Livingston, M.S., and Blewitt, J.P., Particle Accelerators, McGraw-Hill Book Co., 1962.

3. Segrè, E., Nuclei and Particles, W.A. Benjamin, Inc., 1977.

4. Fenyves, E. and Haiman, O., The Physical Principles of Nuclear Radiation Measurements, Academic Press, 1969.

5. Carlson, J.F. and Oppenheimer, J.R., "On Multiplicative Showers," Physical Review, v. 51, pp. 220-230, 15 February 1937.

6. Sandia National Laboratories Report SAND84-0573, ITS: The Integrated TIGER Series of Coupled Electron/Photon Monte Carlo Transport Codes, by J.A. Halbleib and T.A. Menlhorn, 1984.

7. Naval Research Laboratory Report 3335, Calculated Photon Spectra and Radiation Dose from 50 MeV Electrons Stopping in Air, by R.A. Lindgren, 1976.

8. National Bureau of standards Report NBSIR 78-1534, Monte-Carlo Studies of Electrons and Photon Transport at Energies up to 1000 MeV, by S.M. Seltzer and M.J. Berger, 1978.

APPENDIX A

DESCRIPTION OF CYLTRAN AND OUTPUT

The computer code CYLTRAN is a member of the Integrated TIGER Series of Coupled Electron/Photon Monte Carlo Transport Codes developed at Sandia National Laboratories by J.A. Halbleib and W.H. Vandevender. CYLTRAN employs a fully three-dimensional description of particle trajectories within an axisymmetric cylindrical material geometry and finds application in problems involving electron and photon beam sources.[Ref.6: p.6]

CYLTRAN is based primarily on the ETRAN model which combines microscopic photon transport with a macroscopic random walk for electron transport. The code describes the generation and transport of the electron/photon shower from the incident energy down to a specified cut-off energy for photons and electrons. The code can handle up to ten different materials, with the only requirement being that the material geometry be cylindrically symmetric.[Ref.6: p.70]

The user may specify incident particles to be either electrons or photons which may be considered mono-energetic or have a specified energy spectrum. The source reference direction can be monodirectional, isotropic, or have a specified divergence angle.

The default output of CYLTRAN consists of:

a) Energy and number escape fractions (leakage) for electrons, unscattered photons and scattered photons.

b) Charge and energy deposition profiles.

c) An explicit statement of energy conservation.

In addition to the default output, a number of optional outputs may be selected through the use of the appropriate keywords. These are:

a) Escape fractions that are differantial in energy for both electrons and scattered photons.

b) Escape fractions that are differential in angle for both electrons and scattered photons.

c) Coupled energy and angular distributions of escaping electrons and scattered photons.

d) Volume-averaged energy distributions of electron and photon scalar fluxes for selected regions of the problem geometry.

e) Psuedo-pulse-height distributions for selected regions of the problem geonetry-- for example, those regions corresponding to active detector elements.[Ref.6: pp.19,34]

Two basic steps are required for solving any given problem:

a) Generate the cross sections by running the cross section code.

b) Run the Monte Carlo code.

Table A1 is a sample input used for the generations of cross-sections of water, standard air (80% nitogen, 20% oxygen), liquid nitrogen, and silicon. Table A2 is a sample input for the proper execution of CYLTRAN once the cross-sections have been generated. CYLTRAN output for runs of 20,000 incident electron in water, air, and liquid nitrogen is include in Tables A3 thru Table A25.

TABLE A1

SAMPLE INPUT FOR THE GENERATION OF CROSS SECTIONS

```
1 MATERIAL H .111 O .889 DENSITY 1.0
2 MATERIAL N .80 O .20 GAS DENSITY .001226
3 MATERIAL N DENSITY 0.81
4 MATERIAL SI
5 TITLE  100 MeV CROSS SECTIONS FOR H2O AIR N SI
6 ENERGY 100.0
```

TABLE A2

SAMPLE INPUT FOR THE EXECUTION OF CYLTRAN

```
 1 ECHO 1
 2 TITLE
 3 ... 100 MeV ENERGY DEPOSITION IN WATER
 4 **********SOURCE**********
 6 ENERGY 100.0
 7 * DEFAULT SOURCE PHASE SPACE PARAMETERS
 8 POSITION 0.0 0.0 0 0.0
 9    RADIUS 0.4
10 * MONODIRECTIONAL Z-AXIS
11 DIRECTION 0.0 0.0 0.0
12 **********OPTIONS**********
13 HISTORIES 20000
14 BATCHES 10
15 CUTOFFS 0.05 0.001
16 DUMP
17 **********OUTPUT OPTIONS**********
18 ELECTRON-ESCAPE
19    NBINE 2
20    NBINT 4
21 PHOTON-ESCAPE
22    NBINE 2
23    NBINT 4
24 ELECTRON-FLUX 1 10
25   NBINE 2
26 PHOTON -FLUX 1 10
27   NBINE 2
28 **********GEOMETRY**********
29 GEOMETRY 11
30 *ZL      ZR     RI     RO     MAT   IZR   NZ    NR    ECUT    PTCZ
31   0.0    0.2    0.0   10.0  1   1   1   10
32   0.2    9.2    0.0   10.0  1
33   9.2    9.4    0.0   10.0  1   1   1   10
34   9.4   18.5    0.0   10.0  1
35  18.5   18.7    0.0   10.0  1   1   1   10
36  18.7   37.0    0.0   10.0  1
37  37.0   37.2    0.0   10.0  1   1   1   10
38  37.2   55.5    0.0   10.0  1
39  55.5   55.7    0.0   10.0  1   1   1   10
40  55.7   74.0    0.0   10.0  1
```

TABLE A3

ENERGY DEPOSITION FROM 100 MeV ELECTRONS AT 0.0 CM OF WATER

(MeV, normalized to one incident particle)

ZONE	PRIMARIES		KNOCK-ONS		GAMMA-SEC		TOTAL	
1	4.1358E-01	1	-7.0822E-02	8	3.0772E-05	32	3.4279E-01	2
2	5.9498E-06	99	0.0000E+00	99	4.5954E-06	39	1.0545E-05	56
3	0.0000E+00	99	0.0000E+00	99	1.6286E-05	46	1.6286E-05	46
4	0.0000E+00	99	0.0000E+00	99	1.4226E-05	48	1.4226E-05	48
5	0.0000E+00	99	0.0000E+00	99	3.8545E-05	30	3.8545E-05	30
6	0.0000E+00	99	0.0000E+00	99	3.9568E-05	28	3.9568E-05	28
7	0.0000E+00	99	0.0000E+00	99	6.8358E-05	27	6.8358E-05	27
8	0.0000E+00	99	0.0000E+00	99	3.6054E-05	20	3.6054E-05	20
9	0.0000E+00	99	0.0000E+00	99	2.7955E-05	24	2.7955E-05	24
10	0.0000E+00	99	0.0000E+00	99	1.7707E-05	27	1.7707E-05	27

TABLE A4

ENERGY DEPOSITION FROM 100 MeV ELECTRO[illegible] AT 9.2 CM OF WATER

(MeV, normalized to one incident particle)

ZONE	PRIMARIES		KNOCK-ONS		GAMMA-SEC		TOTAL	
1	3.4612E-01	1	-9.0900E-03	79	2.1564E-02	3	3.5860E-01	3
2	4.1494E-02	4	5.8716E-03	13	5.0559E-03	6	5.2422E-02	3
3	3.2950E-03	10	2.5809E-03	11	1.1890E-03	13	7.0649E-03	7
4	8.8955E-04	32	1.0089E-03	19	5.2912E-04	14	2.4276E-03	13
5	5.6419E-04	26	6.3922E-04	34	2.9470E-04	15	1.4981E-03	16
6	1.2424E-04	53	2.5206E-04	46	2.3259E-04	29	6.0889E-04	25
7	6.4327E-05	99	2.6546E-05	99	2.2169E-04	21	3.1256E-04	26
8	3.7499E-05	99	0.0000E+00	99	1.8719E-04	22	2.2469E-04	27
9	2.7798E-05	99	1.3335E-05	99	1.7591E-04	27	2.1704E-04	27
10	9.6048E-05	99	3.3256E-06	99	1.3299E-04	27	2.3236E-04	52

TABLE A5

ENERGY DEPOSITION FROM 100 MeV ELECTRONS AT 18.5 CM OF WATER

(MeV, normalized to one incident particle)

ZONE	PRIMARIES		KNOCK-ONS		GAMMA-SEC		TOTAL	
1	9.3802E-02	2	1.9366E-03	99	2.1264E-02	4	1.1628E-01	3
2	1.4501E-01	1	-2.6641E-03	99	2.4288E-02	3	1.6664E-01	2
3	7.9857E-02	2	-1.6287E-03	99	1.1014E-02	5	8.9242E-02	3
4	3.1456E-02	3	-6.7004E-04	99	4.6207E-03	10	3.5407E-02	5
5	1.1099E-02	6	9.3607E-04	35	2.3969E-03	13	1.4432E-02	
6	4.3910E-03	11	-1.8750E-04	99	9.0475E-04	19	5.1082E-03	13
7	2.1465E-03	13	1.0035E-04	99	8.8232E-04	19	3.1291E-03	8
8	1.2939E-03	19	-2.7840E-05	99	8.1437E-04	24	2.0805E-03	11
9	3.2343E-04	34	3.2177E-05	99	3.0795E-04	35	6.6356E-04	28
10	3.6296E-04	34	-3.9064E-05	99	3.1815E-04	26	7.0540E-04	15

TABLE A6

ENERGY DEPOSITION FROM 100 MeV ELECTRONS AT 37.0 CM OF WATER

(MeV, normalized to one incident particle)

ZONE	PRIMARIES		KNOCK-ONS		GAMMA-SEC		TOTAL	
1	3.5699E-03	6	1.8638E-04	99	6.4026E-03	7	1.0159E-02	6
2	9.8985E-03	5	2.7688E-04	99	1.2411E-02	9	2.2588E-02	6
3	1.5695E-02	5	7.9546E-04	47	1.2498E-02	5	2.8989E-02	3
4	1.7765E-02	2	-3.2412E-04	99	1.1371E-02	6	2.8811E-02	3
5	1.7116E-02	4	-4.8012E-04	91	1.0057E-02	5	2.6693E-02	4
6	1.6461E-02	4	-3.1636E-04	99	6.9207E-03	10	2.3065E-02	7
7	1.3326E-02	4	3.9890E-04	99	5.4832E-03	5	1.9208E-02	2
8	1.0851E-02	7	2.0572E-05	99	4.0098E-03	11	1.4881E-02	7
9	8.4881E-03	5	-1.5392E-04	99	2.4972E-03	11	1.0831E-02	3
10	5.8421E-03	8	-5.2152E-04	79	1.9972E-03	12	7.3178E-03	12

TABLE A7

ENERGY DEPOSITION FROM 100 MeV ELECTRONS AT 55.5 CM OF WATER

(MeV, normalized to one incident particle)

ZONE	PRIMARIES		KNOCK-ONS		GAMMA-SEC		TOTAL	
1	0.0000E+00	99	-2.6725E-06	99	2.3230E-03	11	2.3203E-03	10
2	0.0000E+00	99	-2.3698E-04	72	5.0461E-03	5	4.8092E-03	7
3	0.0000E+00	99	1.5601E-04	85	6.5263E-03	8	6.6824E-03	8
4	0.0000E+00	99	-3.0345E-04	99	5.6263E-03	8	5.3228E-03	12
5	0.0000E+00	99	-2.2656E-04	99	4.6526E-03	6	4.4260E-03	10
6	0.0000E+00	99	-1.1079E-04	99	5.0792E-03	6	4.9684E-03	7
7	0.0000E+00	99	-5.6038E-04	50	4.5326E-03	10	3.9722E-03	13
8	0.0000E+00	99	-4.1497E-05	99	3.6970E-03	11	3.6555E-03	12
9	0.0000E+00	99	5.4584E-05	99	2.8679E-03	11	2.9225E-03	12
10	0.0000E+00	99	4.1243E-05	70	1.9574E-03	14	1.9987E-03	13

TABLE A8

ENERGY DEPOSITION FROM 100 MeV ELECTRONS AT 74.0 CM OF WATER

(MeV, normalized to one incident particle)

ZONE	PRIMARIES		KNOCK-ONS		GAMMA-SEC		TOTAL .	
1	0.0000E+00	99	-1.0679E-04	99	1.3017E-03	14	1.1950E-03	22
2	0.0000E+00	99	-6.5395E-06	99	2.3648E-03	9	2.3582E-03	8
3	0.0000E+00	99	1.1913E-04	89	2.9405E-03	16	3.0596E-03	15
4	0.0000E+00	99	-7.8474E-05	99	3.4973E-03	11	3.4188E-03	11
5	0.0000E+00	99	1.2611E-04	58	3.1229E-03	9	3.2490E-03	8
6	0.0000E+00	99	1.6981E-04	68	3.3080E-03	13	3.4779E-03	12
7	0.0000E+00	99	-3.2978E-05	99	2.8954E-03	10	2.8624E-03	9
8	0.0000E+00	99	9.5110E-05	57	2.2133E-03	9	2.3084E-03	9
9	0.0000E+00	99	-7.2304E-05	99	2.1229E-03	8	2.0506E-03	9
10	0.0000E+00	99	-1.5256E-05	99	1.4860E-03	20	1.4707E-03	24

TABLE A9

ENERGY DEPOSITION FROM 20 MeV ELECTRONS AT 0.0 CM OF WATER

(MeV, normalized to one incident particle)

ZONE	PRIMARIES		KNOCK-ONS		GAMMA-SEC		TOTAL	
1	3.8653E-01	0	-4.3339E-02	5	1.3075E-05	34	3.4320E-01	1
2	0.0000E+00	99	8.5040E-05	44	1.9194E-05	26	1.0423E-04	35
3	2.3183E-04	52	0.0000E+00	99	8.9970E-05	74	3.2180E-04	53
4	9.7953E-05	67	0.0000E+00	99	2.6276E-05	16	1.2423E-04	53
5	1.3600E-05	67	0.0000E+00	99	2.5374E-05	34	3.8974E-05	34
6	1.9934E-04	54	-1.5650E-07	99	2.4546E-05	19	2.2373E-04	49
7	7.6248E-05	76	0.0000E+00	99	2.9266E-05	36	1.0551E-04	55
8	6.4604E-05	99	0.0000E+00	99	4.7860E-05	38	1.1246E-04	57
9	0.0000E+00	99	0.0000E+00	99	1.9127E-05	31	1.9127E-05	31
10	0.0000E+00	99	0.0000E+00	99	1.0790E-05	49	1.0790E-05	49

TABLE A10
ENERGY DEPOSITION FROM 20 MeV ELECTRONS AT 9.2 CM OF WATER

(MeV, normalized to one incident particle)

ZONE	PRIMARIES		KNOCK-ONS		GAMMA-SEC		TOTAL	
1	2.0435E-02	5	3.2765E-05	99	1.6476E-05	99	2.2115E-02	6
2	4.5067E-02	2	5.1233E-04	44	2.1828E-03	11	4.7762E-02	2
3	3.4319E-02	2	5.4297E-05	99	1.4876E-03	15	3.5861E-02	3
4	1.4664E-02	6	-1.2875E-04	44	8.5401E-04	20	1.5389E-02	5
5	2.8407E-03	14	-5.3291E-19	71	5.2936E-04	18	3.3770E-03	11
6	3.7788E-04	37	0.0000E+00	99	5.2519E-04	18	9.0307E-04	23
7	1.9937E-05	99	-4.2845E-05	99	4.1307E-04	29	3.9016E-04	30
8	0.0000E+00	99	0.0000E+00	99	2.0940E-04	24	2.0940E-04	24
9	0.0000E+00	99	0.0000E+00	99	1.0634E-04	33	1.0634E-04	33
10	0.0000E+00	99	0.0000E+00	99	1.0498E-04	47	1.0150E-04	47

TABLE A11

ENERGY DEPOSITION FROM 20 MeV ELECTRONS AT 18.5 CM OF WATER

(MeV, normalized to one incident particle)

ZONE	PRIMARIES		KNOCK-ONS		GAMMA-SEC		TOTAL	
1	0.0000E+00	99	2.8276E-05	99	3.1238E-04	28	3.4066E-04	27
2	0.0000E+00	99	2.0326E-05	99	7.2579E-04	18	7.4611E-04	17
3	0.0000E+00	99	4.6803E-05	99	7.8105E-04	15	8.2785E-04	14
4	0.0000E+00	99	0.0000E+00	99	6.9166E-04	20	6.9166E-04	20
5	0.0000E+00	99	0.0000E+00	99	5.0592E-04	22	5.0592E-04	22
6	0.0000E+00	99	0.0000E+00	99	4.3682E-04	47	4.3682E-04	47
7	0.0000E+00	99	-2.6645E-19	99	4.6562E-04	31	4.6562E-04	31
8	0.0000E+00	99	0.0000E+00	99	3.7421E-04	23	3.7421E-04	23
9	0.0000E+00	99	0.0000E+00	99	2.9957E-04	26	2.9957E-04	26
10	0.0000E+00	99	-1.9274E-05	99	2.2572E-04	36	2.0644E-04	39

TABLE A12

ENERGY DEPOSITION FROM 20 MeV ELECTRONS AT 37.0 CM OF WATER

(MeV, normalized to one incident particle)

ZONE	PRIMARIES		KNOCK-ONS		GAMMA-SEC		TOTAL	
1	0.0000E+00	99	0.0000E+00	99	4.3169E-05	62	4.3169E-05	62
2	0.0000E+00	99	0.0000E+00	99	1.0936E-04	41	1.0936E-04	41
3	0.0000E+00	99	-1.7764E-19	99	1.8084E-04	26	1.8084E-04	26
4	0.0000E+00	99	0.0000E+00	99	1.0664E-04	38	1.0664E-04	38
5	0.0000E+00	99	0.0000E+00	99	4.3403E-05	41	4.3403E-05	41
6	0.0000E+00	99	0.0000E+00	99	1.6936E-04	34	1.6936E-04	34
7	0.0000E+00	99	0.0000E+00	99	1.2069E-04	33	1.2069E-04	33
8	0.0000E+00	99	0.0000E+00	99	2.0810E-04	29	2.0810E-04	29
9	0.0000E+00	99	0.0000E+00	99	1.1385E-04	41	1.1385E-04	41
10	0.0000E+00	99	0.0000E+00	99	1.3556E-04	42	1.3556E-04	42

TABLE A13
ENERGY DEPOSITION FROM 20 MeV ELECTRONS AT 55.5 CM OF WATER

(MeV, normalized to one incident particle)

ZONE	PRIMARIES		KNOCK-ONS		GAMMA-SEC		TOTAL	
1	0.0000E+00	99	0.0000E+00	99	5.7519E-05	86	5.7519E-05	86
2	0.0000E+00	99	0.0000E+00	99	4.0860E-06	99	4.0860E-06	99
3	0.0000E+00	99	-1.7764E-19	99	6.9462E-05	60	6.9462E-05	60
4	0.0000E+00	99	0.0000E+00	99	1.6826E-04	60	1.6826E-04	60
5	0.0000E+00	99	0.0000E+00	99	9.9525E-05	66	9.9525E-05	66
6	0.0000E+00	99	0.0000E+00	99	7.9949E-05	55	7.9949E-05	55
7	0.0000E+00	99	0.0000E+00	99	9.8235E-05	55	9.8235E-05	55
8	0.0000E+00	99	0.0000E+00	99	1.1126E-04	63	1.1126E-04	63
9	0.0000E+00	99	0.0000E+00	99	1.2446E-05	99	1.2446E-05	99
10	0.0000E+00	99	0.0000E+00	99	6.3564E-05	40	6.3564E-05	40

TABLE A14

ENERGY DEPOSITION FROM 20 MeV ELECTRONS AT 74.0 CM OF WATER

(MeV, normalized to one incident particle)

ZONE	PRIMARIES		KNOCK-ONS		GAMMA-SEC		TOTAL	
1	0.0000E+00	99	0.0000E+00	99	0.0000E+00	99	0.0000E+00	99
2	0.0000E+00	99	0.0000E+00	99	0.0000E+00	99	0.0000E+00	99
3	0.0000E+00	99	-1.7764E-19	99	4.1282E-05	67	4.1282E-05	67
4	0.0000E+00	99	0.0000E+00	99	4.4739E-05	71	4.4739E-05	71
5	0.0000E+00	99	0.0000E+00	99	1.1964E-05	71	1.1964E-05	71
6	0.0000E+00	99	0.0000E+00	99	1.6701E-05	99	1.6701E-05	99
7	0.0000E+00	99	0.0000E+00	99	4.0066E-05	66	4.0066E-05	66
8	0.0000E+00	99	-2.7874E-05	99	1.9880E-05	99	-7.9936E-06	99
9	0.0000E+00	99	0.0000E+00	99	1.8621E-05	73	1.8621E-05	73
10	0.0000E+00	99	0.0000E+00	99	5.3425E-05	67	5.3425E-05	67

TABLE A15
ENERGY DEPOSITION FROM 100 MeV ELECTRONS AT 0.0 M OF AIR

(MeV, normalized to one incident particle)

ZONE	PRIMARIES		KNOCK-ONS		GAMMA-SEC		TOTAL	
1	2.8344E-01	1	-3.7217E-02	14	9.6919E-06	64	2.4623E-01	3
2	0.0000E+00	99	2.3119E-05	99	2.0178E-06	59	2.5137E-05	91
3	0.0000E+00	99	0.0000E+00	99	4.0565E-06	42	4.0565E-06	42
4	0.0000E+00	99	2.5746E-05	99	1.6071E-05	39	4.1817E-05	62
5	0.0000E+00	99	0.0000E+00	99	2.5504E-05	42	2.5504E-05	42
6	0.0000E+00	99	0.0000E+00	99	9.3378E-06	34	9.3378E-06	34
7	0.0000E+00	99	0.0000E+00	99	1.3360E-05	43	1.3360E-05	43
8	0.0000E+00	99	0.0000E+00	99	1.9238E-05	36	1.9238E-05	36
9	0.0000E+00	99	0.0000E+00	99	1.1033E-05	47	1.1033E-05	47
10	0.0000E+00	99	0.0000E+00	99	9.0893E-06	51	9.0893E-06	51

TABLE A16
ENERGY DEPOSITION FROM 100 MeV ELECTRONS AT 76.8 M OF AIR

(MeV, normalized to one incident particle)

ZONE	PRIMARIES		KNOCK-ONS		GAMMA-SEC		TOTAL	
1	2.4807E-01	1	-7.8895E+01	56	1.3832E-02	5	2.5402E-01	3
2	1.9389E-02	5	2.7530E-03	61	2.6628E-03	7	2.1481E-01	6
3	2.1309E-03	15	1.1093E-03	23	8.1654E-04	21	4.0568E-03	9
4	8.1601E-04	33	5.4671E-04	17	2.9823E-04	35	1.6609E-03	18
5	3.4005E-04	33	2.8156E-04	41	1.4427E-04	32	7.6587E-04	28
6	1.3220E-04	64	-1.8487E-04	99	1.7337E-04	23	1.2071E-04	99
7	1.3930E-04	56	4.5731E-05	78	1.1615E-05	32	3.0118E-04	40
8	8.4710E-05	79	6.0121E-06	99	8.9680E-05	47	1.8040E-04	40
9	1.0073E-04	83	0.0000E+00	99	4.5172E-05	28	1.4590E-04	55
10	1.0505E-04	99	0.0000E+00	99	5.9532E-05	25	1.6458E-04	61

TABLE A17

ENERGY DEPOSITION FROM 100 MeV ELECTRONS AT 153.5 M OF AIR

(MeV, normalized to one incident particle)

ZONE	PRIMARIES		KNOCK-ONS		GAMMA-SEC		TOTAL	
1	6.0558E-02	3	5.3843E-03	23	1.1662E-02	5	7.7604E-02	3
2	9.3455E-02	1	2.4235E-03	43	1.4000E-02	4	1.0988E-01	2
3	5.3233E-02	2	-2.5835E-03	72	5.6759E-03	5	5.6242E-02	4
4	1.9699E-02	5	-9.8918E-05	99	2.3253E-03	13	2.1925E-02	6
5	6.6715E-03	7	5.9743E-04	29	1.3110E-03	15	8.2999E-03	7
6	2.5666E-03	17	1.8186E-04	79	5.2242E-04	15	3.1709E-03	17
7	1.3664E-03	13	1.1369E-04	69	4.4142E-04	19	1.9215E-03	11
8	1.1379E-03	16	1.8589E-06	99	2.5871E-04	15	1.3984E-03	15
9	3.3818E-04	22	1.3621E-05	99	2.2045E-04	23	5.7226E-04	17
10	3.0485E-04	31	-1.3323E-18	93	1.4225E-04	31	4.4711E-04	29

TABLE A18
ENERGY DEPOSITION FROM 100 MeV ELECTRONS AT 307 M OF AIR

(MeV, normalized to one incident particle)

ZONE	PRIMARIES		KNOCK-ONS		GAMMA-SEC		TOTAL	
1	1.7119E-04	13	7.3188E-05	99	4.1002E-03	7	5.8853E-03	7
2	4.9354E-03	5	4.3134E-04	99	8.0540E-03	5	1.3422E-02	6
3	7.5822E-03	5	-3.0777E-04	99	7.5123E-03	5	1.4787E-02	6
4	7.9392E-03	5	-1.9492E-04	99	6.2450E-03	5	1.3888E-02	5
5	8.3857E-03	3	5.2199E-04	61	5.1270E-03	12	1.4033E-02	6
6	7.0361E-03	6	-3.5439E-04	95	3.7161E-03	8	1.0398E-02	4
7	6.0272E-03	7	-2.1551E-05	99	2.4940E-03	11	8.4996E-03	9
8	4.9155E-03	5	1.5663E-04	71	2.0459E-03	12	7.1180E-03	5
9	4.0861E-03	9	2.6810E-06	99	1.1934E-03	19	5.2821E-03	8
10	3.1359E-03	10	3.9832E-05	99	1.0100E-03	14	4.1850E-03	10

TABLE A19

ENERGY DEPOSITION FROM 100 MeV ELECTRONS AT 460.5 M OF AIR

(MeV, normalized to one incident particle)

ZONE	PRIMARIES		KNOCK-ONS		GAMMA-SEC		TOTAL	
1	0.0000E+00	99	4.0771E-05	99	1.4402E-03	16	1.4809E-03	16
2	0.0000E+00	99	2.6544E-04	37	3.2886E-03	5	3.5541E-03	5
3	0.0000E+00	99	2.0090E-04	58	3.8934E-03	4	4.0943E-03	5
4	0.0000E+00	99	3.1686E-05	99	3.3126E-03	7	3.3443E-03	7
5	0.0000E+00	99	1.9029E-04	41	2.8428E-03	14	3.0331E-03	14
6	0.0000E+00	99	-8.0847E-05	99	2.4017E-03	10	2.3208E-03	10
7	0.0000E+00	99	-6.0717E-05	99	2.1503E-03	7	2.0896E-03	9
8	0.0000E+00	99	3.9528E-06	99	1.6772E-03	9	1.6811E-03	15
9	0.0000E+00	99	-2.2157E-04	84	1.5826E-03	13	1.3610E-03	8
10	0.0000E+00	99	-5.3823E-05	90	1.3179E-03	17	1.2641E-03	18

TABLE A20

ENERGY DEPOSITION FROM 100 MeV ELECTRONS AT 0.0 CM OF LIQUID NITROGEN

(MeV, normalized to one incident particle)

ZONE	PRIMARIES		KNOCK-ONS		GAMMA-SEC		TOTAL	
1	3.1376E-01	1	-4.3907E-02	10	2.2752E-05	49	2.6987E-01	2
2	0.0000E+00	99	3.9232E-05	99	2.0393E-05	49	5.9736E-05	66
3	0.0000E+00	99	0.0000E+00	99	1.9265E-05	24	1.9265E-05	24
4	0.0000E+00	99	3.2825E-05	99	1.0080E-05	53	4.2906E-05	75
5	0.0000E+00	99	0.0000E+00	99	2.0080E-05	39	2.0080E-05	39
6	0.0000E+00	99	0.0000E+00	99	1.4801E-05	31	1.4801E-05	31
7	0.0000E+00	99	0.0000E+00	99	2.3271E-05	46	2.3271E-05	46
8	0.0000E+00	99	0.0000E+00	99	6.4380E-06	42	6.4380E-06	42
9	0.0000E+00	99	0.0000E+00	99	4.8463E-06	62	4.8463E-06	62
10	0.0000E+00	99	0.0000E+00	99	1.3843E-05	50	1.3843E-05	50

TABLE A21

ENERGY DEPOSITION FROM 100 MeV ELECTRONS AT 11.9 CM OF LIQUID NITROGEN

(MeV, normalized to one incident particle)

ZONE	PRIMARIES		KNOCK-ONS		GAMMA-SEC		TOTAL	
1	2.4642E-01	2	-1.4010E-02	37	1.5646E-02	4	2.4806E-01	3
2	5.9950E-02	4	1.2247E-03	99	5.0433E-03	4	6.6218E-02	5
3	6.0281E-03	11	2.6944E-03	23	1.7132E-03	16	1.0436E-02	10
4	1.9365E-03	14	3.6443E-04	96	6.9067E-04	21	2.9916E-03	16
5	5.0826E-04	26	4.2144E-04	27	2.5366E-04	32	1.1833E-03	16
6	3.8864E-04	35	2.1501E-04	49	1.9262E-04	39	7.9627E-04	23
7	3.9717E-05	99	1.0669E-04	48	7.9617E-05	21	2.2603E-04	30
8	7.3029E-05	59	9.0364E-05	74	1.7392E-04	25	3.3732E-04	31
9	5.8897E-05	75	-2.3039E-04	93	1.4890E-04	42	-2.2600E-05	99
10	0.0000E+00	99	3.3888E-05	99	5.4708E-05	49	8.8596E-05	44

TABLE A22

ENERGY DEPOSITION FROM 100 MeV ELECTRONS AT 23.8 CM OF LIQUID NITROGEN

(MeV, normalized to one incident particle)

ZONE	PRIMARIES		KNOCK-ONS		GAMMA-SEC		TOTAL	
1	4.4770E-02	3	-1.6708E-04	99	1.1914E-02	5	5.6516E-02	2
2	9.2995E-02	2	1.8310E-03	95	1.6342E-02	4	1.1117E-01	3
3	7.6223E-02	3	-2.3932E-03	81	1.0173E-02	8	8.4003E-02	4
4	3.8853E-02	3	-1.9318E-03	64	6.3378E-03	7	4.3259E-02	3
5	1.6980E-02	5	5.9162E-04	68	2.7241E-03	9	2.0296E-02	5
6	7.5181E-03	8	3.9643E-04	89	1.3422E-03	22	9.2568E-03	8
7	3.4120E-03	5	1.0832E-04	99	5.9281E-04	12	4.1823E-03	8
8	1.9411E-03	12	4.4515E-05	99	3.5570E-04	20	2.3413E-03	13
9	1.5531E-03	16	-1.2189E-04	99	5.2957E-04	31	1.9588E-03	20
10	7.0420E-04	21	0.0000E+00	99	4.5226E-04	32	1.1565E-03	20

TABLE A23

ENERGY DEPOSITION FROM 100 MeV ELECTRONS AT 47.7 CM OF LIQUID NITROGEN

(MeV, normalized to one incident particle)

ZONE	PRIMARIES		KNOCK-ONS		GAMMA-SEC		TOTAL	
1	1.6029E-03	13	2.2473E-04	99	3.4626E-03	11	5.2902E-03	11
2	4.5064E-03	8	-7.0198E-04	42	7.6267E-03	6	1.1431E-02	5
3	7.2659E-03	7	-4.8385E-04	99	7.5162E-03	7	1.4298E-02	4
4	9.4584E-03	8	4.1425E-04	99	7.2344E-03	7	1.7107E-02	7
5	1.0588E-02	5	1.3719E-04	99	6.9451E-03	4	1.7670E-02	3
6	1.0473E-02	5	7.4036E-05	99	5.7827E-03	5	1.6330E-02	3
7	1.0928E-02	7	3.2656E-04	76	4.2122E-03	8	1.5467E-03	5
8	9.8891E-03	4	3.9004E-04	52	3.4286E-03	6	1.3708E-02	3
9	7.3698E-03	4	2.6517E-04	47	2.5241E-03	10	1.0116E-02	3
10	6.5975E-03	6	6.4422E-05	99	2.1489E-03	11	8.8107E-03	5

TABLE A24

ENERGY DEPOSITION FROM 100 MeV ELECTRONS AT 71.5 CM OF LIQUID NITROGEN

(MeV, normalized to one incident particle)

ZONE	PRIMARIES		KNOCK-ONS		GAMMA-SEC		TOTAL	
1	0.0000E+00	99	-1.8999E-05	99	1.1323E-03	16	1.1133E-03	19
2	0.0000E+00	99	-5.8410E-04	86	3.2199E-03	16	2.5470E-03	17
3	0.0000E+00	99	3.2031E-04	43	3.3039E-03	9	3.6242E-03	9
4	0.0000E+00	99	4.6074E-05	99	3.4108E-03	8	3.4569E-03	8
5	0.0000E+00	99	2.5240E-04	39	3.2433E-03	13	3.4597E-03	13
6	0.0000E+00	99	-2.6163E-04	87	2.9747E-03	11	2.7131E-03	14
7	0.0000E+00	99	9.9899E-05	99	2.8571E-03	9	2.9570E-03	11
8	0.0000E+00	99	-1.8774E-04	99	2.3162E-03	10	2.1285E-03	19
9	0.0000E+00	99	9.1558E-05	67	2.1568E-03	13	2.2483E-03	13
10	0.0000E+00	99	1.0458E-04	36	1.5644E-03	18	1.6690E-03	18

AD-A164 523 STUDY OF OFF-AXIS RADIATION EXPOSURE FROM RELATIVISTIC ELECTRONS TRAVERSING THROUGH MATTER(U) NAVAL POSTGRADUATE SCHOOL MONTEREY CA R D FITZPATRICK DEC 85 2/2

UNCLASSIFIED F/G 20/8 NL

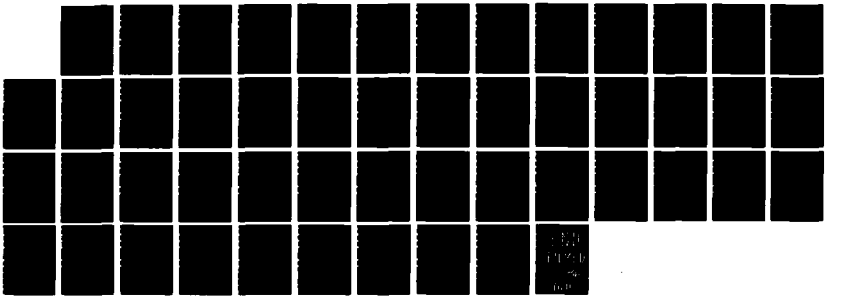

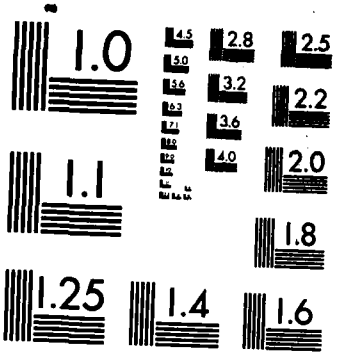

TABLE A25

ENERGY DEPOSITION FROM 100 MeV ELECTRONS AT 95.4 CM OF LIQUID NITROGEN

(MeV, normalized to one incident particle)

ZONE	PRIMARIES		KNOCK-ONS		GAMMA-SEC		TOTAL	
1	0.0000E+00	99	4.0315E-05	67	4.4337E-04	27	4.8369E-04	24
2	0.0000E+00	99	1.0030E-04	87	1.5208E-03	16	1.6211E-03	14
3	0.0000E+00	99	1.9102E-04	32	1.3465E-03	17	1.5375E-03	17
4	0.0000E+00	99	6.1450E-06	99	2.0000E-03	16	2.0061E-03	16
5	0.0000E+00	99	1.1667E-04	84	1.9115E-03	10	2.0282E-03	10
6	0.0000E+00	99	-3.6596E-04	93	2.0871E-03	14	1.7211E-03	28
7	0.0000E+00	99	-2.2827E-04	99	1.9225E-03	8	1.6942E-03	18
8	0.0000E+00	99	1.1085E-04	42	1.8938E-03	10	2.0047E-03	11
9	0.0000E+00	99	-1.7341E-06	99	1.6160E-03	21	1.6143E-03	18
10	0.0000E+00	99	-1.1863E-04	99	1.1306E-03	12	1.0119E-03	15

APPENDIX B

TABLE B1 : Calculated Off-Axis Dose From 100 MeV Electrons in Water

Zone	x-axis avg (cm)	Mass (gm)	Volume (cm3)	Energy Deposition (MeV/Particle)	Rads/Coulomb	1-Sigma Uncertainty
z axis-0.0 cm						
1	0.5	6.2832E-01	6.2832E-01	3.4279E-01	5.4557E+10	2
2	1.5	1.8850E+00	1.8850E+00	1.0545E-05	5.5942E+05	56
3	2.5	3.1416E+00	3.1416E+00	1.6286E-05	5.1840E+05	46
4	3.5	4.3982E+00	4.3982E+00	1.4226E-05	3.2345E+05	48
5	4.5	5.6549E+00	5.6549E+00	3.8545E-05	6.8162E+05	30
6	5.5	6.9115E+00	6.9115E+00	3.9568E-05	5.7250E+05	28
7	6.5	8.1681E+00	8.1681E+00	6.8358E-05	8.3689E+05	27
8	7.5	9.4248E+00	9.4248E+00	3.6054E-05	3.8254E+05	20
9	8.5	1.0068E+01	1.0068E+01	2.7955E-05	2.7766E+05	24
10	9.5	1.1938E+01	1.1938E+01	1.7707E-05	1.4832E+05	27
z axis- 9.2 cm						
1	0.5	6.2832E-01	6.2832E-01	3.5860E-01	5.7073E+10	3
2	1.5	1.8850E+00	1.8850E+00	5.2422E-02	2.7810E+09	3
3	2.5	3.1416E+00	3.1416E+00	7.0649E-03	2.2488E+08	7
4	3.5	4.3982E+00	4.3982E+00	2.4276E-03	5.5195E+07	13
5	4.5	5.6549E+00	5.6549E+00	1.4981E-03	2.6492E+07	16
6	5.5	6.9115E+00	6.9115E+00	6.0889E-04	8.8098E+06	25
7	6.5	8.1681E+00	8.1681E+00	3.1256E-04	3.8266E+06	26
8	7.5	9.4248E+00	9.4248E+00	2.2469E-04	2.3840E+06	27
9	8.5	1.0068E+01	1.0068E+01	2.1704E-04	2.1557E+06	27
10	9.5	1.1938E+01	1.1938E+01	2.3236E-04	1.9464E+06	52

z axis- 18.5 cm

1	0.5	6.2832E-01	6.2832E-01	1.1628E-01	1.8506E+10	3
2	1.5	1.8850E+00	1.8850E+00	1.6664E-01	8.8403E+09	2
3	2.5	3.1416E+00	3.1416E+00	8.9242E-02	2.8407E+09	3
4	3.5	4.3982E+00	4.3982E+00	3.5407E-02	8.0503E+08	5
5	4.5	5.6549E+00	5.6549E+00	1.4432E-02	2.5521E+08	4
6	5.5	6.9115E+00	6.9115E+00	5.1082E-03	7.3909E+07	13
7	6.5	8.1681E+00	8.1681E+00	3.1291E-03	3.8309E+07	8
8	7.5	9.4248E+00	9.4248E+00	2.0805E-03	2.2075E+07	11
9	8.5	1.0068E+01	1.0068E+01	6.6356E-04	6.5907E+06	28
10	9.5	1.1938E+01	1.1938E+01	7.0543E-04	5.9091E+06	15

z axis- 37.0 cm

1	0.5	6.2832E-01	6.2832E-01	1.0159E-02	1.6169E+09	6
2	1.5	1.8850E+00	1.8850E+00	2.2588E-02	1.1983E+09	6
3	2.5	3.1416E+00	3.1416E+00	2.8989E-02	9.2275E+08	3
4	3.5	4.3982E+00	4.3982E+00	2.8811E-02	6.5506E+08	3
5	4.5	5.6549E+00	5.6549E+00	2.6693E-02	4.7203E+08	4
6	5.5	6.9115E+00	6.9115E+00	2.3065E-02	3.3372E+08	7
7	6.5	8.1681E+00	8.1681E+00	1.9208E-02	2.3516E+08	2
8	7.5	9.4248E+00	9.4248E+00	1.4881E-02	1.5789E+08	7
9	8.5	1.0068E+01	1.0068E+01	1.0831E-02	1.0758E+08	3
10	9.5	1.1938E+01	1.1938E+01	7.3178E-03	6.1298E+07	12

z axis- 55.5 cm						
1	0.5	6.2832E-01	6.2832E-01	2.3203E-03	3.6929E+08	10
2	1.5	1.8850E+00	1.8850E+00	4.8092E-03	2.5513E+08	7
3	2.5	3.1416E+00	3.1416E+00	6.6824E-03	2.1271E+08	8
4	3.5	4.3982E+00	4.3982E+00	5.3228E-03	1.2102E+08	12
5	4.5	5.6549E+00	5.6549E+00	4.4260E-03	7.8268E+07	10
6	5.5	6.9115E+00	6.9115E+00	4.9684E-03	7.1886E+07	7
7	6.5	8.1681E+00	8.1681E+00	3.9722E-03	4.8631E+07	13
8	7.5	9.4248E+00	9.4248E+00	3.6555E-03	3.8786E+07	12
9	8.5	1.0068E+01	1.0068E+01	2.9225E-03	2.9027E+07	12
10	9.5	1.1938E+01	1.1938E+01	1.9987E-03	1.6742E+07	13
z axis- 74.0 cm						
1	0.5	6.2832E-01	6.2832E-01	1.1950E-03	1.9019E+08	22
2	1.5	1.8850E+00	1.8850E+00	2.3582E-03	1.2510E+08	8
3	2.5	3.1416E+00	3.1416E+00	3.0596E-03	9.7390E+07	15
4	3.5	4.3982E+00	4.3982E+00	3.4188E-03	7.7732E+07	11
5	4.5	5.6549E+00	5.6549E+00	3.2490E-03	5.7455E+07	8
6	5.5	6.9115E+00	6.9115E+00	3.4779E-03	5.0320E+07	12
7	6.5	8.1681E+00	8.1681E+00	2.8624E-03	3.5044E+07	9
8	7.5	9.4248E+00	9.4248E+00	2.3084E-03	2.4493E+07	9
9	8.5	1.0068E+01	1.0068E+01	2.0506E-03	2.0367E+07	9
10	9.5	1.1938E+01	1.1938E+01	1.4707E-03	1.2319E+07	24

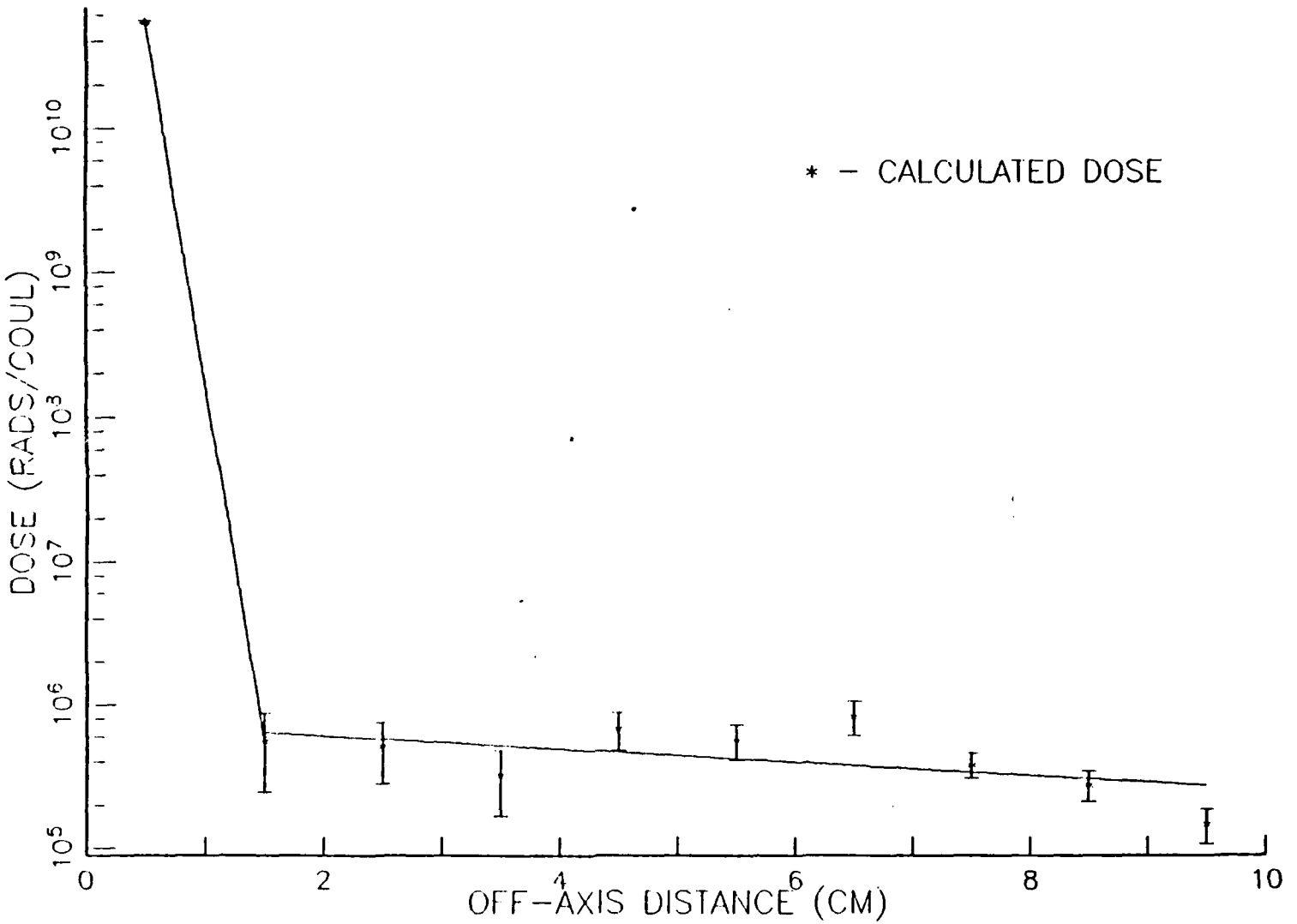

Figure B1: Calculated Dose Due to 100 MeV Electrons in Water-0.0 cm

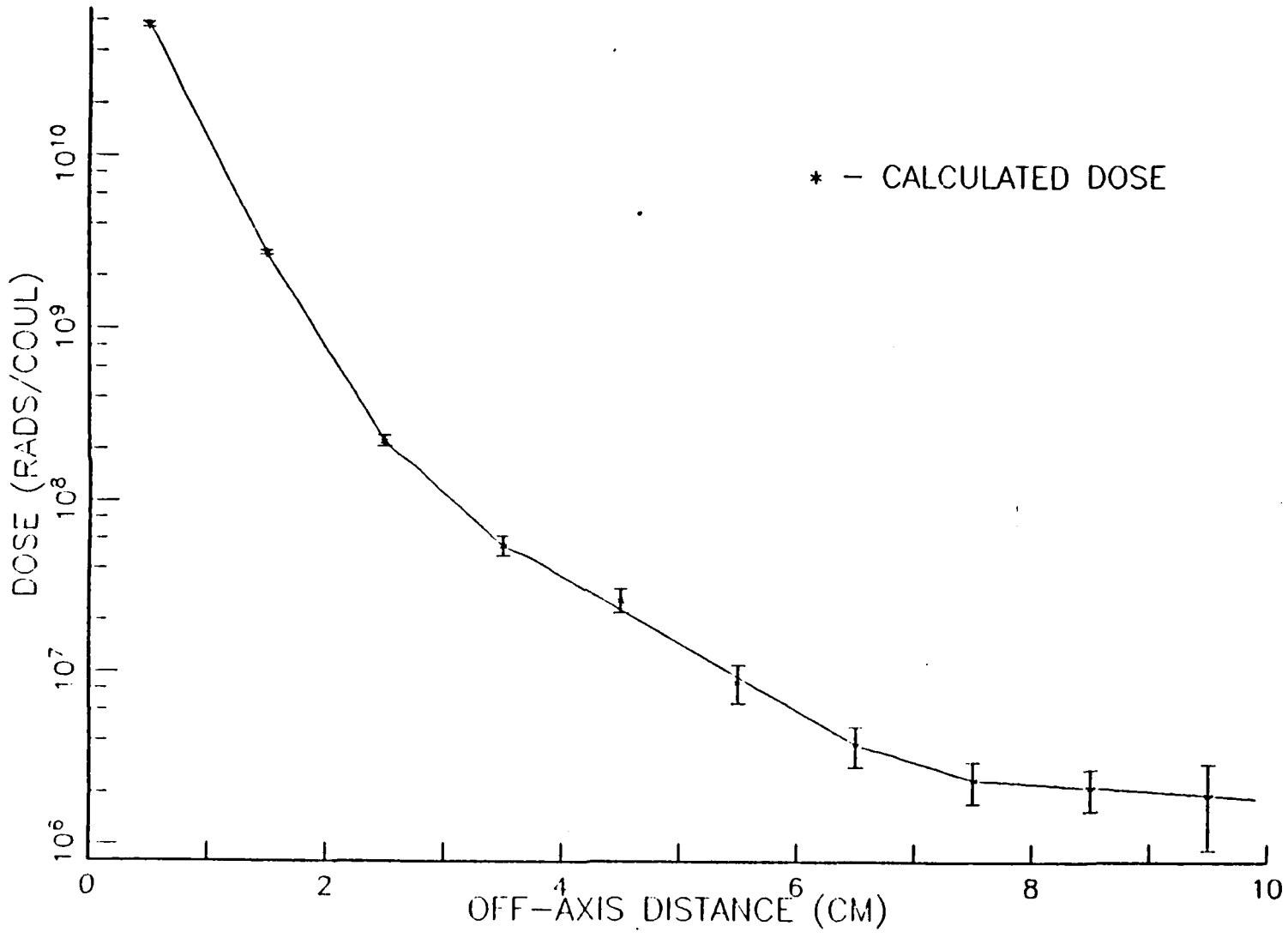

Figure B2: Calculated Dose Due to 100 MeV Electrons in Water–9.2 cm

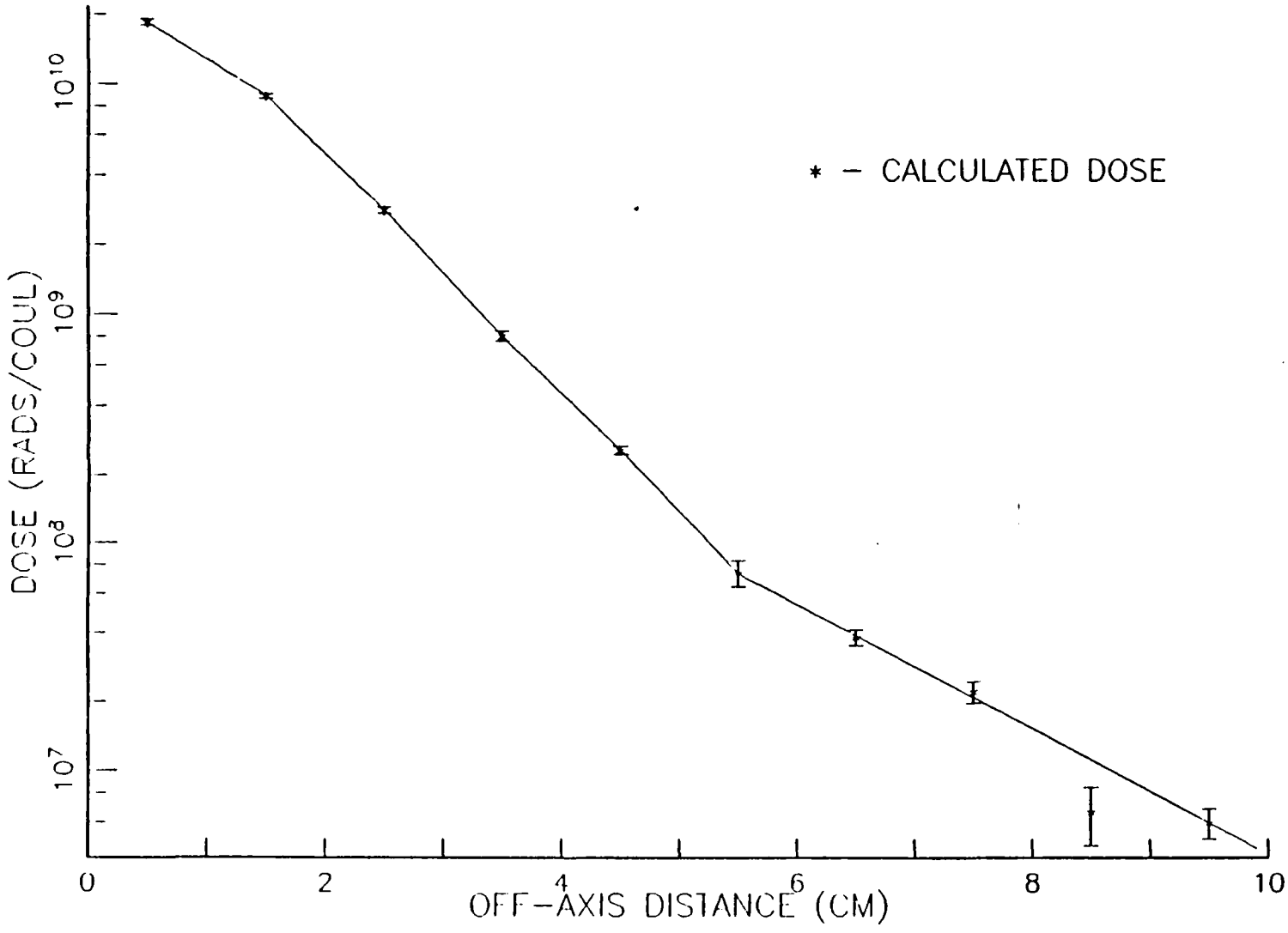

Figure B3: Calculated Dose Due to 100 MeV Electrons in Water-18.5 cm

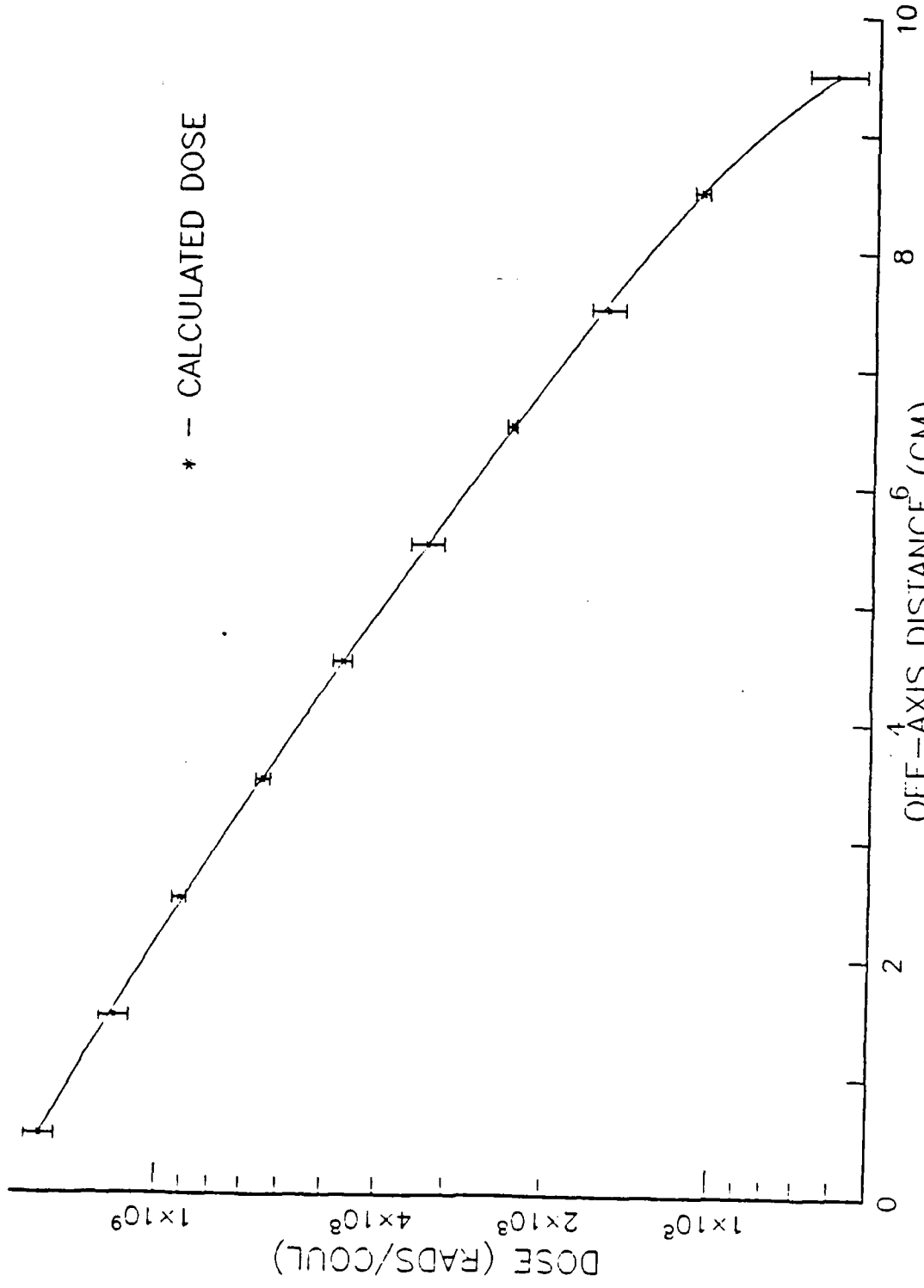

Figure B4: Calculated Dose Due to 100 MeV Electrons in Water-37.0 cm

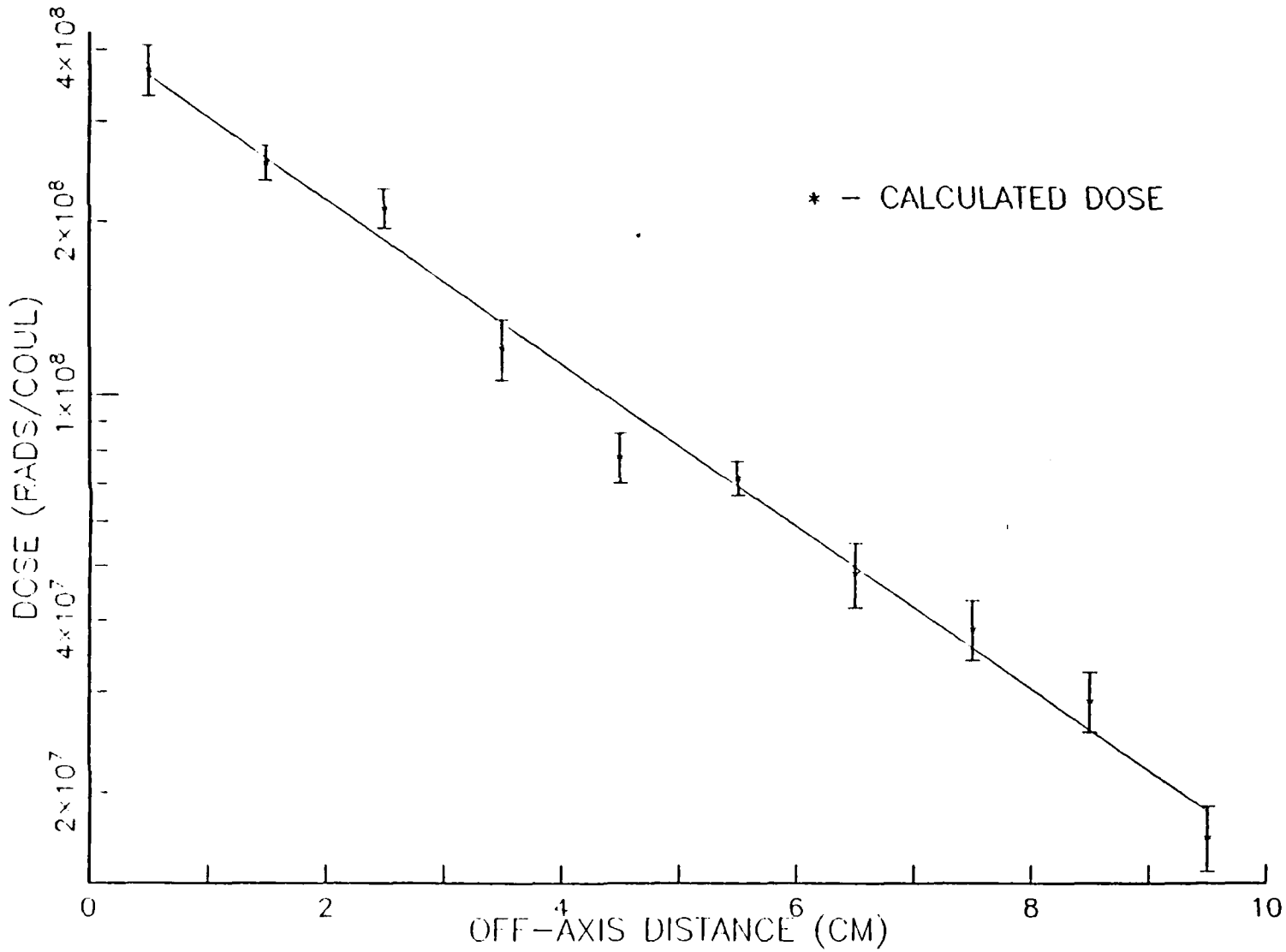

Figure B5: Calculated Dose Due to 100 MeV Electrons in Water-55.5 cm

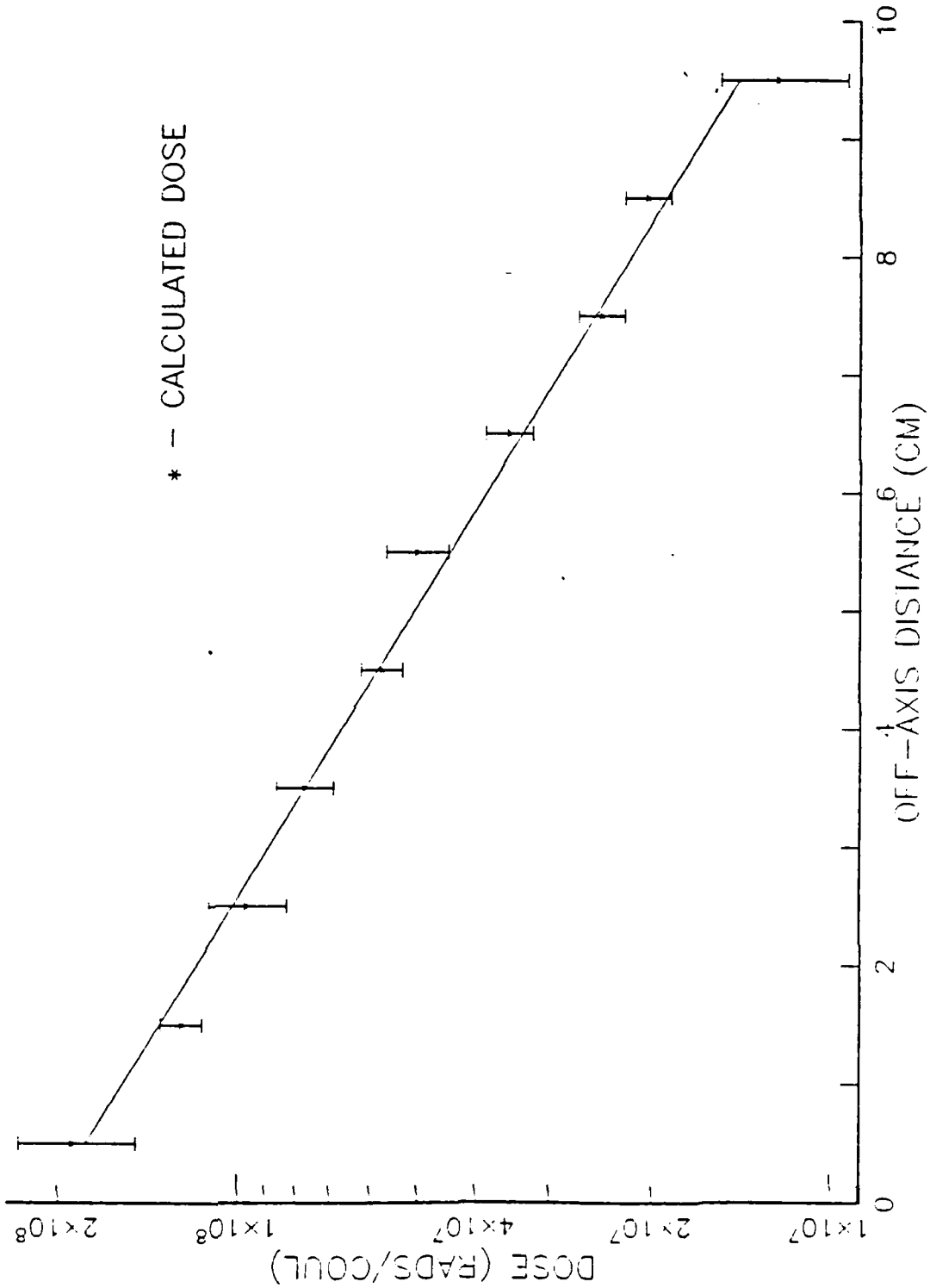

Figure B6: Calculated Dose Due to 100 MeV Electrons in Water-74.0 cm

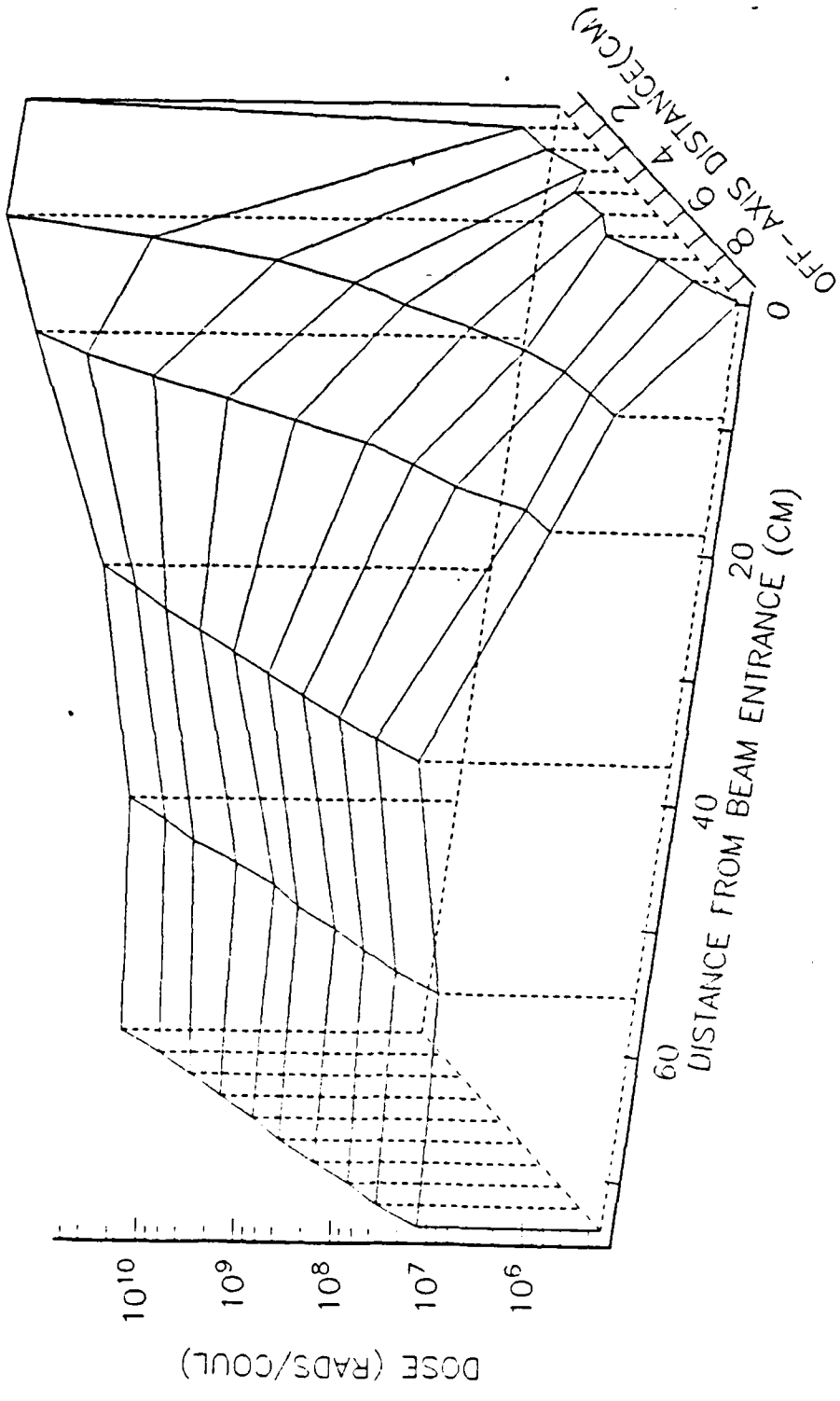

Figure B7: Unsmoothed Surface Plot of Dose Due to 100 MeV Electrons in Water

APPENDIX C

TABLE C1 : CALCULATED OFF-AXIS DOSE FROM 100 MeV ELECTRONS IN AIR

Zone	x-axis avg (m)	Mass (gm)	Volume (m3)	Energy Deposition (MeV/Particle)	Rads/Coulomb	1-Sigma Uncertainty
z axis-0.0 m						
1	4.15	2.6533E+05	2.1642E+08	2.4623E-01	9.2801E+04	3
2	12.45	7.9601E+05	6.4927E+08	2.5137E-05	3.1579E+00	91
3	20.75	1.3267E+06	1.0821E+09	4.0565E-06	3.0577E-01	42
4	29.05	1.8574E+06	1.5150E+09	4.1817E-05	2.2514E+00	62
5	37.35	2.3880E+06	1.9478E+09	2.5504E-05	1.0680E+00	42
6	45.65	2.9187E+06	2.3807E+09	9.3378E-06	3.1993E-01	34
7	53.95	3.4494E+06	2.8135E+09	1.3360E-05	3.8732E-01	43
8	62.25	3.9801E+06	3.2464E+09	1.9238E-05	4.8336E-01	36
9	70.55	4.5107E+06	3.6792E+09	1.1033E-05	2.4460E-01	47
10	78.85	5.0414E+06	4.1121E+09	9.0893E-06	1.8029E-01	51
z axis- 76.8 m						
1	4.15	2.6533E+05	2.1642E+08	2.5402E-01	9.5737E+04	3
2	12.45	7.9601E+05	6.4927E+08	2.4805E-02	3.1162E+03	6
3	20.75	1.3267E+06	1.0821E+09	4.0568E-03	3.0579E+02	9
4	29.05	1.8574E+06	1.5150E+09	1.6609E-03	8.9421E+01	18
5	37.35	2.3880E+06	1.9478E+09	7.6587E-04	3.2072E+01	28
6	45.65	2.9187E+06	2.3807E+09	1.2070E-04	4.1353E+00	99
7	53.95	3.4494E+06	2.8135E+09	3.0118E-04	8.7315E+00	40
8	62.25	3.9801E+06	3.2464E+09	1.8040E-04	4.5326E+00	40
9	70.55	4.5107E+06	3.6792E+09	1.4590E-04	3.2345E+00	55
10	78.85	5.0414E+06	4.1121E+09	1.6458E-04	3.2645E+00	61

z axis- 153.5 m

1	4.15	2.6533E+05	2.1642E+08	7.7604E-02	2.9248E+04	3
2	12.45	7.9601E+05	6.4927E+08	1.0988E-01	1.3804E+04	2
3	20.75	1.3267E+06	1.0821E+09	5.6242E-02	4.2394E+03	4
4	29.05	1.8574E+06	1.5150E+09	2.1925E-02	1.1804E+03	6
5	37.35	2.3880E+06	1.9478E+09	8.2999E-03	3.4757E+02	7
6	45.65	2.9187E+06	2.3807E+09	3.2709E-03	1.1207E+02	17
7	53.95	3.4494E+06	2.8135E+09	1.9215E-03	5.5706E+01	11
8	62.25	3.9801E+06	3.2464E+09	1.3984E-03	3.5135E+01	15
9	70.55	4.5107E+06	3.6792E+09	5.7226E-04	1.2687E+01	17
10	78.85	5.0414E+06	4.1121E+09	4.4711E-04	8.8687E+00	29

z axis- 307.0 m

1	4.15	2.6533E+05	2.1642E+08	5.8853E-03	2.2181E+03	7
2	12.45	7.9601E+05	6.4927E+08	1.3422E-02	1.6862E+03	6
3	20.75	1.3267E+06	1.0821E+09	1.4787E-02	1.1146E+03	6
4	29.05	1.8574E+06	1.5150E+09	1.3888E-02	7.4772E+02	5
5	37.35	2.3880E+06	1.9478E+09	1.4033E-02	5.8765E+02	6
6	45.65	2.9187E+06	2.3807E+09	1.0398E-02	3.5625E+02	4
7	53.95	3.4494E+06	2.8135E+09	8.4996E-03	2.4641E+02	9
8	62.25	3.9801E+06	3.2464E+09	7.1180E-03	1.7884E+02	5
9	70.55	4.5107E+06	3.6792E+09	5.2821E-03	1.1710E+02	8
10	78.85	5.0414E+06	4.1121E+09	4.1858E-03	8.3028E+01	10

z axis- 460.5 m

1	4.15	2.6533E+05	2.1642E+08	1.4809E-03	5.5813E+02	16
2	12.45	7.9601E+05	6.4927E+08	3.5441E-03	4.4524E+02	5
3	20.75	1.3267E+06	1.0821E+09	4.0943E-03	3.0862E+02	5
4	29.05	1.8574E+06	1.5150E+09	3.3443E-03	1.8005E+02	7
5	37.35	2.3880E+06	1.9478E+09	3.0331E-03	1.2701E+02	14
6	45.65	2.9187E+06	2.3807E+09	2.3208E-03	7.9514E+01	10
7	53.95	3.4494E+06	2.8135E+09	2.0896E-03	6.0580E+01	9
8	62.25	3.9801E+06	3.2464E+09	1.6811E-03	4.2238E+01	15
9	70.55	4.5107E+06	3.6792E+09	1.3610E-03	3.0173E+01	8
10	78.85	5.0414E+06	4.1121E+09	1.2641E-03	2.5074E+01	18

z axis- 614.0 m

1	4.15	2.6533E+05	2.1642E+08	0.0000E+00	0.0000E+00	99
2	12.45	7.9601E+05	6.4927E+08	0.0000E+00	0.0000E+00	99
3	20.75	1.3267E+06	1.0821E+09	0.0000E+00	0.0000E+00	99
4	29.05	1.8574E+06	1.5150E+09	0.0000E+00	0.0000E+00	99
5	37.35	2.3880E+06	1.9478E+09	0.0000E+00	0.0000E+00	99
6	45.65	2.9187E+06	2.3807E+09	0.0000E+00	0.0000E+00	99
7	53.95	3.4494E+06	2.8135E+09	0.0000E+00	0.0000E+00	99
8	62.25	3.9801E+06	3.2464E+09	0.0000E+00	0.0000E+00	99
9	70.55	4.5107E+06	3.6792E+09	0.0000E+00	0.0000E+00	99
10	78.85	5.0414E+06	4.1121E+09	0.0000E+00	0.0000E+00	99

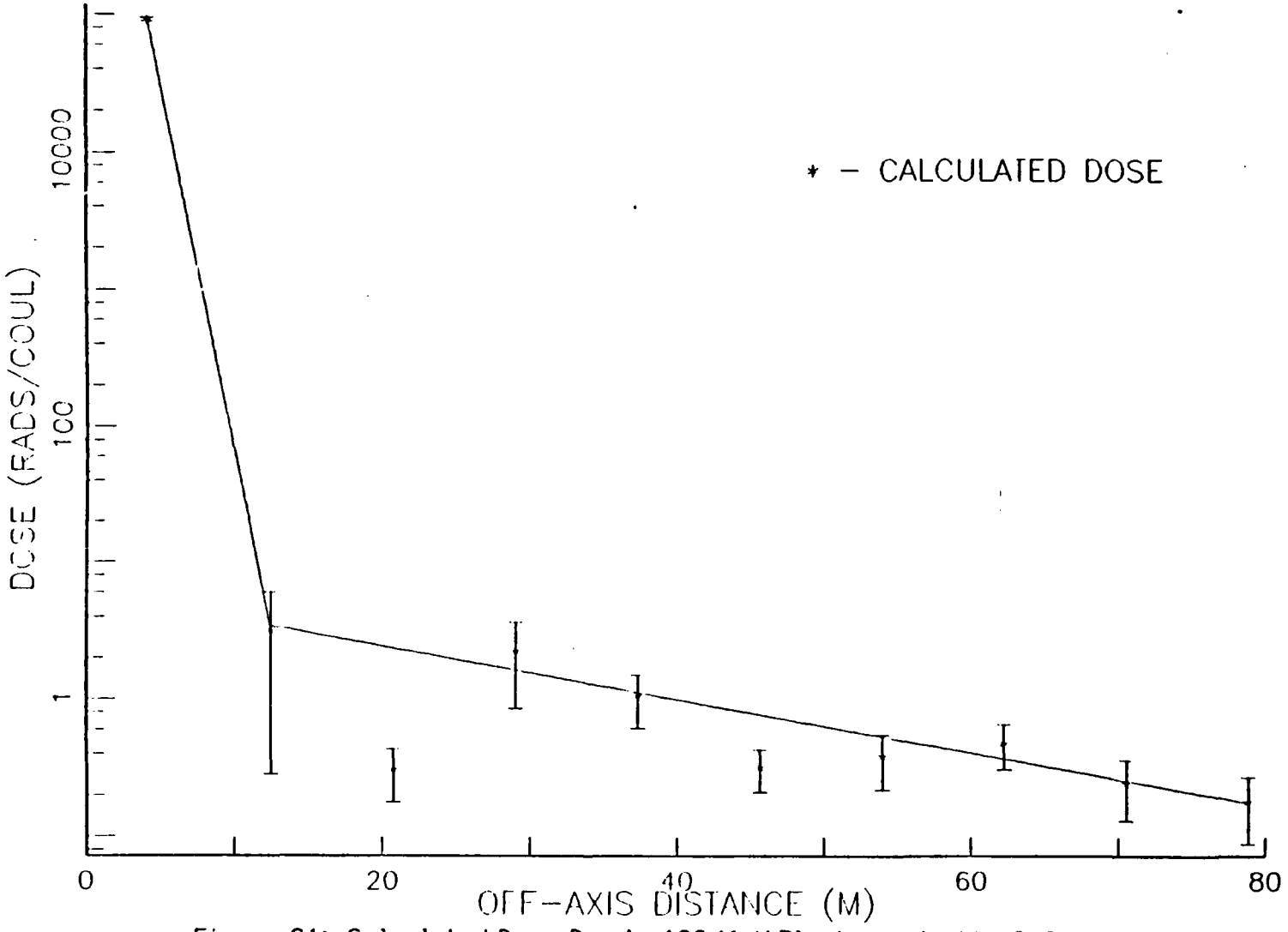

Figure C1: Calculated Dose Due to 100 MeV Electrons in Air-0.0 m

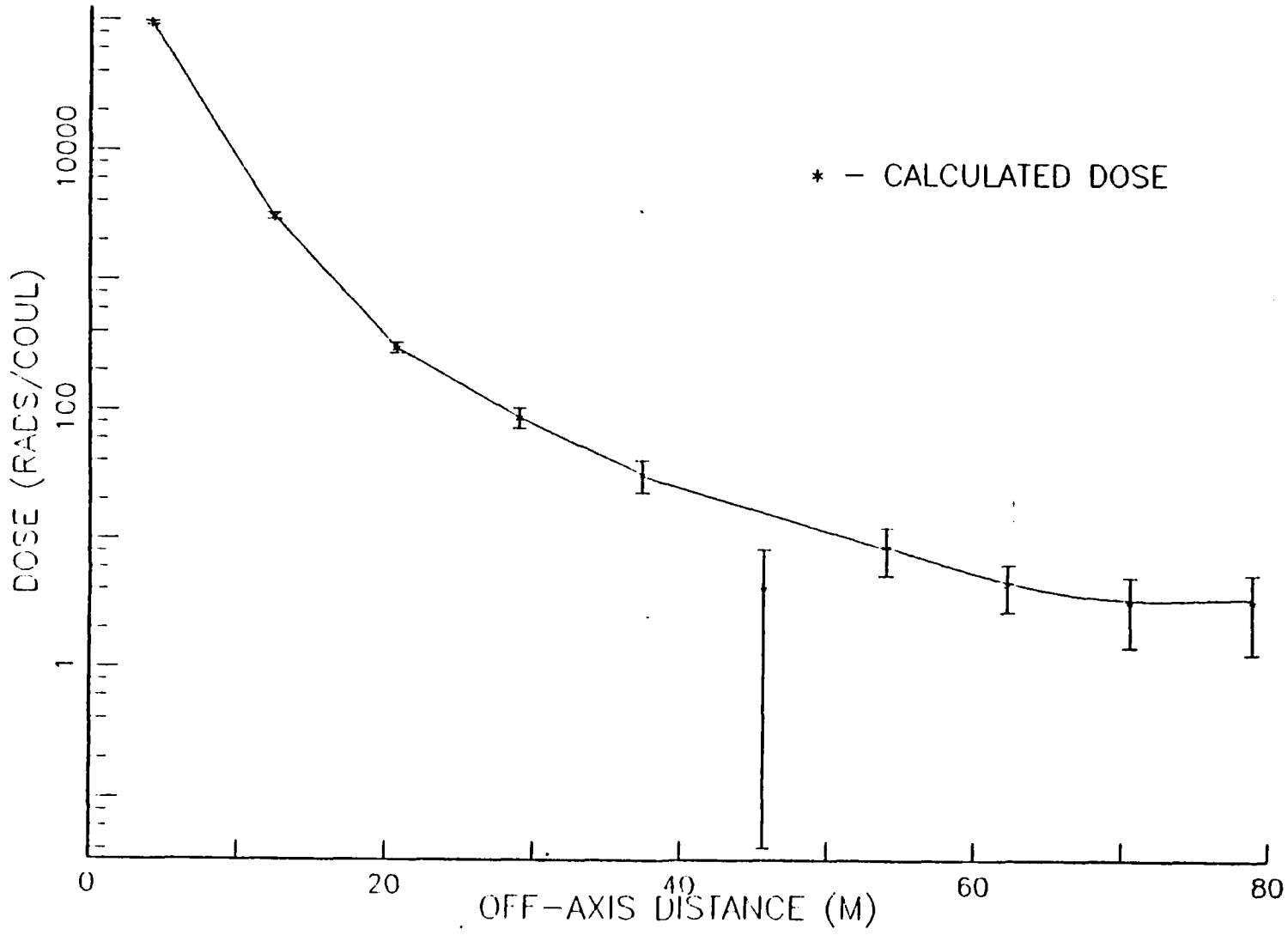

Figure C2: Calculated Dose Due to 100 MeV Electrons in Air-76.8 m

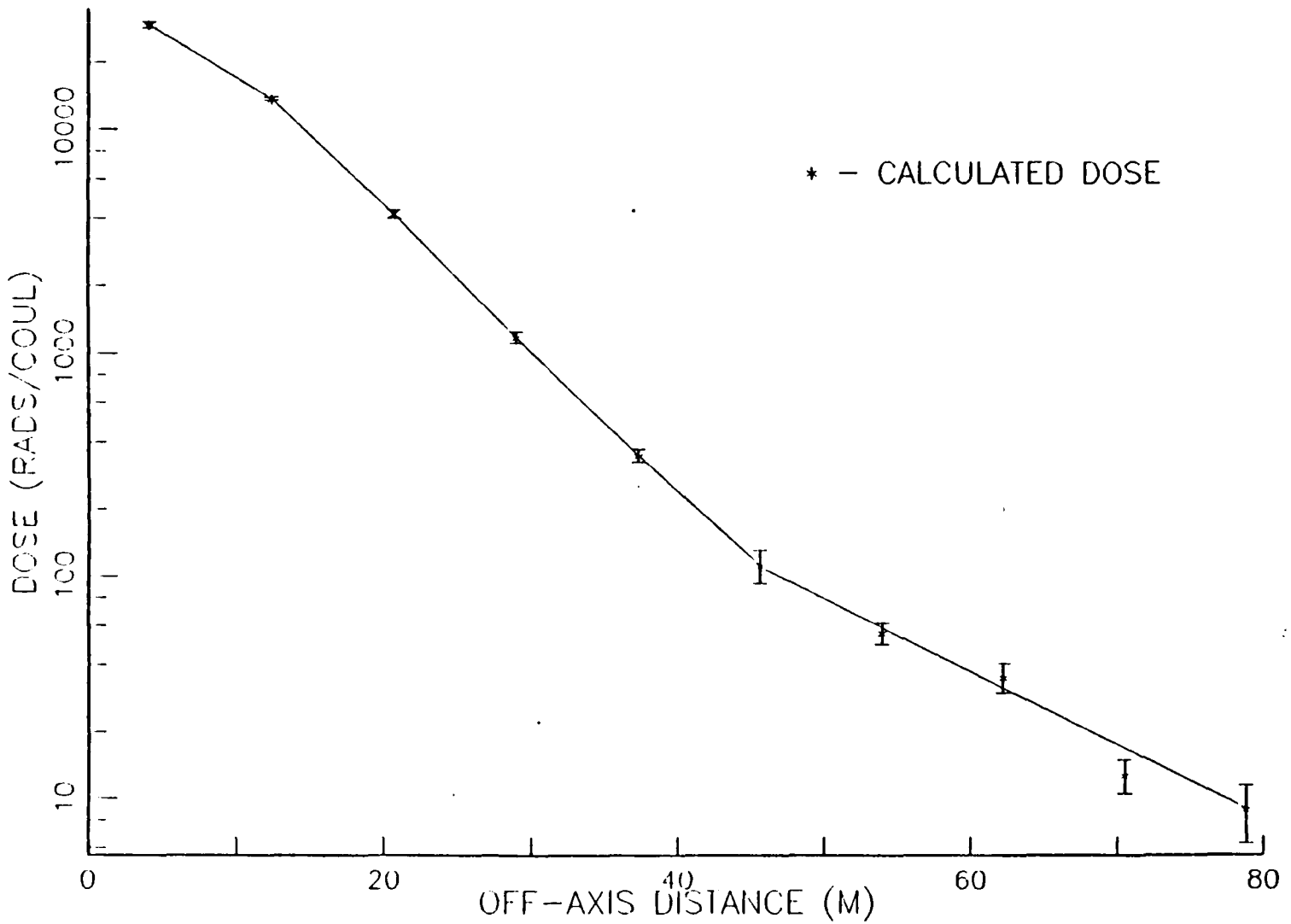

Figure C3: Calculated Dose Due to 100 MeV Electrons in Air–153.5 m

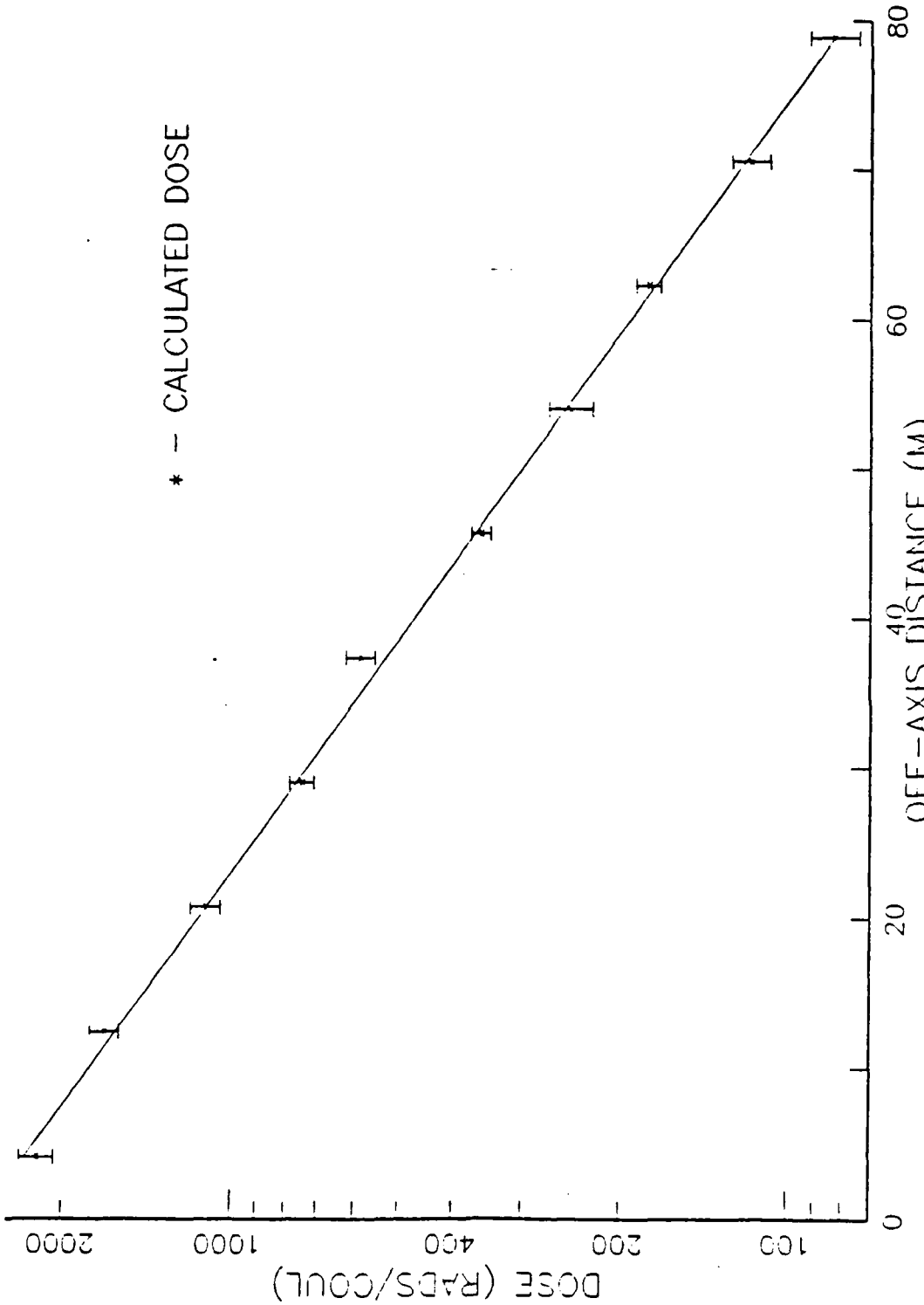

Figure C4: Calculated Dose Due to 100 MeV Electrons in Air-307 m

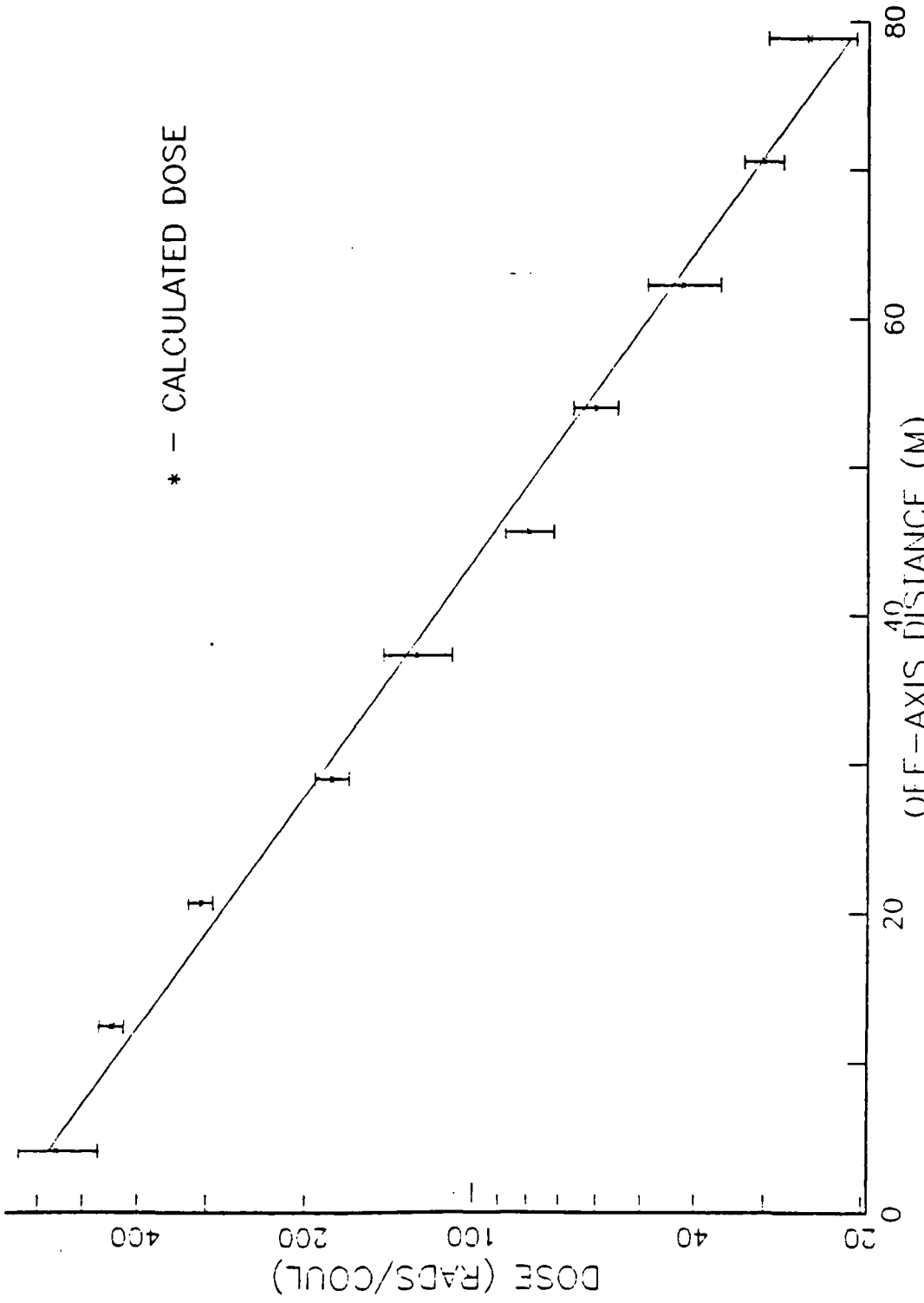

Figure C5: Calculated Dose Due to 100 MeV Electrons in Air-460.5 m

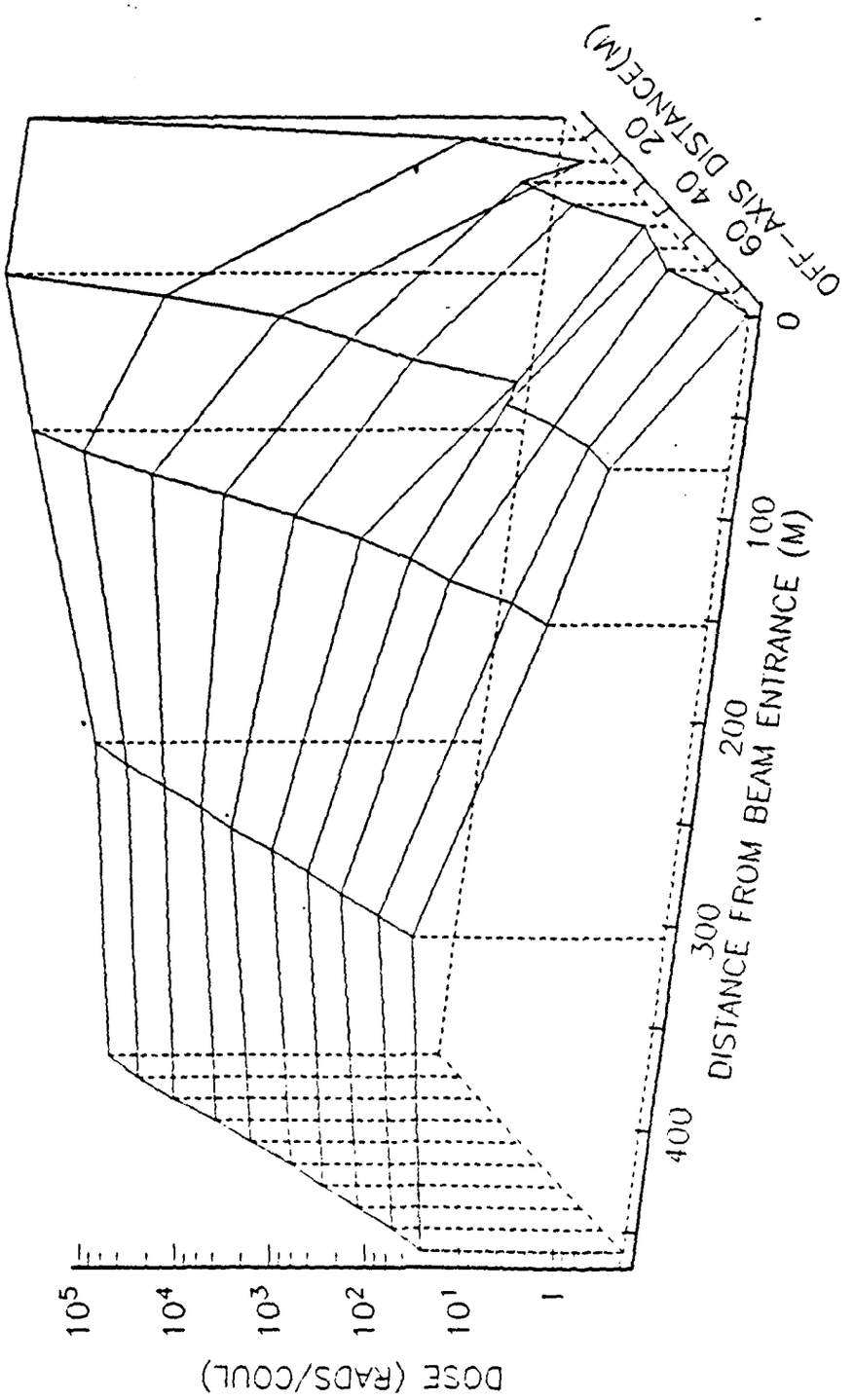

Figure C6: Unsmoothed Surface Plot of Dose Due to 100 MeV Electrons in Air

APPENDIX D

TABLE D1 : CALCULATED OFF-AXIS DOSE FROM 100 MeV ELECTRONS IN LIQUID NITROGEN

Zone	x-axis avg (cm)	Mass (gm)	Volume (cm3)	Energy Deposition (MeV/Particle)	Rads/Coulomb	1-Sigma Uncertainty
z axis-0.0 cm						
1	0.5	5.0894E-01	6.2832E-01	2.6897E-01	5.2849E+10	2
2	1.5	1.5269E+00	1.8850E+00	5.9736E-05	3.9124E+06	66
3	2.5	2.5447E+00	3.1416E+00	1.9265E-05	7.5706E+05	24
4	3.5	3.5625E+00	4.3982E+00	4.2906E-05	1.2044E+06	75
5	4.5	4.5805E+00	5.6549E+00	2.0801E-05	4.5412E+05	39
6	5.5	5.5983E+00	6.9115E+00	1.4804E-05	2.6444E+05	31
7	6.5	6.6162E+00	8.1681E+00	2.3270E-05	3.5171E+05	46
8	7.5	7.6341E+00	9.4248E+00	6.4380E-06	8.4332E+04	42
9	8.5	8.1552E+00	1.0068E+01	4.8463E-06	5.9426E+04	62
10	9.5	9.6698E+00	1.1938E+01	1.3843E-05	1.4316E+05	50
z axis- 11.9 cm						
12	0.5	5.0894E-01	6.2832E-01	2.4806E-01	4.8741E+10	3
13	1.5	1.5269E+00	1.8850E+00	6.6218E-02	4.3369E+09	5
14	2.5	2.5447E+00	3.1416E+00	1.0436E-02	4.1011E+08	10
15	3.5	3.5625E+00	4.3982E+00	2.9916E-03	8.3974E+07	16
16	4.5	4.5805E+00	5.6549E+00	1.1833E-03	2.5834E+07	16
17	5.5	5.5983E+00	6.9115E+00	7.9627E-04	1.4223E+07	23
18	6.5	6.6162E+00	8.1681E+00	2.2603E-04	3.4163E+06	30
19	7.5	7.6341E+00	9.4248E+00	3.3732E-04	4.4186E+06	31
20	8.5	8.1552E+00	1.0068E+01	0.0000E+00	0.0000E+00	99
21	9.5	9.6698E+00	1.1938E+01	8.8596E-05	9.1622E+05	44

z axis- 23.8 cm

23	0.5	5.0894E-01	6.2832E-01	5.6516E-02	1.1105E+10	2
24	1.5	1.5269E+00	1.8850E+00	1.1117E-01	7.2810E+09	3
25	2.5	2.5447E+00	3.1416E+00	8.4003E-02	3.3011E+09	4
26	3.5	3.5625E+00	4.3982E+00	4.3259E-02	1.2143E+09	3
27	4.5	4.5805E+00	5.6549E+00	2.0296E-02	4.4310E+08	5
28	5.5	5.5983E+00	6.9115E+00	9.2568E-03	1.6535E+08	8
29	6.5	6.6162E+00	8.1681E+00	4.1823E-03	6.3213E+07	8
30	7.5	7.6341E+00	9.4248E+00	2.3413E-03	3.0669E+07	13
31	8.5	8.1552E+00	1.0068E+01	1.9588E-03	2.4019E+07	20
32	9.5	9.6698E+00	1.1938E+01	1.1565E-03	1.1960E+07	20

z axis- 47.7 cm

34	0.5	5.0894E-01	6.2832E-01	5.2902E-03	1.0395E+09	11
35	1.5	1.5269E+00	1.8850E+00	1.1431E-02	7.4867E+08	5
36	2.5	2.5447E+00	3.1416E+00	1.4298E-02	5.6187E+08	4
37	3.5	3.5625E+00	4.3982E+00	1.7107E-02	4.8019E+08	7
38	4.5	4.5805E+00	5.6549E+00	1.7670E-02	3.8577E+08	3
39	5.5	5.5983E+00	6.9115E+00	1.6330E-02	2.9169E+08	3
40	6.5	6.6162E+00	8.1681E+00	1.5467E-02	2.3378E+08	5
41	7.5	7.6341E+00	9.4248E+00	1.3708E-02	1.7956E+08	3
42	8.5	8.1552E+00	1.0068E+01	1.0159E-02	1.2457E+08	3
43	9.5	9.6698E+00	1.1938E+01	8.8107E-03	9.1116E+07	5

z axis- 71.5 cm						
45	0.5	5.0894E-01	6.2832E-01	1.1133E-03	2.1875E+08	19
46	1.5	1.5269E+00	1.8850E+00	2.5457E-03	1.6673E+08	17
47	2.5	2.5447E+00	3.1416E+00	3.6242E-03	1.4242E+08	9
48	3.5	3.5625E+00	4.3982E+00	3.4569E-03	9.7035E+07	8
49	4.5	4.5805E+00	5.6549E+00	3.4957E-03	7.6318E+07	13
50	5.5	5.5983E+00	6.9115E+00	2.7131E-03	4.8463E+07	14
51	6.5	6.6162E+00	8.1681E+00	2.9570E-03	4.4694E+07	11
52	7.5	7.6341E+00	9.4248E+00	2.1285E-03	2.7882E+07	19
53	8.5	8.1552E+00	1.0068E+01	2.2483E-03	2.7569E+07	13
54	9.5	9.6698E+00	1.1938E+01	1.6690E-03	1.7260E+07	18
z axis- 95.4 cm						
56	0.5	5.0894E-01	6.2832E-01	4.8369E-04	9.5039E+07	24
57	1.5	1.5269E+00	1.8850E+00	1.6211E-03	1.0617E+08	14
58	2.5	2.5447E+00	3.1416E+00	1.5375E-03	6.0420E+07	17
59	3.5	3.5625E+00	4.3982E+00	2.0061E-03	5.6311E+07	16
60	4.5	4.5805E+00	5.6549E+00	2.0282E-03	4.4279E+07	10
61	5.5	5.5983E+00	6.9115E+00	1.7211E-03	3.0743E+07	28
62	6.5	6.6162E+00	8.1681E+00	1.6942E-03	2.5607E+07	18
63	7.5	7.6341E+00	9.4248E+00	2.0047E-03	2.6260E+07	11
64	8.5	8.1552E+00	1.0068E+01	1.6143E-03	1.9795E+07	18
65	9.5	9.6698E+00	1.1938E+01	1.0119E-03	1.0465E+07	15

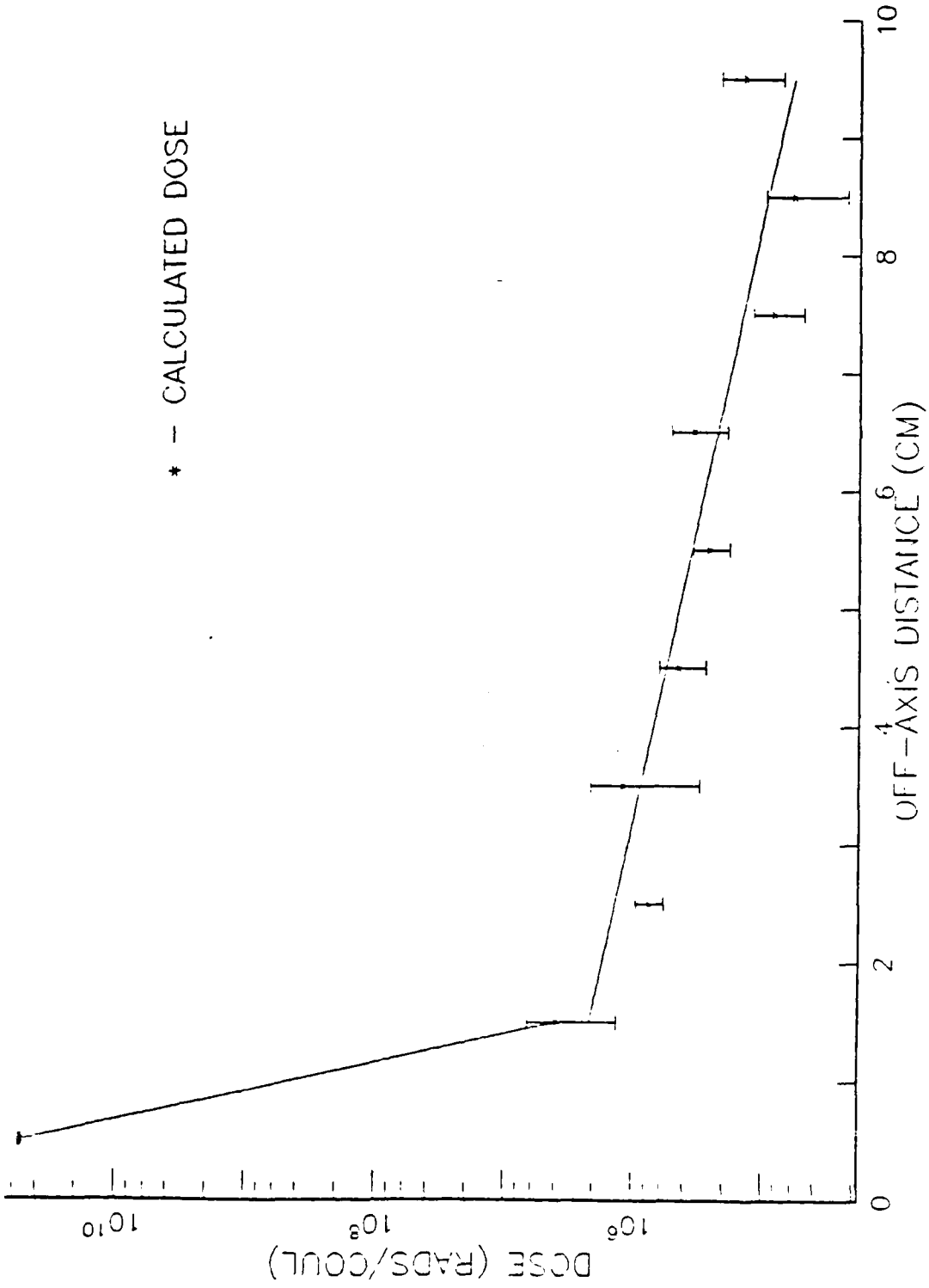

Figure D1: Calculated Dose Due to 100 MeV Electrons in LN_2-0.0 cm

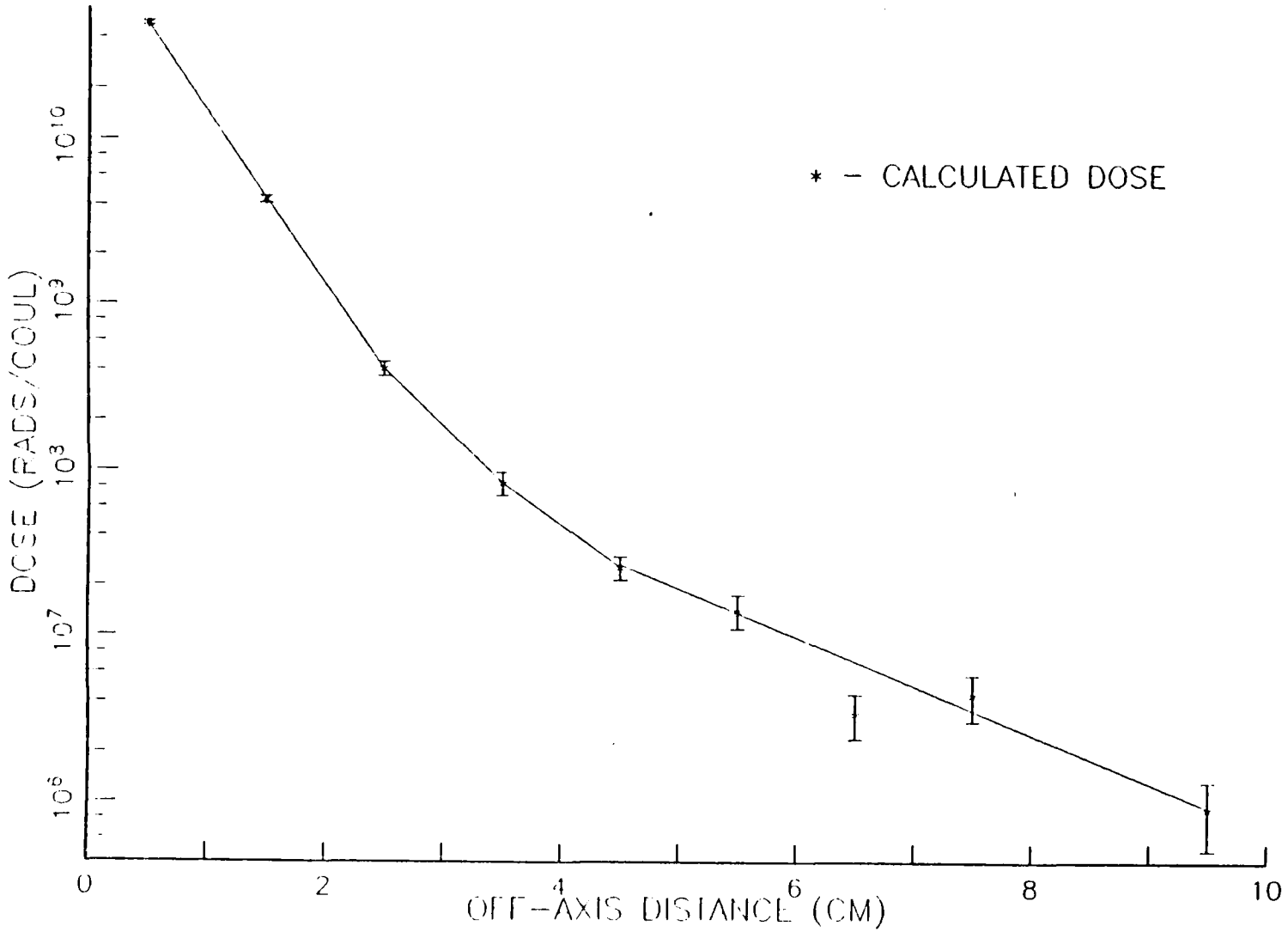

Figure D2: Calculated Dose Due to 100 MeV Electrons in LN_2-11.9 cm

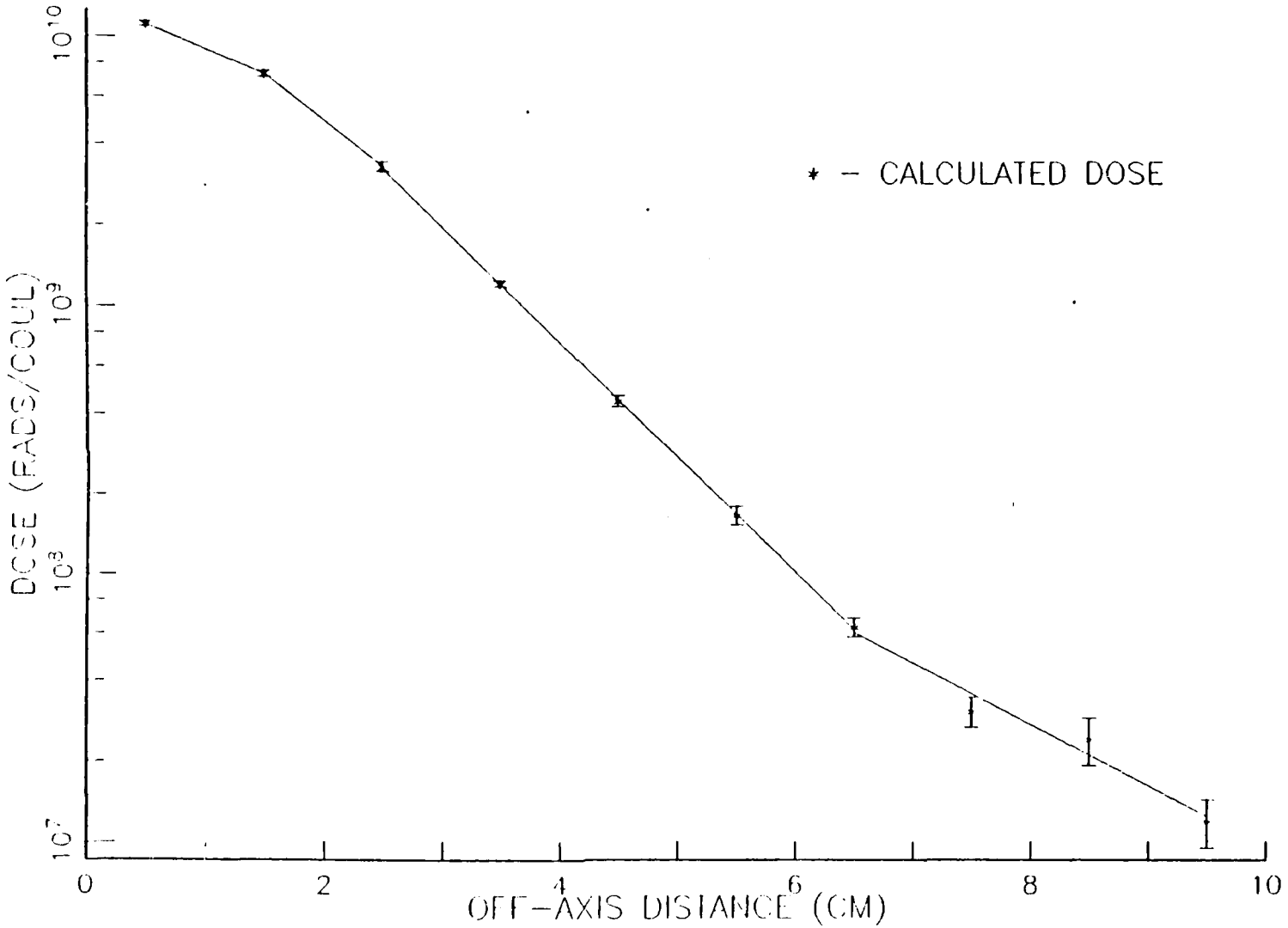

Figure D3: Calculated Dose Due to 100 MeV Electrons in LN_2-23.8 cm

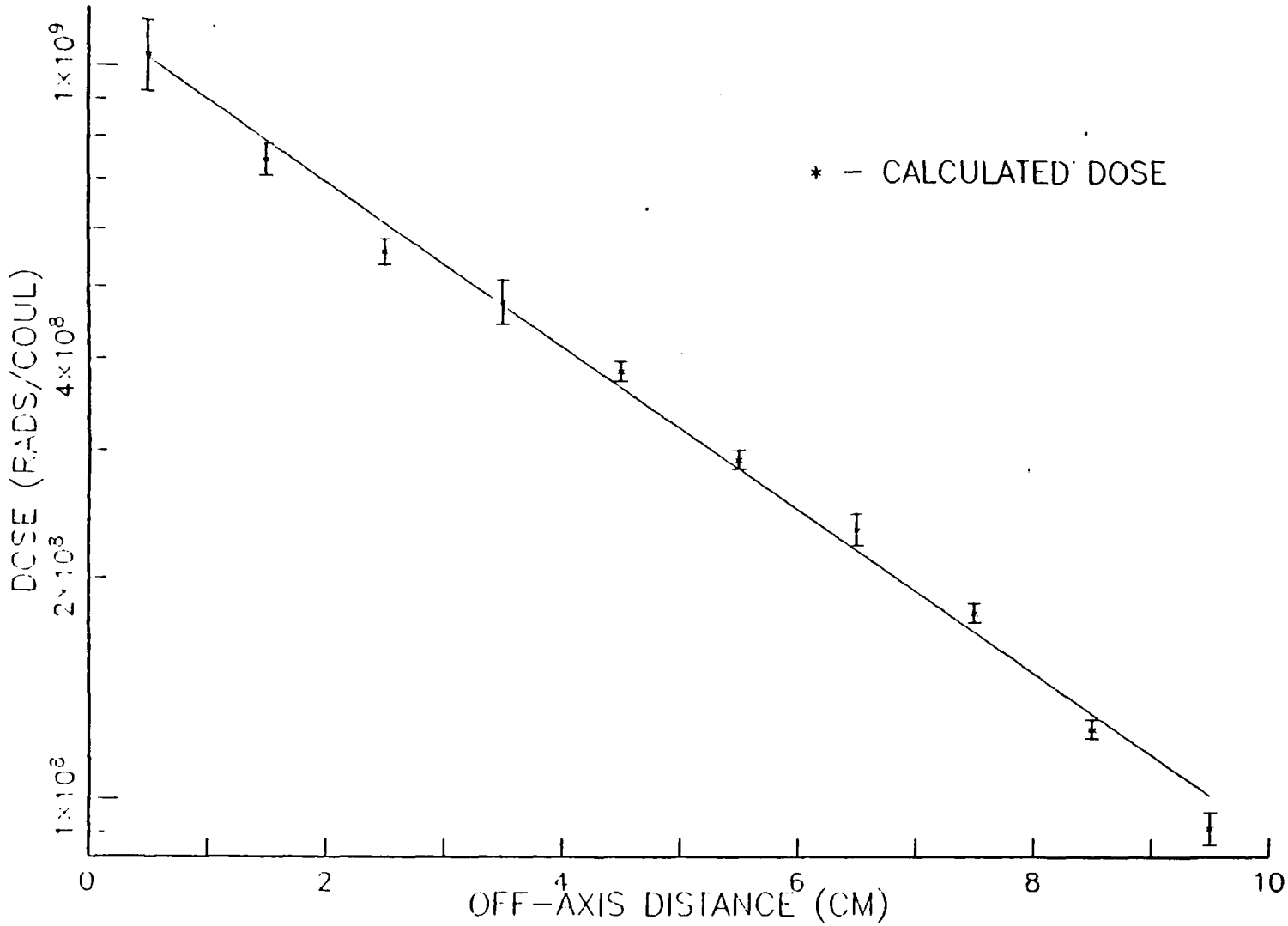

Figure D4: Calculated Dose Due to 100 MeV Electrons in LN_2-47.7 cm

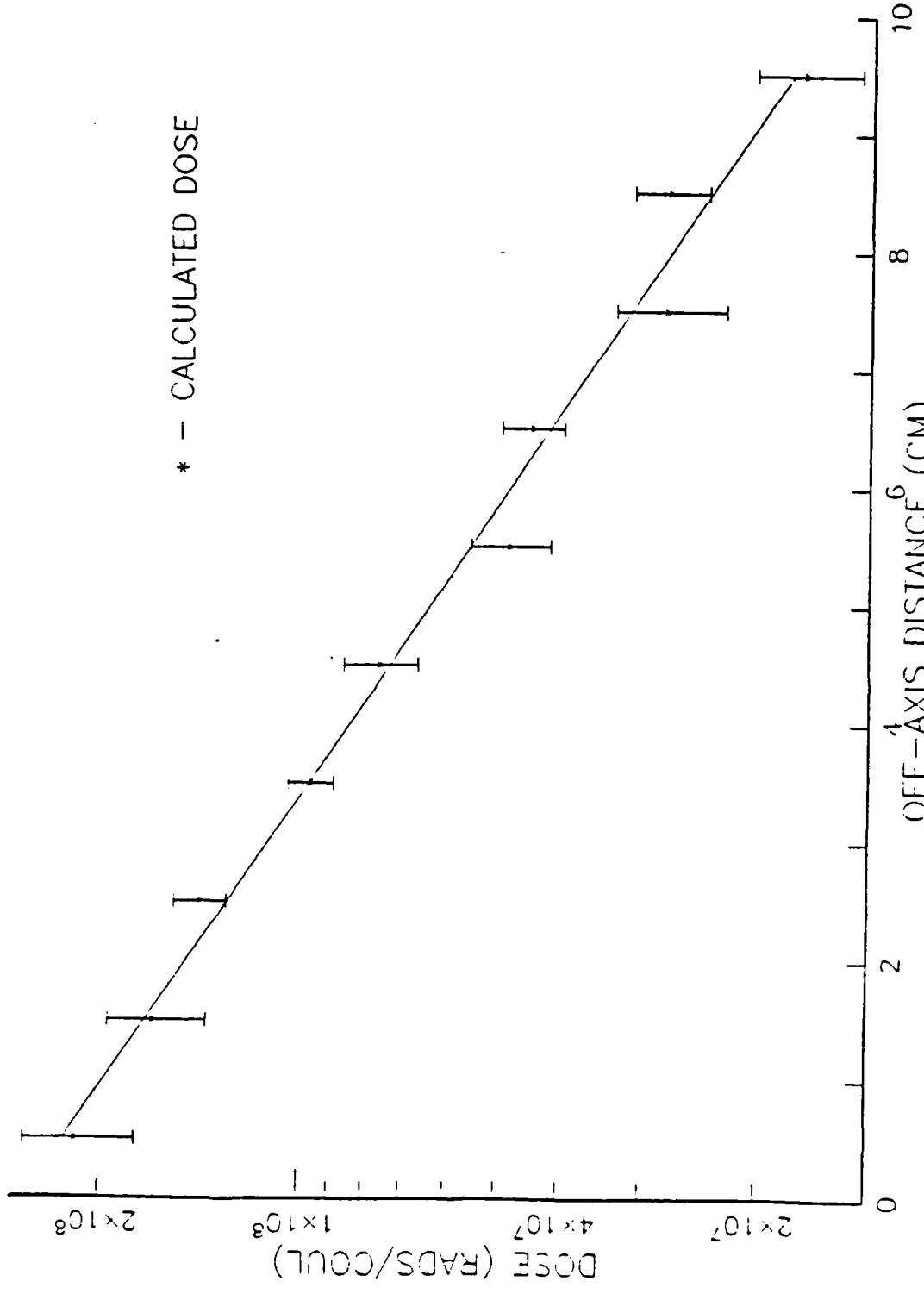

Figure D5: Calculated Dose Due to 100 MeV Electrons in LN_2-71.5 cm

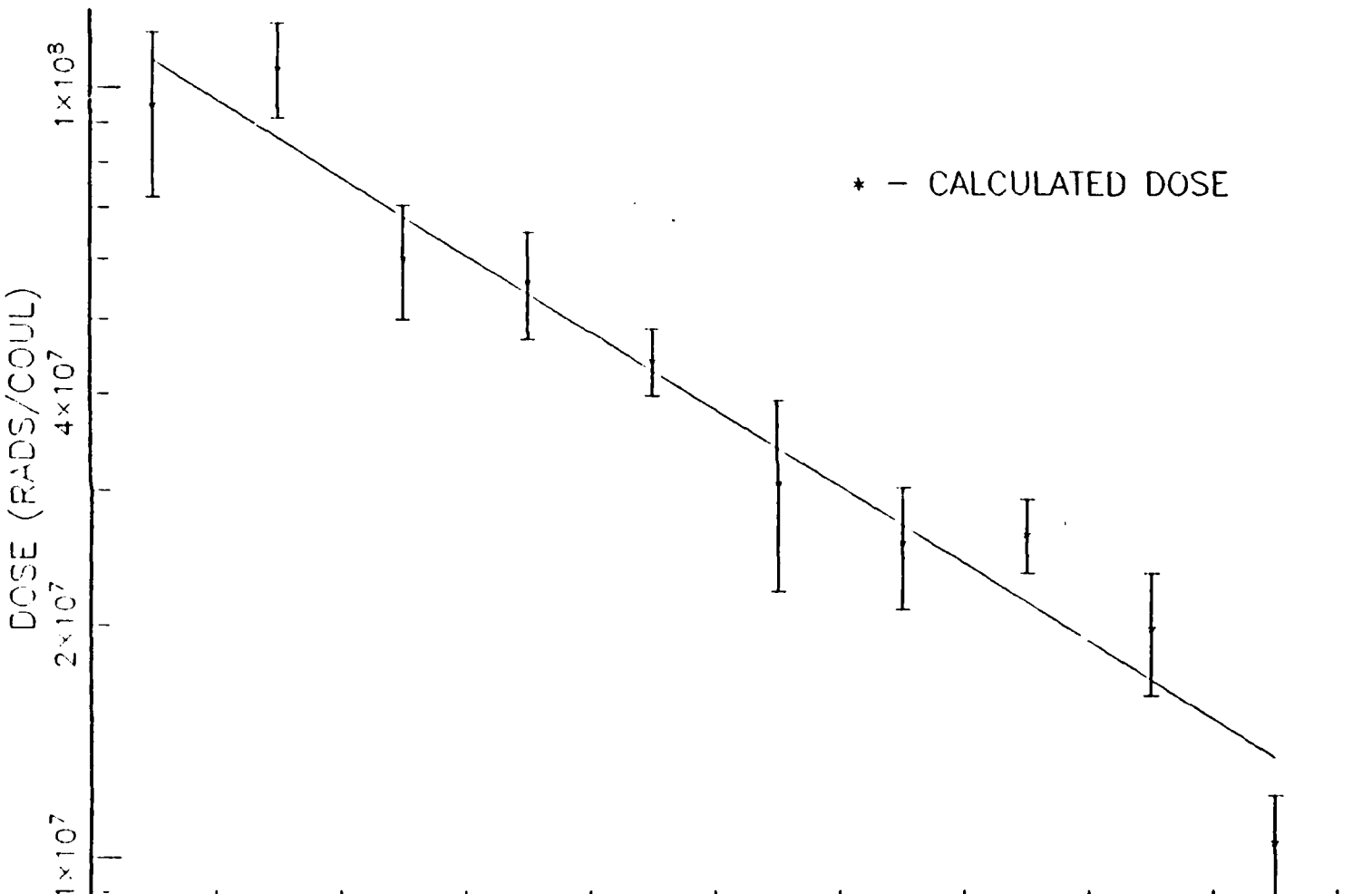

Figure D6: Calculated Dose Due to 100 MeV Electrons in LN_2-95.4 cm

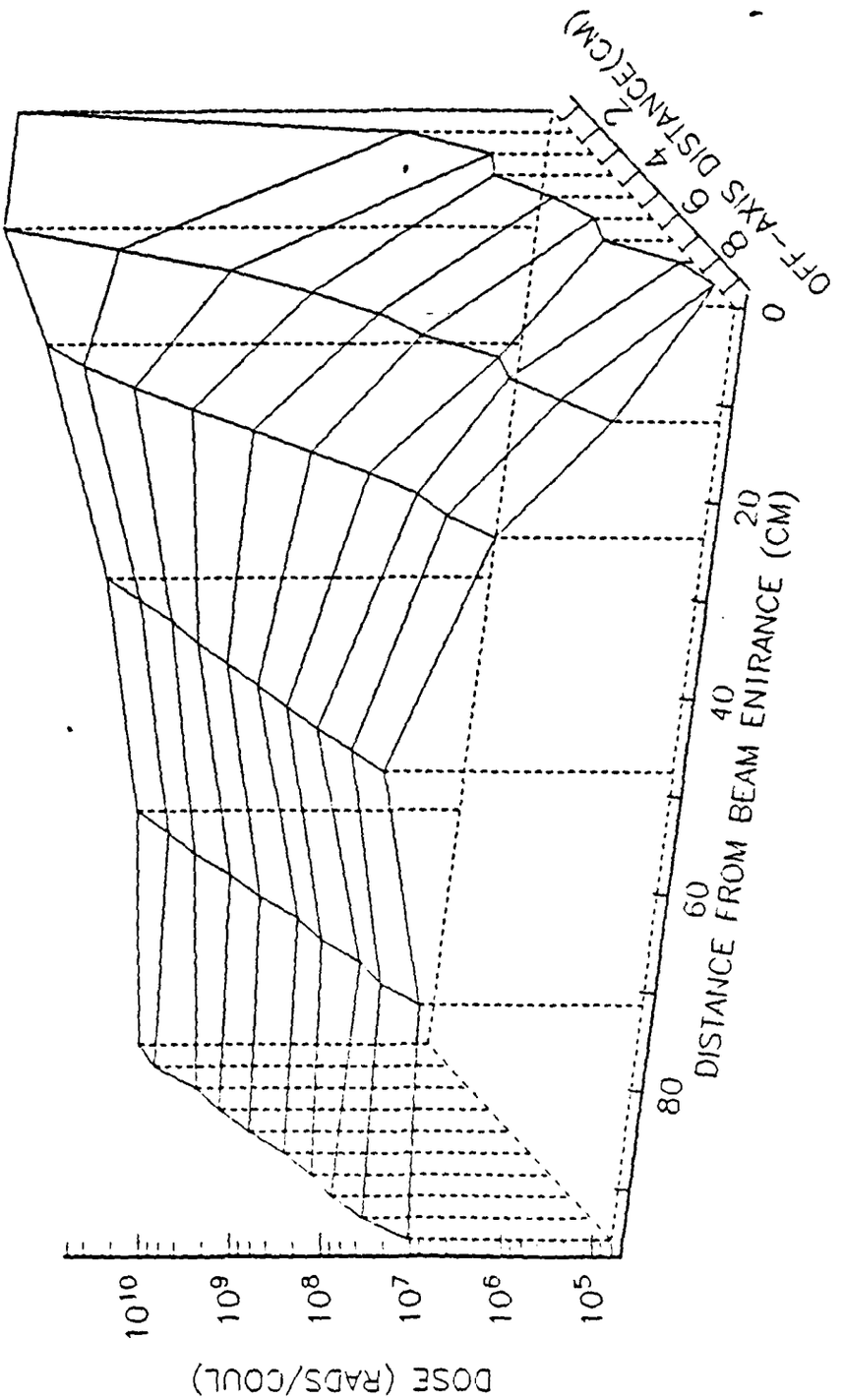

Figure D7: Unsmoothed Surface Plot of Dose Due to 100 MeV Electrons in LN_2

APPENDIX E

TABLE E1 : CALCULATED OFF-AXIS DOSE FROM 20 MeV ELECTRONS IN WATER

Zone	x-axis avg (cm)	Mass (gm)	Volume (cm3)	Energy Deposition (MeV/Particle)	Rads/Coulomb	1-Sigma Uncertainty
z axis-0.0cm						
1	0.5	6.2832E-01	6.2832E-01	3.4320E-01	5.4622E+10	1
2	1.5	1.8850E+00	1.8850E+00	1.0423E-04	5.5294E+06	35
3	2.5	3.1416E+00	3.1416E+00	3.2180E-04	1.0243E+07	53
4	3.5	4.3982E+00	4.3982E+00	1.2423E-04	2.8246E+06	53
5	4.5	5.6549E+00	5.6549E+00	3.8974E-05	6.8921E+05	34
6	5.5	6.9115E+00	6.9115E+00	2.2373E-04	3.2371E+06	49
7	6.5	8.1681E+00	8.1681E+00	1.0551E-04	1.2917E+06	55
8	7.5	9.4248E+00	9.4248E+00	1.1246E-04	1.1932E+06	57
9	8.5	1.0068E+01	1.0068E+01	1.9127E-05	1.8998E+05	31
10	9.5	1.1938E+01	1.1938E+01	1.0790E-05	9.0384E+04	49
z axis- 9.2 cm						
12	0.5	6.2832E-01	6.2832E-01	2.2115E-02	3.5197E+09	6
13	1.5	1.8850E+00	1.8850E+00	4.7762E-02	2.5338E+09	2
14	2.5	3.1416E+00	3.1416E+00	3.5861E-02	1.1415E+09	3
15	3.5	4.3982E+00	4.3982E+00	1.5389E-02	3.4989E+08	5
16	4.5	5.6549E+00	5.6549E+00	3.3701E-03	5.9596E+07	11
17	5.5	6.9115E+00	6.9115E+00	9.0307E-04	1.3066E+07	23
18	6.5	8.1681E+00	8.1681E+00	3.9016E-04	4.7766E+06	30
19	7.5	9.4248E+00	9.4248E+00	2.0940E-04	2.2218E+06	24
20	8.5	1.0068E+01	1.0068E+01	1.0634E-04	1.0562E+06	33
21	9.5	1.1938E+01	1.1938E+01	1.0498E-04	8.7938E+05	47

z axis- 18.5 cm						
23	0.5	6.2832E-01	6.2832E-01	3.4066E-04	5.4218E+07	27
24	1.5	1.8850E+00	1.8850E+00	7.4611E-04	3.9581E+07	17
25	2.5	3.1416E+00	3.1416E+00	8.2785E-04	2.6351E+07	14
26	3.5	4.3982E+00	4.3982E+00	6.9166E-04	1.5726E+07	20
27	4.5	5.6549E+00	5.6549E+00	5.0592E-04	8.9466E+06	22
28	5.5	6.9115E+00	6.9115E+00	4.3682E-04	6.3202E+06	47
29	6.5	8.1681E+00	8.1681E+00	4.6562E-04	5.7005E+06	31
30	7.5	9.4248E+00	9.4248E+00	3.7421E-04	3.9705E+06	23
31	8.5	1.0068E+01	1.0068E+01	2.9957E-04	2.9754E+06	26
32	9.5	1.1938E+01	1.1938E+01	2.0644E-04	1.7293E+06	39
z axis- 37.0 cm						
34	0.5	6.2832E-01	6.2832E-01	4.3169E-05	6.8705E+06	62
35	1.5	1.8850E+00	1.8850E+00	1.0936E-04	5.8016E+06	41
36	2.5	3.1416E+00	3.1416E+00	1.8084E-04	5.7563E+06	26
37	3.5	4.3982E+00	4.3982E+00	1.0664E-04	2.4246E+06	38
38	4.5	5.6549E+00	5.6549E+00	4.3403E-05	7.6753E+05	41
39	5.5	6.9115E+00	6.9115E+00	1.6936E-04	2.4504E+06	34
40	6.5	8.1681E+00	8.1681E+00	1.2069E-04	1.4776E+06	33
41	7.5	9.4248E+00	9.4248E+00	2.0810E-04	2.2080E+06	29
42	8.5	1.0068E+01	1.0068E+01	1.1385E-04	1.1308E+06	41
43	9.5	1.1938E+01	1.1938E+01	1.3556E-04	1.1355E+06	42

z axis- 55.5 cm

45	0.5	6.2832E-01	6.2832E-01	5.7519E-05	9.1544E+06	86
46	1.5	1.8850E+00	1.8850E+00	4.0860E-06	2.1676E+05	99
47	2.5	3.1416E+00	3.1416E+00	6.9462E-05	2.2110E+06	60
48	3.5	4.3982E+00	4.3982E+00	1.6826E-04	3.8257E+06	60
49	4.5	5.6549E+00	5.6549E+00	9.9525E-05	1.7600E+06	66
50	5.5	6.9115E+00	6.9115E+00	7.9949E-05	1.1568E+06	55
51	6.5	8.1681E+00	8.1681E+00	9.8235E-05	1.2027E+06	55
52	7.5	9.4248E+00	9.4248E+00	1.1126E-04	1.1805E+06	63
53	8.5	1.0068E+01	1.0068E+01	1.2446E-05	1.2362E+05	99
54	9.5	1.1938E+01	1.1938E+01	6.3564E-05	5.3245E+05	40

z axis- 74.0 cm

56	0.5	6.2832E-01	6.2832E-01	0.0000E+00	0.0000E+00	99
57	1.5	1.8850E+00	1.8850E+00	0.0000E+00	0.0000E+00	99
58	2.5	3.1416E+00	3.1416E+00	0.0000E+00	0.0000E+00	67
59	3.5	4.3982E+00	4.3982E+00	0.0000E+00	0.0000E+00	71
60	4.5	5.6549E+00	5.6549E+00	0.0000E+00	0.0000E+00	71
61	5.5	6.9115E+00	6.9115E+00	0.0000E+00	0.0000E+00	99
62	6.5	8.1681E+00	8.1681E+00	0.0000E+00	0.0000E+00	66
63	7.5	9.4248E+00	9.4248E+00	0.0000E+00	0.0000E+00	99
64	8.5	1.0068E+01	1.0068E+01	0.0000E+00	0.0000E+00	73
65	9.5	1.1938E+01	1.1938E+01	0.0000E+00	0.0000E+00	67

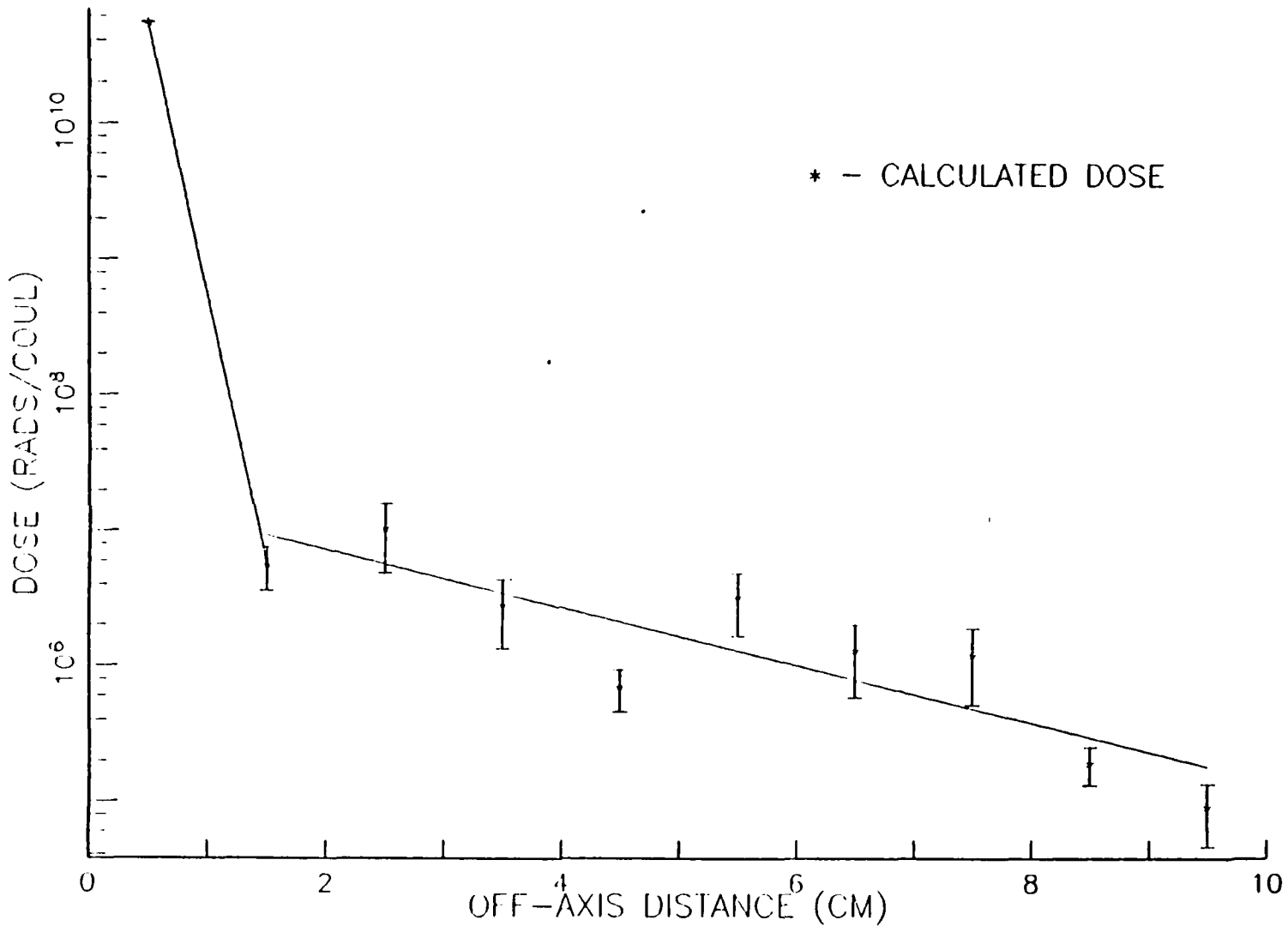

Figure E1: Calculated Dose Due to 20 MeV Electrons in Water–0.0 cm

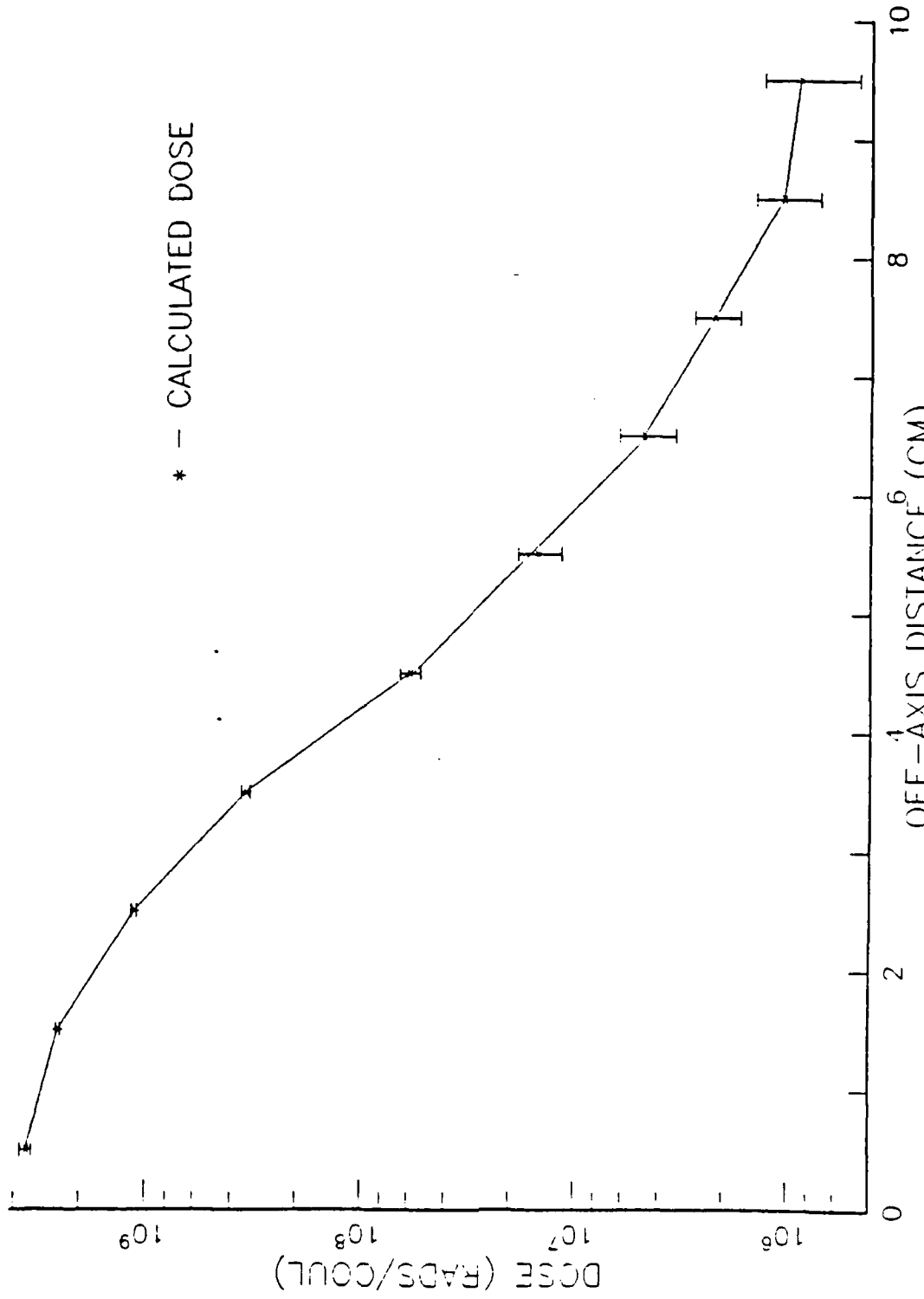

Figure E2: Calculated Dose Due to 20 MeV Electrons in Water-9.2 cm

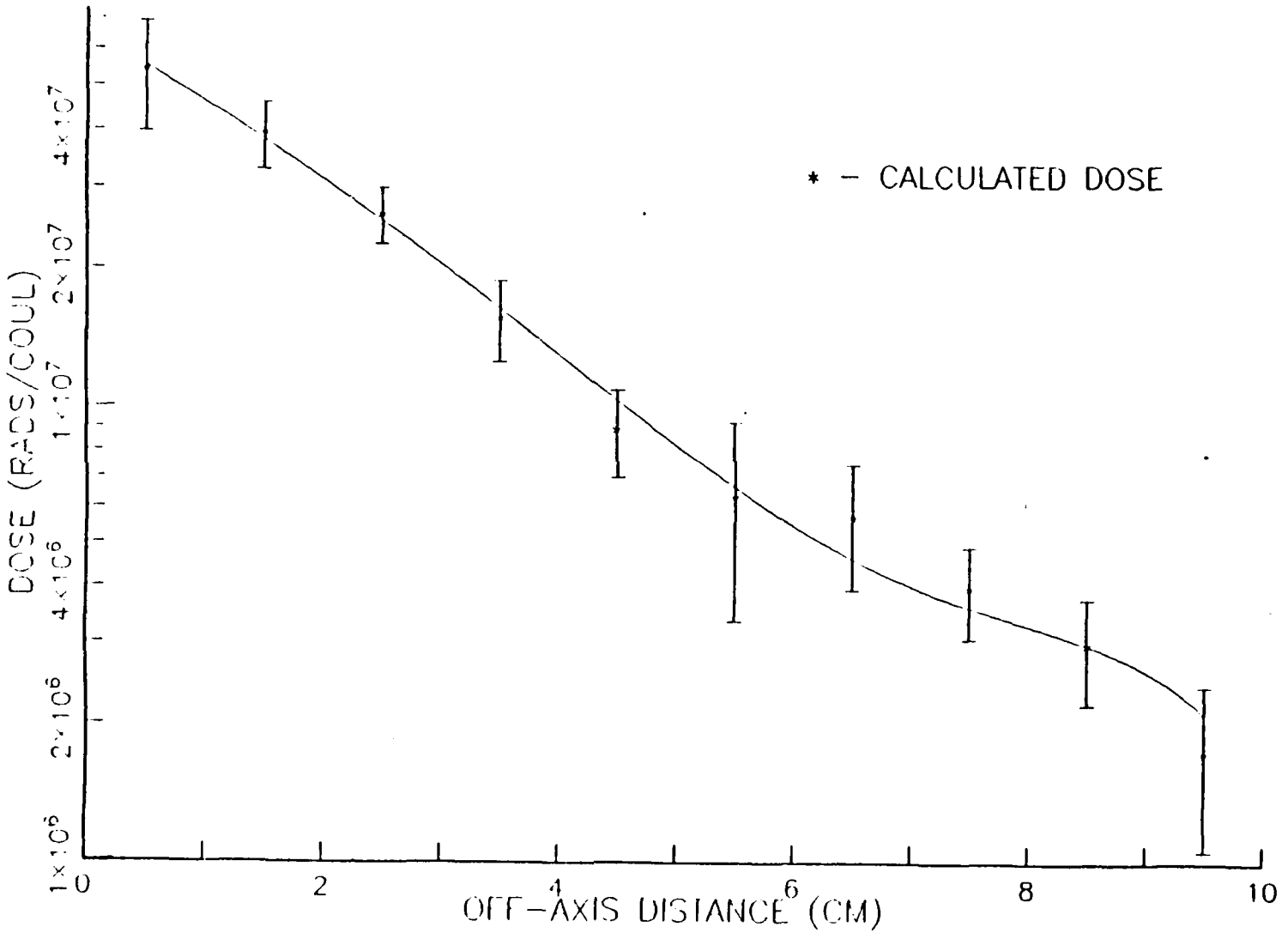

Figure E3: Calculated Dose Due to 20 MeV Electrons in Water-18.5 cm

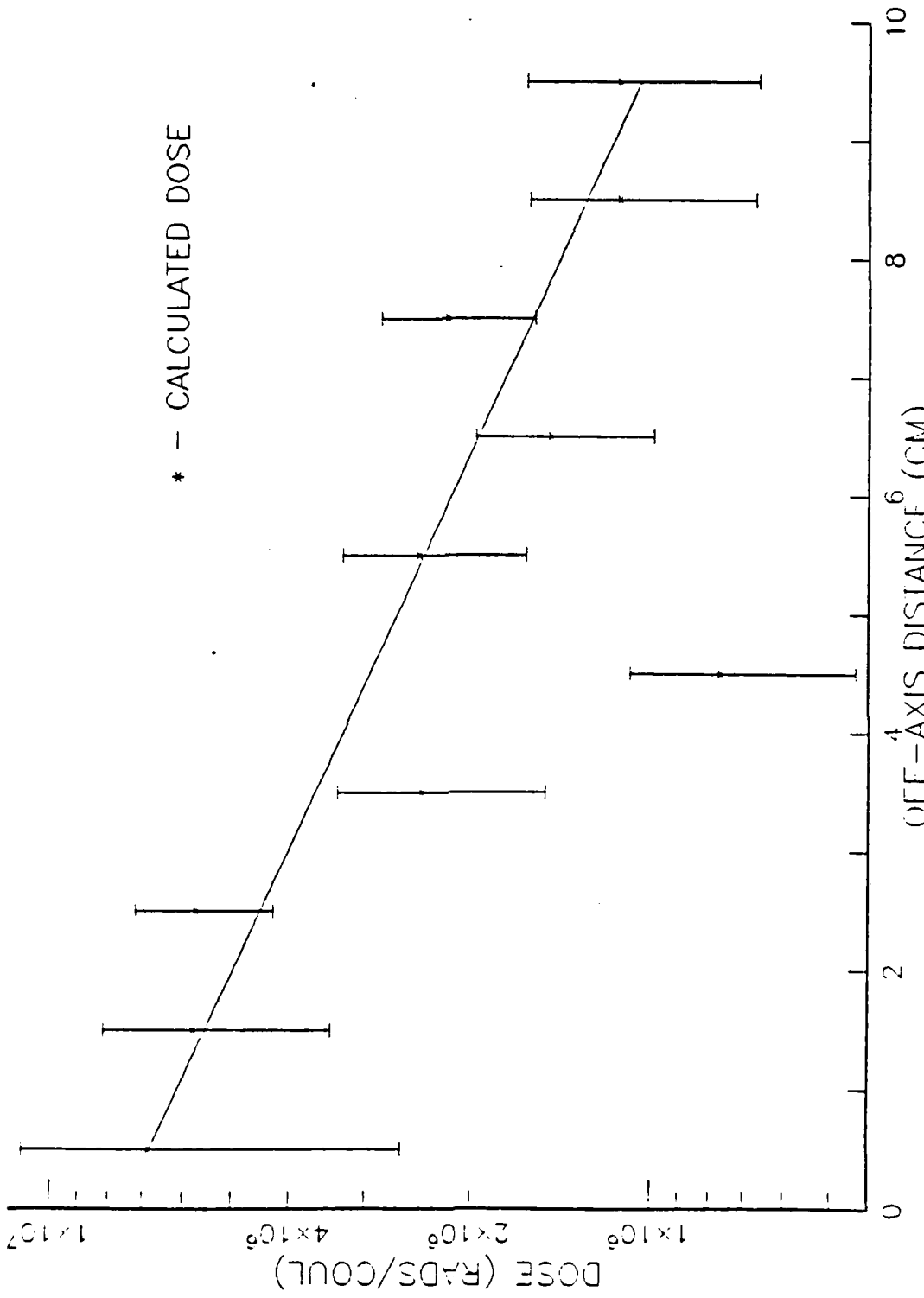

Figure E4: Calculated Dose Due to 20 MeV Electrons in Water–37.0 cm

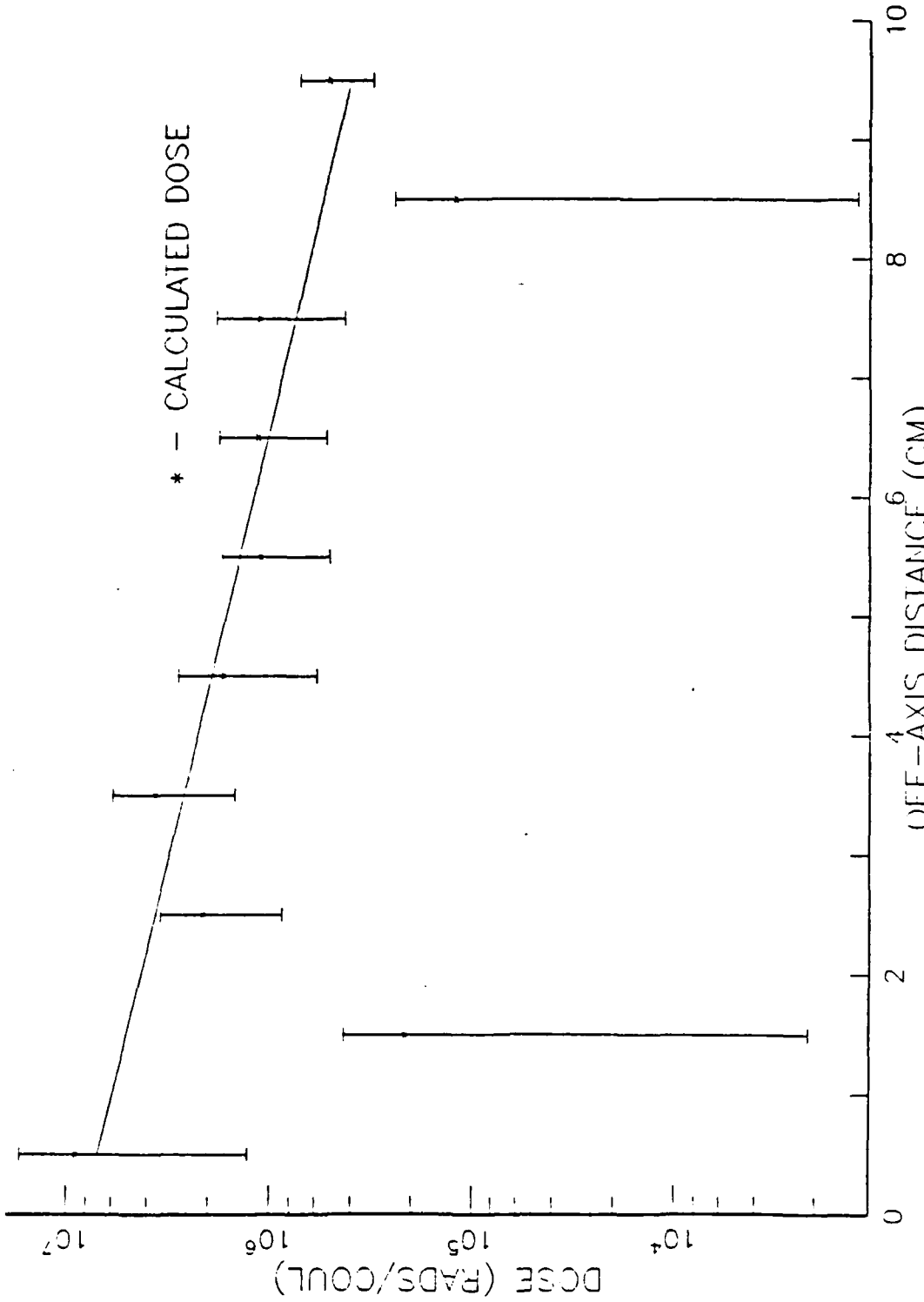

Figure E5: Calculated Dose Due to 20 MeV Electrons in Water-55.5 cm

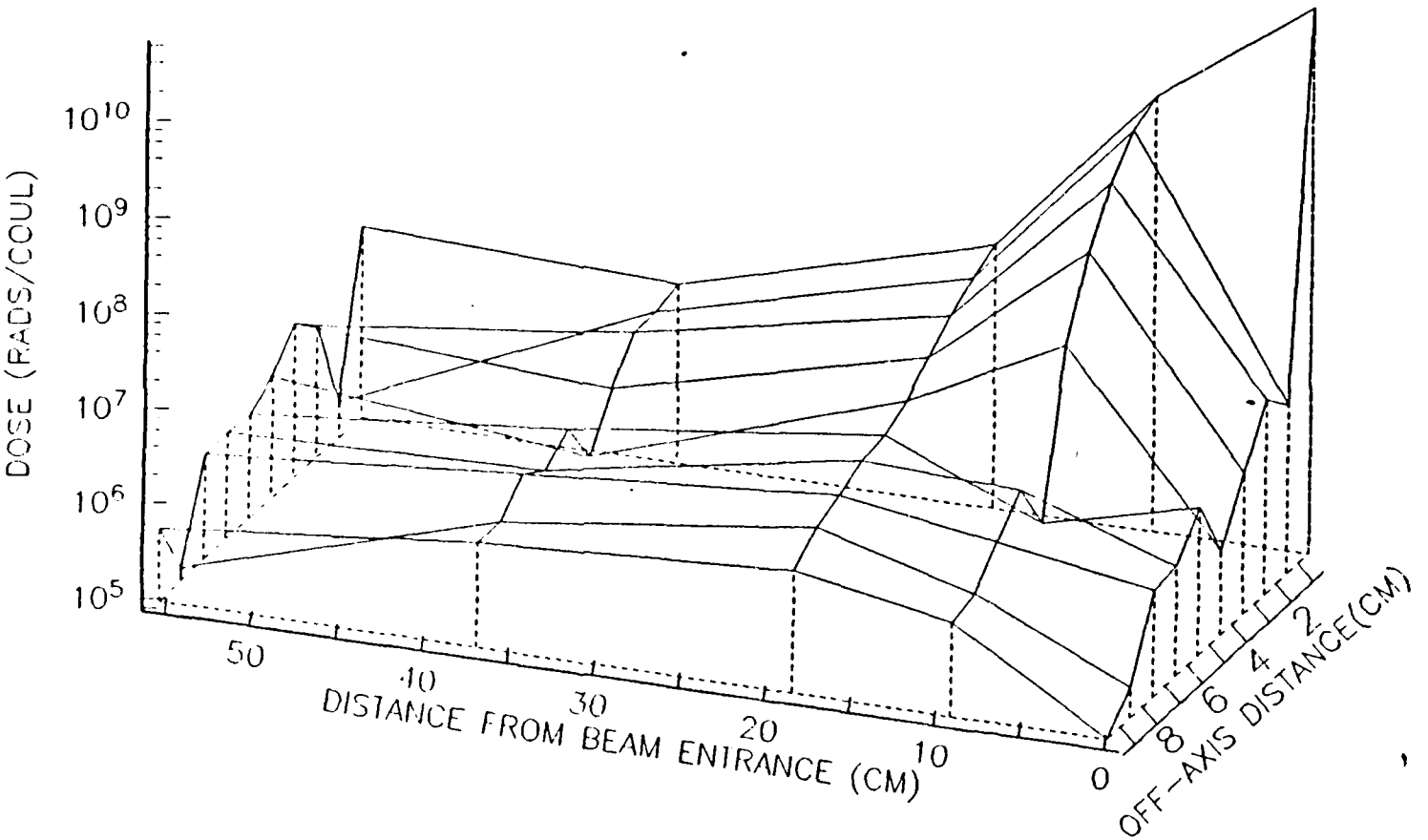

Figure E6: Unsmoothed Surface Plot of Dose Due to 20 MeV Electrons in Water

APPENDIX F

EQUATIONS USED FOR CURVE FITTING

TABLE F1 : 100 MEV ELECTRONS IN WATER

0.0 cm				
	$0.5 \leq x \leq 1.5$	$y=1.71$	$\times 10^{13}$	$e^{-11.49x}$
	$1.5 < x \leq 10$	$y=7.516$	$\times 10^{5}$	$e^{-0.1061x}$
9.2 cm				
	$0.5 \leq x \leq 1.5$	$y=2.59$	$\times 10^{11}$	$e^{-3.022x}$
	$1.5 < x \leq 2.5$	$y=1.211$	$\times 10^{11}$	$e^{-2.515x}$
	$2.5 < x \leq 3.5$	$y=7.514$	$\times 10^{9}$	$e^{-1.405x}$
	$3.5 < x \leq 6.5$	$y=1.359$	$\times 10^{9}$	$e^{-0.9046x}$
	$6.5 < x \leq 7.5$	$y=8.291$	$\times 10^{7}$	$e^{-0.4732x}$
	$7.5 < x \leq 10$	$y=5.1014$	$\times 10^{6}$	$e^{-0.1014x}$
18.5 cm				
	$0.5 \leq x \leq 1.5$	$y=2.6675$	$\times 10^{10}$	$e^{-0.7388x}$
	$1.5 < x \leq 2.5$	$y=4.8532$	$\times 10^{10}$	$e^{-1.1352x}$
	$2.5 < x \leq 3.5$	$y=6.6444$	$\times 10^{10}$	$e^{-1.1352x}$
	$3.5 < x \leq 4.5$	$y=4.4876$	$\times 10^{10}$	$e^{-1.1488x}$
	$4.5 < x \leq 5.5$	$y=6.7422$	$\times 10^{10}$	$e^{-1.2393x}$
	$5.5 < x \leq 10$	$y=2.2332$	$\times 10^{9}$	$e^{-0.629x}$
37.0 cm				
	$0.5 \leq x \leq 10$	$y=1.848-4.871 \times 10^{8}x+4.807 \times 10^{7}x^{2}-1.748 \times 10^{6}x^{3}$		
55.5 cm				
	$0.5 \leq x \leq 10$	$y=4.26$	$\times 10^{8}$	$e^{-0.3299x}$
74.0				
	$0.5 \leq x \leq 10$	$y=2.074$	$\times 10^{8}$	$e^{-0.282x}$

TABLE F2 : 100 MEV ELECTRONS IN AIR

0.0 m				
	$4 \leq x \leq 12$	$y=1.587$	$\times 10^{7}$	$e^{-1.24x}$
	$12 < x \leq 80$	$y=5.972$	$\times$	$e^{-0.0446x}$
76.8 m				
	$4 \leq x \leq 12$	$y=5.297$	$\times 10^{5}$	$e^{-0.4126x}$
	$12 < x \leq 20$	$y=1.017$	$\times 10^{5}$	$e^{-0.2792x}$
	$20 < x \leq 28$	$y=6.614$	$\times 10^{3}$	$e^{-0.1481x}$
	$28 < x \leq 36$	$y=3.236$	$\times 10^{3}$	$e^{-0.1253x}$
	$36 < x \leq 54$	$y=5.50$	$\times 10^{2}$	$e^{-0.07838x}$
	$54 < x \leq 80$	$y=215.3-8.25x+0.1066x^{2}-.000458x^{3}$		
153.5 m				
	$4 \leq x \leq 12$	$y=4.262$	$\times 10^{4}$	$e^{-0.0905x}$
	$12 < x \leq 20$	$y=8.1107$	$\times 10^{4}$	$e^{-0.1422x}$
	$20 < x \leq 28$	$y=1.0363$	$\times 10^{5}$	$e^{-0.1540x}$
	$28 < x \leq 36$	$y=8.5209$	$\times 10^{4}$	$e^{-0.1473x}$
	$36 < x \leq 44$	$y=5.6628$	$\times 10^{4}$	$e^{-0.1364x}$
	$44 < x \leq 80$	$y=4.1004$	$\times 10^{3}$	$e^{-0.0789x}$
307.0 m				
	$4 \leq x \leq 80$	$y=2.802$	$\times 10^{3}$	$e^{-0.04468x}$
460.5 m				
	$4 \leq x \leq 80$	$y=6.90$	$\times 10^{2}$	$e^{-0.04427x}$

TABLE F3 : 100 MeV Electrons in Liquid Nitrogen

0.0 cm				
	$0.5 \leq x \leq 1.5$	$y=6.166$	$\times 10^{12}$	$e^{-11.49x}$
	$1.5 < x \leq 10$	$y=4.198$	$\times 10^{6}$	$e^{-0.1061x}$
11.9 cm				
	$0.5 \leq x \leq 2.5$	$y=1.593$	$\times 10^{11}$	$e^{-3.022x}$
	$2.5 < x \leq 3.5$	$y=2.162$	$\times 10^{10}$	$e^{-2.515x}$
	$3.5 < x \leq 4.5$	$y=5.198$	$\times 10^{9}$	$e^{-1.405x}$
	$4.5 < x \leq 10$	$y=5.525$	$\times 10^{8}$	$e^{-0.9046x}$
23.8 cm				
	$0.5 \leq x \leq 1.5$	$y=1.369$	$\times 10^{10}$	$e^{-0.7388x}$
	$1.5 < x \leq 2.5$	$y=2.397$	$\times 10^{10}$	$e^{-1.1352x}$
	$2.5 < x \leq 6.5$	$y=3.873$	$\times 10^{10}$	$e^{-1.1352x}$
	$6.5 < x \leq 10$	$y=1.853$	$\times 10^{10}$	$e^{-1.1488x}$
47.7 cm				
	$0.5 \leq x \leq 10$	$y=1.17$	$\times 10^{9}$	$e^{-0.258x}$
71.5 cm				
	$0.5 \leq x \leq 10$	$y=2.61$	$\times 10^{8}$	$e^{-0.2817x}$
95.4				
	$0.5 \leq x \leq 10$	$y=1.221$	$\times 10^{8}$	$e^{-0.2319x}$

TABLE F4 : 20 MeV Electrons in Water

0.0 cm	$0.5 \leq x \leq 1.5$	$y=5.4289 \times 10^{12}$	$e^{-9.1981x}$
	$1.5 < x \leq 10$	$y=1.9199 \times 10^{7}$	$e^{-0.4918x}$
9.2 cm			
	$0.5 \leq x \leq 1.5$	$y=4.1483 \times 10^{9}$	$e^{-0.3287x}$
	$1.5 < x \leq 2.5$	$y=8.3790 \times 10^{9}$	$e^{-0.7938x}$
	$2.5 < x \leq 3.5$	$y=2.1945 \times 10^{10}$	$e^{-1.1825x}$
	$3.5 < x \leq 4.5$	$y=1.7157 \times 10^{11}$	$e^{-1.77x}$
	$4.5 < x \leq 6.5$	$y=1.6720 \times 10^{10}$	$e^{-1.262x}$
	$6.5 < x \leq 7.5$	$y=6.9153 \times 10^{8}$	$e^{-0.7654x}$
	$7.5 < x \leq 8.5$	$y=5.8735 \times 10^{8}$	$e^{-0.7436x}$
	$8.5 < x \leq 10$	$y=5.0129 \times 10^{6}$	$e^{-0.1832x}$
18.5 cm			
	$0.5 \leq x \leq 10$	$y=6.5584 \times 10^{7} - 2.1939 \times 10^{7}x + 2.6384 \times 10^{6}x^{2} - 1.0869 \times 10^{5}x^{3}$	
37.0 cm			
	$0.5 \leq x \leq 10$	$y=7.572 \times 10^{6}$	$e^{-0.209x}$
55.5 cm			
	$0.5 \leq x \leq 10$	$y=8.286 \times 10^{6}$	$e^{-0.3157x}$

APPENDIX G

EXPERIMENTAL RESULTS

Table G1 contains the results of the 100 MeV experimental run. The uncertainties involved include the TLD position on the stretcher (± 0.5 cm), the strecher location with respect to the central axis of the test tank (± 1.0 cm), and the skewness of the beam with respect the center line of the tank (±2.0 degrees). Uncertainty in the charge delivered is five percent and uncertainty in the normalized dose is ten percent.

TABLE G1

Experimental Run #1: 100 Mev Electrons in Water

Test day - 28 JUNE 1985
Test Medium - Water
Beam Diameter - 0.5 cm
(0.4 cm above the horizontal axis)
SEM Efficiency - 0.028
Capacitor - 1×10^{-6} Farad
TLD Type - CaF_2

TLD Number	z-axis (cm)	x-axis (cm)	Rads	Coulomb	Rads/Coul
1	0.0	2.0	35.6702	1.03E-06	3.46E+07
2	0.0	4.0	15.8316	1.03E-06	1.54E+07
3	0.0	6.0	64.0929	1.36E-05	4.71E+06
4	0.0	8.0	49.6843	1.36E-05	3.65E+06
5	9.2	1.0	2348.76	1.03E-06	2.28E+09
6	9.2	2.0	631.758	1.03E-06	6.13E+08
7	9.2	3.0	183.113	1.03E-06	1.78E+08
8	9.2	4.0	78.6993	1.03E-06	7.64E+07
9	9.2	5.0	42.9735	1.03E-06	4.17E+07
10	9.2	6.0	22.6433	1.03E-06	2.20E+07
11	9.2	7.0	18.3424	1.03E-06	1.78E+07
12	9.2	8.0	111.069	1.36E-05	8.17E+06
13	9.2	9.0	111.267	1.36E-05	8.18E+06

TABLE G1 (cont'd)

TLD Number	z- axis (cm)	x-axis (cm)	Rads	Coulomb	Rads/Coul
14	18.5	1.0	12188.1	1.03E-06	1.18E+10
15	18.5	2.0	4085.73	1.03E-06	3.97E+09
16	18.5	3.0	2407.99	1.03E-06	2.34E+09
17	18.5	4.0	516.688	1.03E-06	5.02E+08
18	18.5	5.0	297.201	1.03E-06	2.89E+08
19	18.5	6.0	97.8459	1.03E-06	9.50E+07
20	18.5	7.0	453.528	1.36E-05	3.33E+07
21	18.5	8.0	340.428	1.36E-05	2.50E+07
22	18.5	9.0	194.366	1.36E-05	1.43E+07
23	18.5	10.0	156.074	1.36E-05	1.15E+07
24	37.0	1.0	1282.73	1.03E-06	1.25E+09
25	37.0	2.0	1783.29	1.03E-06	1.73E+09
26	37.0	4.0	3612.04	1.36E-05	2.66E+08
27	37.0	6.0	5309.53	1.36E-05	3.90E+08
28	37.0	8.0	4737.13	1.02E-04	4.64E+07
29	37.0	10.0	7204.42	1.02E-04	7.06E+07
30	55.5	1.0	5743.79	1.36E-05	4.22E+08
31	55.5	2.0	1189.37	1.36E-05	8.75E+07
32	55.5	4.0	13359.7	1.02E-04	1.31E+08
33	55.5	6.0	3039.64	1.02E-04	2.98E+07
34	55.5	8.0	4717.41	1.02E-04	4.62E+07
35	55.5	10.0	1047.85	1.02E-04	1.03E+07
36	74.0	2.0	2625.15	1.36E-05	1.93E+08
37	74.0	4.0	2625.15	1.02E-04	2.57E+07
38	74.0	6.0	7757.14	1.02E-04	7.61E+07
39	74.0	8.0	1181.88	1.02E-04	1.16E+07

INITIAL DISTRIBUTION LIST

		No. Copies
1.	Defence Technical Information Center Cameron Station Alexandria, Virginia 22304-6145	2
2.	Library, Code 0142 Naval Postgraduate School Monterey, California 93943-5100	2
3.	Professor F.R. Buskirk, Code 61 Bs Department of Physics Naval Postgraduate School Monterey, California 93943-5100	5
4.	Xavier Maruyama, Rm. B108, Bldg 245 Center fo Radiation Research National Bureau of Standards Gaithersburg, Maryland 20899	5
5.	Professor J.R. Neighbors, Code 61 Nb Department of Physics Naval Postgraduate School Monterey, California 93943-5100	2
6.	Mr. Donald Snyder, Code 61 Ds Department of Physics Naval Postgraduate School Monterey, California 93943-5100	1
7.	Joe Mack Code M-4 Los Alamos National Laboratory Los Alamos, New Mexico 87545	1
8.	Gene Nolting Naval Surface Weapons Center Code H23 White Oak, Maryland 20810	2

9. Ms. Louise Miles — 1
Naval Surface Weapons Center
Code H23
White Oak, Maryland 20810

10. Dr. Ken Struve — 1
P.O. Box 808
Lawrence Livermore National Laboratory
Livermore, California 94550

11. Dr. R.A. Lindgren — 1
Department of Physics
University of Massachussets
Amherst, Massachussets 01033

12. Lt R.D. Fitzpatrick — 2
647 Tewkesbury Ln
Severna Park, Maryland 21146

END

FILMED

3 -86

DTIC